

NEGOM-COH Technical Report

Nearshore bottom properties over the northeastern shelves of the Gulf of Mexico as observed during early May 1998

W. D. Nowlin, Jr.
A. E. Jochens
M. K. Howard
S. F. DiMarco

TAMU Oceanography
Technical Report No. 98-3-T
December 1998

Department of Oceanography
Texas A&M University
College Station, TX 77843-3146

Table of Contents

Prologue.....	1
Background.....	1
Nearshore bottom properties observed on cruise N2	1
Some observed temporal changes.....	2
Acknowledgement.....	4
Reference.....	4
Figures	5

Nearshore bottom properties over the northeastern shelves of the Gulf of Mexico as observed during early May 1998

Prologue

During June and July of 1998, numerous instances of unusually cool bottom waters were reported along the Florida coast west of Cape San Blas. In some cases, low oxygenated (even hypoxic) bottom waters and biological mortalities were reported.

Prior to that period Texas A&M University had conducted in May a cruise sampling the shelf between 89°W and 27.5°N for physical and chemical oceanographic properties. That cruise was part of the Northeastern Gulf of Mexico Physical Oceanography Program: Chemical Oceanography and Hydrography Study sponsored by the Minerals Management Service (MMS). (Here we refer to this cruise as NEGOM cruise N2.)

This informal technical report briefly describing the results of this May 1998 NEGOM cruise, with a focus on nearshore bottom properties, was prepared to provide possible assistance to those attempting to interpret the reports of unusual temperatures, oxygen levels, and ecological disruptions.

Background

NEGOM cruise N2 took samples from 5 through 16 May 1998. Figure 1 shows CTD/bottle station locations. Numbers are in sequence of occupation. Lines are referred to as 1 through 11 from west to southeast. Lines 11-4 were occupied sequentially beginning with 11, after which, lines 1-3 were occupied in that order.

Surface meteorological observations are generally available from the locations shown in Figure 2. Figure 3 shows vector surface winds from ten of these locations for the period May through August 1998, indicating the spatial coherence of the wind field for this period. During most of this period, surface winds were generally weak with speeds averaging near 4 m·s⁻¹. During April there were periods of westerly winds favorable for coastal upwelling and eastward nearshore currents in the region west of Cape San Blas; otherwise winds were generally easterly. During the month of May, winds were light and variable.

Figure 4 shows the sea surface height anomaly from satellite altimeter data averaged over the period 21 April - 4 May 1998, just prior to the beginning of cruise N2. Seen are two anticyclonic features impinging on the shelf edge in the region of DeSoto Canyon and west of Tampa.

Nearshore bottom properties observed on cruise N2

The distribution of geopotential anomaly for the sea surface (3 m) relative to 800 m (Figure 5) also shows an anticyclonic feature over the DeSoto Canyon and a second anticyclone encroaching over the outer shelf edge west of Tampa. The circulation indicated by these features is substantiated by the shipboard ADCP measurements. Shown in Figure 6 is the gridded ADCP field at 50 m, which is representative of other levels as well. An anticyclonic feature is seen located over the upper canyon (centered near 29°N, 87°W). There is evidence for along-isobath flow along the northern edge of the canyon and cross-isobath flow, directed inshore, at the canyon axis. This results in inshore penetration of deep water along the canyon sides. Such a flow will lead to transport in a bottom Ekman layer that is to the left of the flow—leading to even more penetration of bottom waters upslope in the canyon. Upwelling is clearly seen in the bottom distribution of temperature (Figure 7) showing maximum inshore penetration of cool bottom water near the head of DeSoto Canyon (lines 5 and 6).

Vertical sections of hydrographic properties give clear evidence that onshore, near-bottom flow extending in most cases to the innermost stations (10-m isobath) had occurred prior to the cruise. Figures 8a - 8k show temperature in vertical sections. Apparently, upwelling had been stronger prior to the time of the cruise as evidenced by cooler water at the bottom at the innermost stations. Southeast of Cape San Blas (lines 8-11) this onshore upwelling generally did not extend to the shallowest stations.

The high vertical stability associated with the temperature distribution is enhanced west of Cape San Blas by a layer of relatively fresh surface water. On lines 3-7 (Figures 9c-9g) the freshest water is found somewhat further offshore. This could have been caused by nearshore upwelling and associated movement of surface water offshore or by advection from the west due to the anticyclonic circulation over DeSoto Canyon. On lines 1 and 2 (Figures 9a and 9b) the freshest surface water was observed at the inshore stations—evidence of local river sources for this water. East of Cape San Blas the freshest water was also found in the surface layers at the inshore stations. Figure 9h gives the extreme example, with lowest salinities, from line 9. The extent, core, and possible source of the fresh water lens may be deduced from the observed distributions of surface (3.5 m) salinity (Figure 10).

The combination of cool bottom water and a lens of fresh surface water resulted in a very strong pycnocline over the inner and mid shelf regions. West of Cape San Blas the pycnocline was much stronger than to the east; compare Figure 11a for line 3 with Figure 11b for line 9. It is likely that this stability contributed to the relatively low oxygen values found at the bottom over much of the survey region (Figure 12). Many values were near $3 \text{ ml}\cdot\text{l}^{-1}$ and values approached $2 \text{ ml}\cdot\text{l}^{-1}$ near the Mississippi Sound. Bottom dissolved oxygens were not particularly low east of Cape San Blas. That could have been due to differences in stratification or to the fact that the region east of the Cape was sampled earlier in the cruise.

Percent light transmission at the 660 nm wavelength observed during cruise N2 on lines 4 through 11 was generally 80% to greater than 90%, as shown in the example for line 4 (Figure 13d). High light transmission values in the cool bottom waters nearshore gives further evidence that these are upwelled offshore waters. By contrast, approaching the Mississippi Sound, light transmission decreased inshore, toward the surface, and to the west; see values on lines 1-3 shown in Figures 13a-13c.

Nutrient distributions over the mid and inner shelf seem to have been increased at locations corresponding to the cooler upwelled waters. As an example, nitrate in vertical section on line 4 is shown in Figure 14. High nitrate values at the bottom seem well correlated with low oxygen values; for example, compare Figure 14 with Figure 15 that shows dissolved oxygen in vertical section for line 4. The 3.5 m and bottom distributions of nitrate observed on cruise N2 are shown in Figure 16. Effects of river discharge and primary production are clear in the surface distribution. The bottom distribution shows the effects of onshore movement of bottom waters and may be compared with bottom oxygen distributions shown in Figure 12. For completeness, we show in Figures 17-19 the distributions of silicate, phosphate, and nitrite at 3.5 m and near bottom based on cruise N2 measurements.

Some observed temporal changes

In search of cool upwelling events prior to cruise N2 or during the summer of 1998, we examined time series of temperatures from SAIC moorings in the DeSoto Canyon from early April to early August 1998 (SAIC, 1998). Figure 20 shows mooring locations. We focused on locations A1, A2, B2 (B1 was not recovered), C1, C2, D1, D2, and E1. Temperature records for the near-bottom instruments on moorings A1, C1, D1, and E1 at approximately the 100-m isobath are

shown in Figure 21. Lower than average temperatures were recorded during periods in April and early May at C1, D1, and E1. During two periods in mid April pulses of cool water appeared at mooring locations C1 and D1 at approximately the same time. These cool water pulses appeared at E1, at the head of DeSoto Canyon about ten days later. This cool water penetration over the 100-m isobath was not seen at A1. (We examined temperature records at the bottom at A1 and B1 for March and early April and found no indication of such penetration.) These intrusions likely set the stage for the cool bottom water observed during cruise N2.

Note the presence of another influx of cooler water over the 100-m isobath in mid July. Again its presence was found at D1 about ten days before E1. The intensity of this intrusion was less than those in April.

Figures 22a-22d show time histories of isotherm depths from 50 to 300 m at the locations of moorings A2, B2, C2, and D2 along the northeast wall of DeSoto Canyon as constructed by SAIC. At all locations there was a general increase in temperatures at the deeper levels from April until early June. Pronounced cooling occurred throughout the water column in late June and early July at A2. At B2 this cooling was somewhat later in time and confined to the deeper layers. At C2 and D2 the cooling trend continued through July and August.

We examined nearshore meteorological station records for surface temperature and found records from stations 42007 and Dauphin Island (see Figure 2 for locations). At both locations (Figure 23) there was a pronounced warming trend during spring, as expected. A cool event lasting several weeks with a magnitude of near 5°C occurred at both locations in early June 1998.

Figures 24a through 24d show surface winds (vectors as well as north and east components) for early April through early August from four locations arrayed from west to east (see Figure 2 for locations): stations 42007, Dauphin Island, Cape San Blas, and Cedar Key. As described before, we see generally weak and variable winds with some periods favorable to coastal upwelling. However, at the end of the first week in June a strong offshore wind event occurred from the Mississippi Sound to Cape San Blas. This event might have effected offshore flow and upwelling; its timing corresponds with the cool event in observed surface temperatures (Figure 23).

We have examined the evolution of sea surface height anomaly (SSHA) over the northeastern Gulf of Mexico (depths greater than 200 m) using a product prepared by Robert Leben (CCAR) based on a combination of altimeter data from T/P and ERS-2. We looked at one SSHA distribution per week beginning April 1, 1998 and continuing through August 1998. The data have been spatially and temporally smoothed using decorrelation scales of 100 km and 12 days, respectively. Therefore, features may tend to be weaker than in reality and smaller scale features may have been removed.

A series of SSHA distributions was selected to illustrate variability offshore of the NEGOM study area. That offshore region is pictured in the upper panel of each figure; a broader SSHA coverage of the eastern Gulf north of 25°N is shown in the lower panels.

On April 1 (Figure 25) most of the off-shelf NEGOM area was cyclonic flow except for one small anticyclone over DeSoto Canyon. A strong extension of the anticyclone centered at 25.5°N, 88°W is seen extending toward the shelf break west-southwest of Tampa. The anticyclone off Tampa had extended to the 200-m isobath by April 8 and, after separation of a weak anticyclone near the shelf edge, subsequently withdrew. By April 29 (Figure 26) the anticyclone over DeSoto Canyon had consistently strengthened. Shortly thereafter the two anticyclonic features at the shelf edge extended toward one another, coalesced and strengthened, resulting in the peanut-shaped feature seen in Figure 27 for May 20.

Several weeks later (June 3) this feature had reformed into that shown in Figure 28. Then, the feature strengthened and straightened into an east-west orientation as shown in Figure 29 for July 1. Connections began to form with the larger anticyclonic feature to the south until by July 22 (Figure 30) both ends of the anticyclone offshore the NEGOM region appeared to be connected to the larger anticyclone. For the next three weeks, it again separated and diminished somewhat in spatial extent, appearing on August 12 as shown in Figure 31. By August 26 (Figure 32), the feature had renewed a connection with an anticyclone to the southwest and was oriented over the axis of the DeSoto Canyon with considerable strength.

There may be some evidence for the counterclockwise movement along the continental slope of small anticyclones. However, the reality of weak features in the SSHA field near the shelf edge probably should be viewed with caution.

Acknowledgment

This work was carried out as part of the Northeastern Gulf of Mexico Physical Oceanography Program: Chemical Oceanography and Hydrography study sponsored by the Minerals Management Service (MMS) of the U.S. Department of Interior under MMS OCS contract No. 1435-01-97-CT-30851.

Reference

SAIC. 1998. DeSoto Canyon Eddy Intrusion Study. Data Products: Set 4 April 1998-August 1998. SAIC, 615 Oberlin Road, Suite 300, Raleigh, NC 27605.

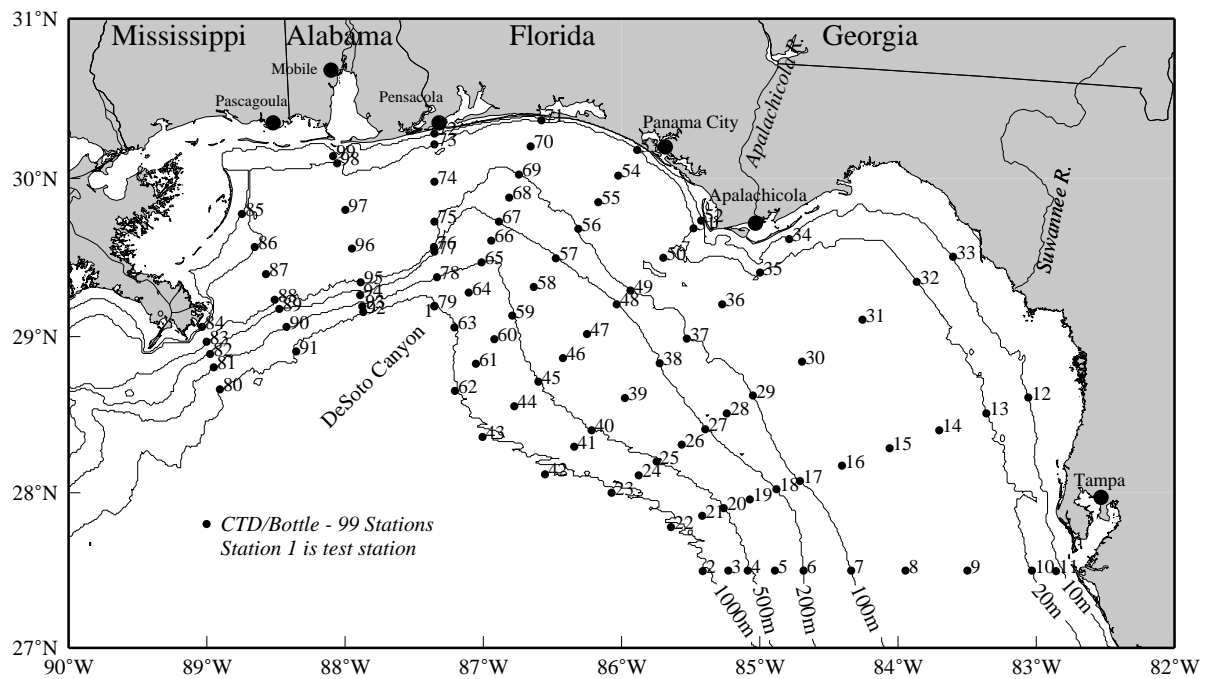


Figure 1. Station numbers for CTD stations on cruise N2 conducted on 5-16 May 1998.

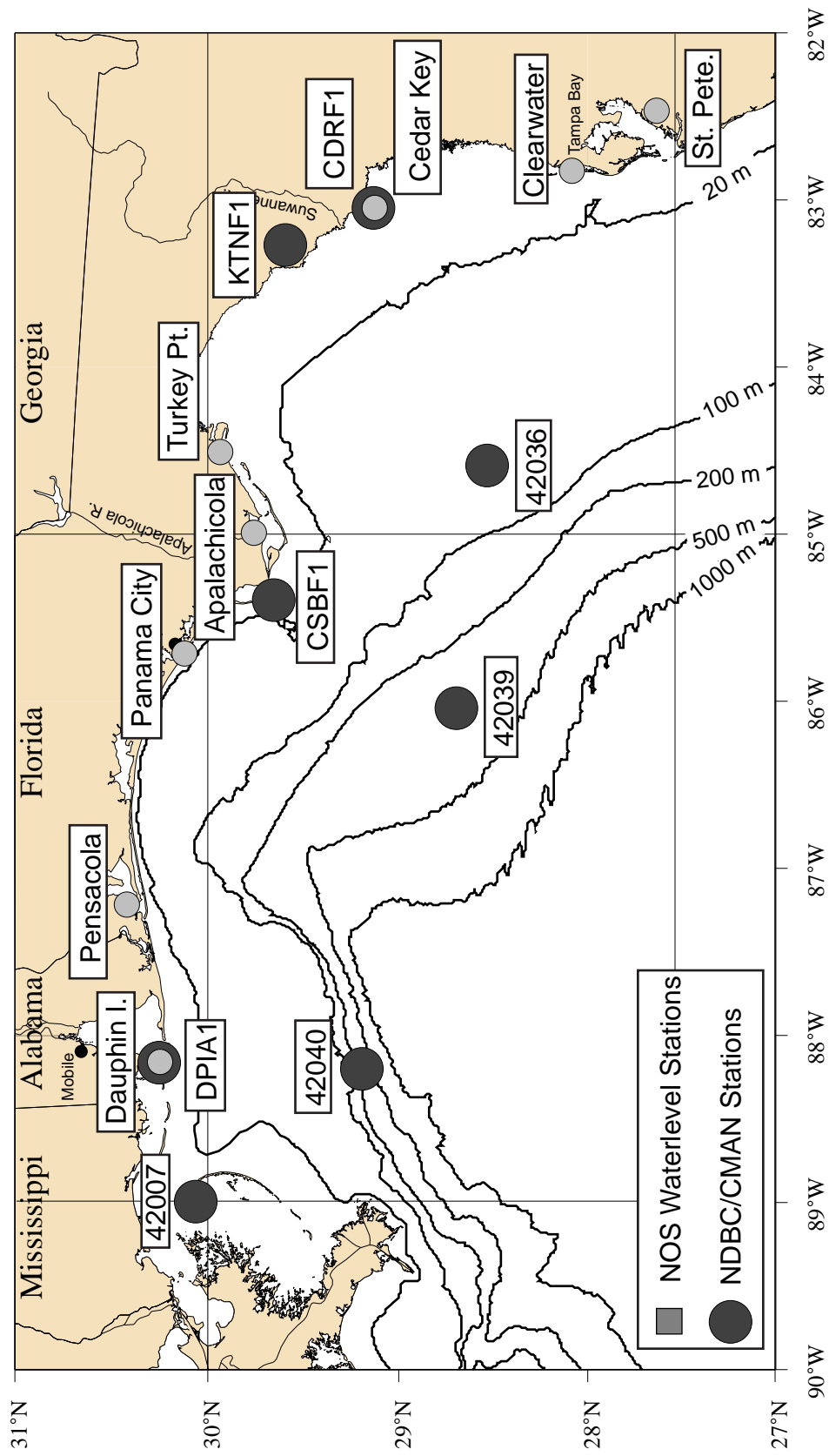


Figure 2. Locations of National Ocean Service water level stations and NDBC/CMAN stations.

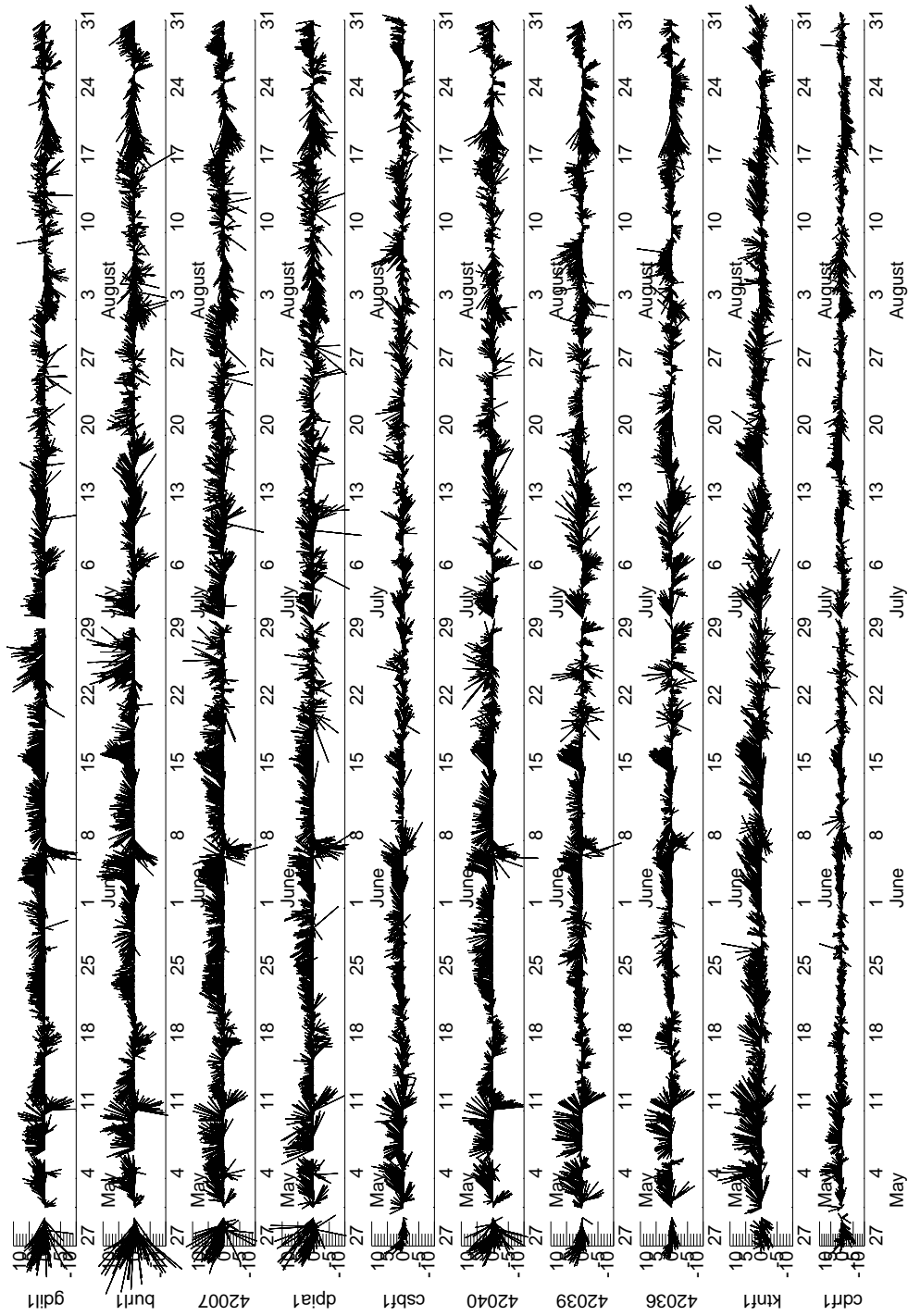


Figure 3. Time series of vector surface winds from ten locations shown in Figure 2 for the period May-August 1998.

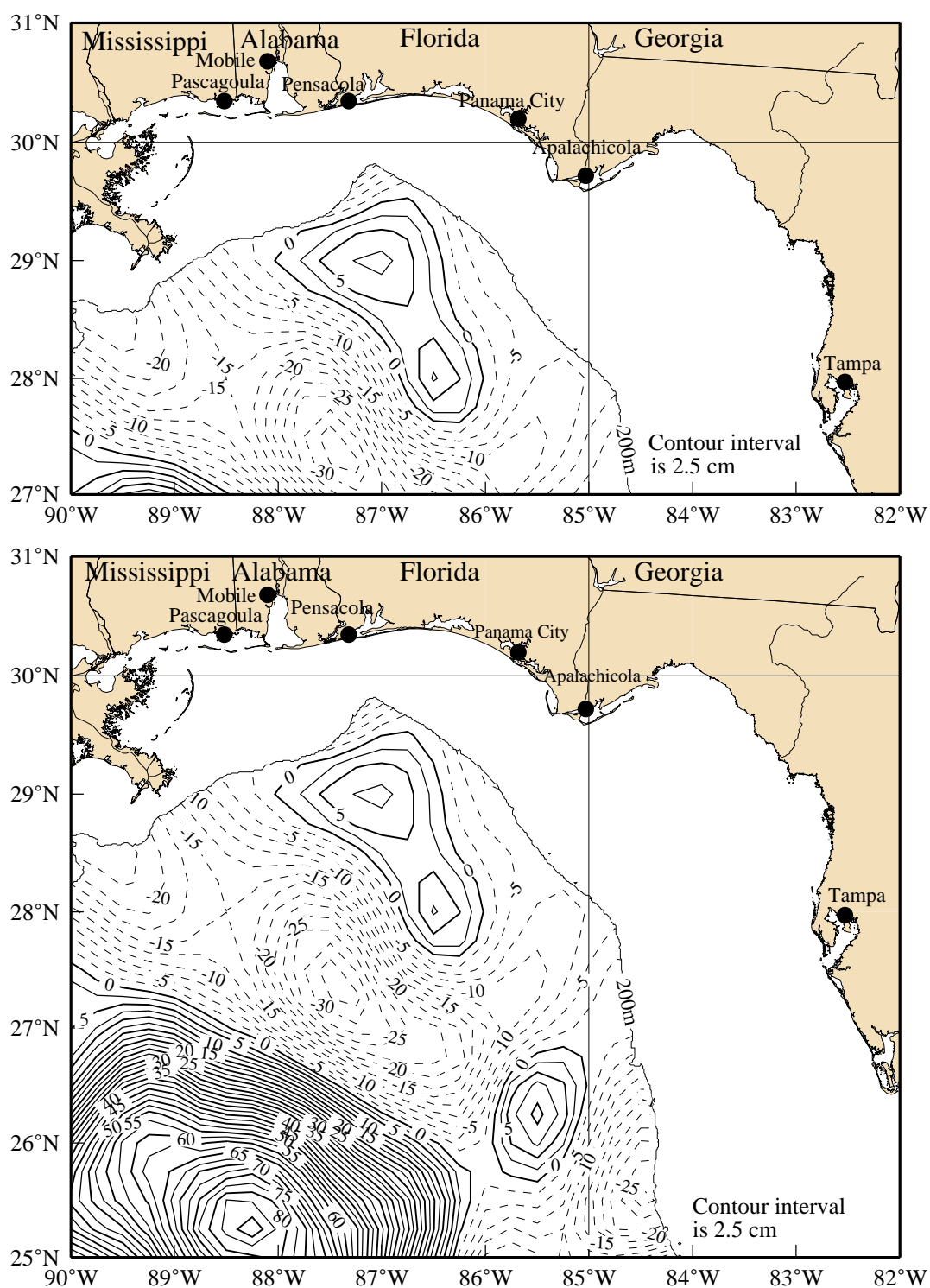


Figure 4. Sea surface height anomaly from satellite altimeter data showing NEGOM study area (upper) and extended region (lower) averaged for 21 April—4 May 1998. (Courtesy of Robert Leben, University of Colorado.)

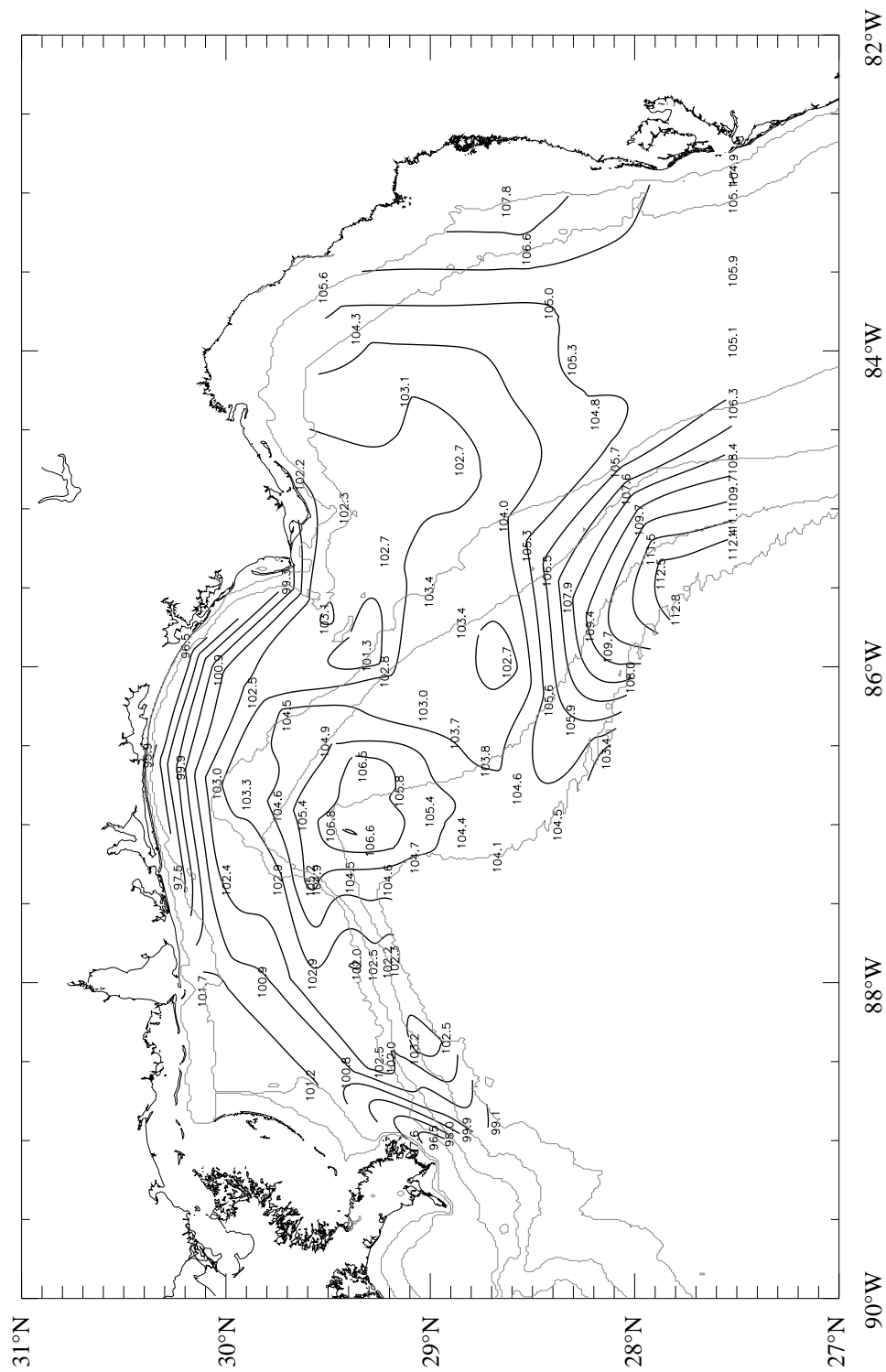


Figure 5. Geopotential anomaly of 3-m surface relative to 800 m constructed from CTD data taken 5-16 May 1998.

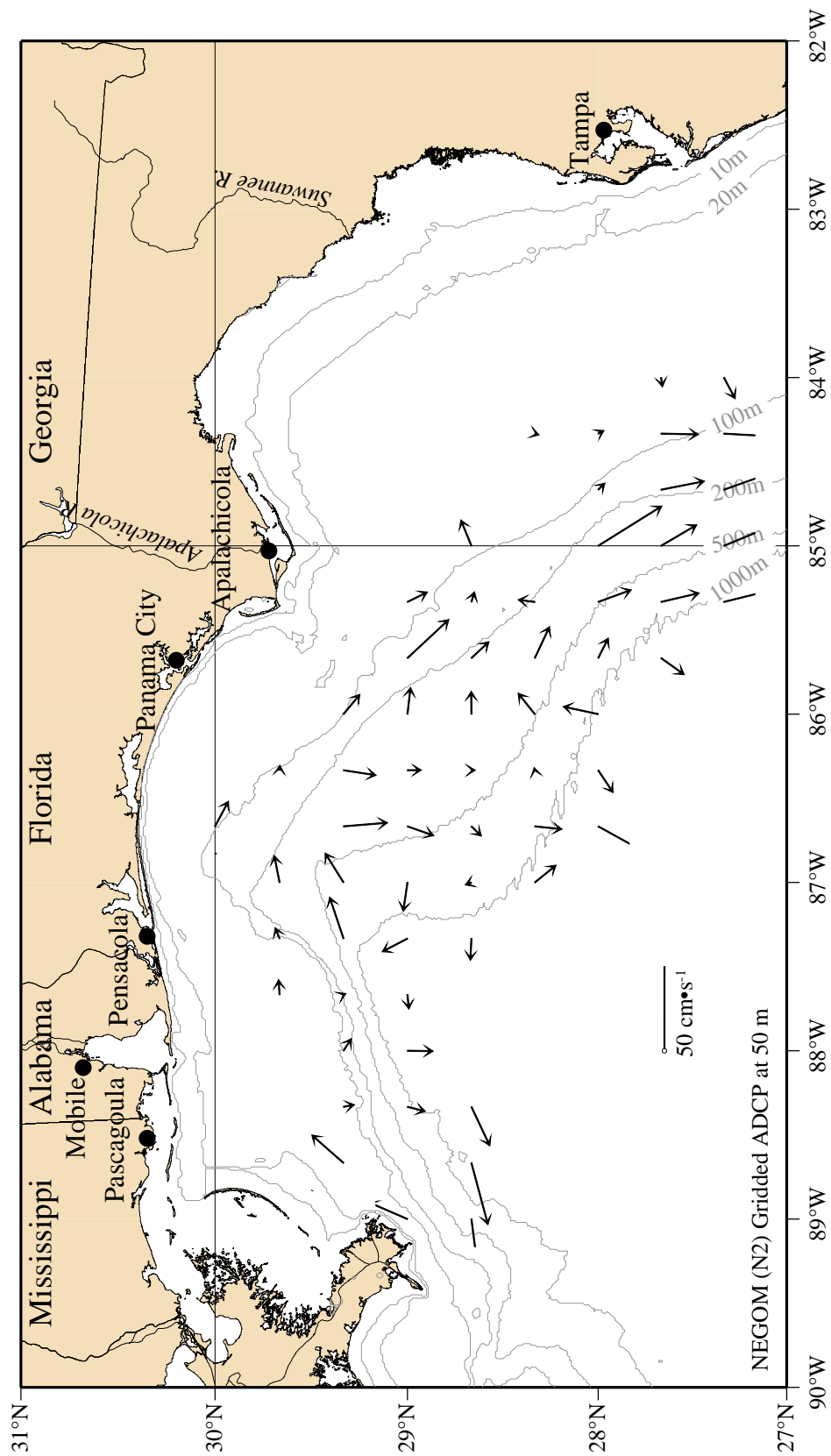


Figure 6. Gridded shipboard ADCP data at 50 m taken 5-16 May 1998.

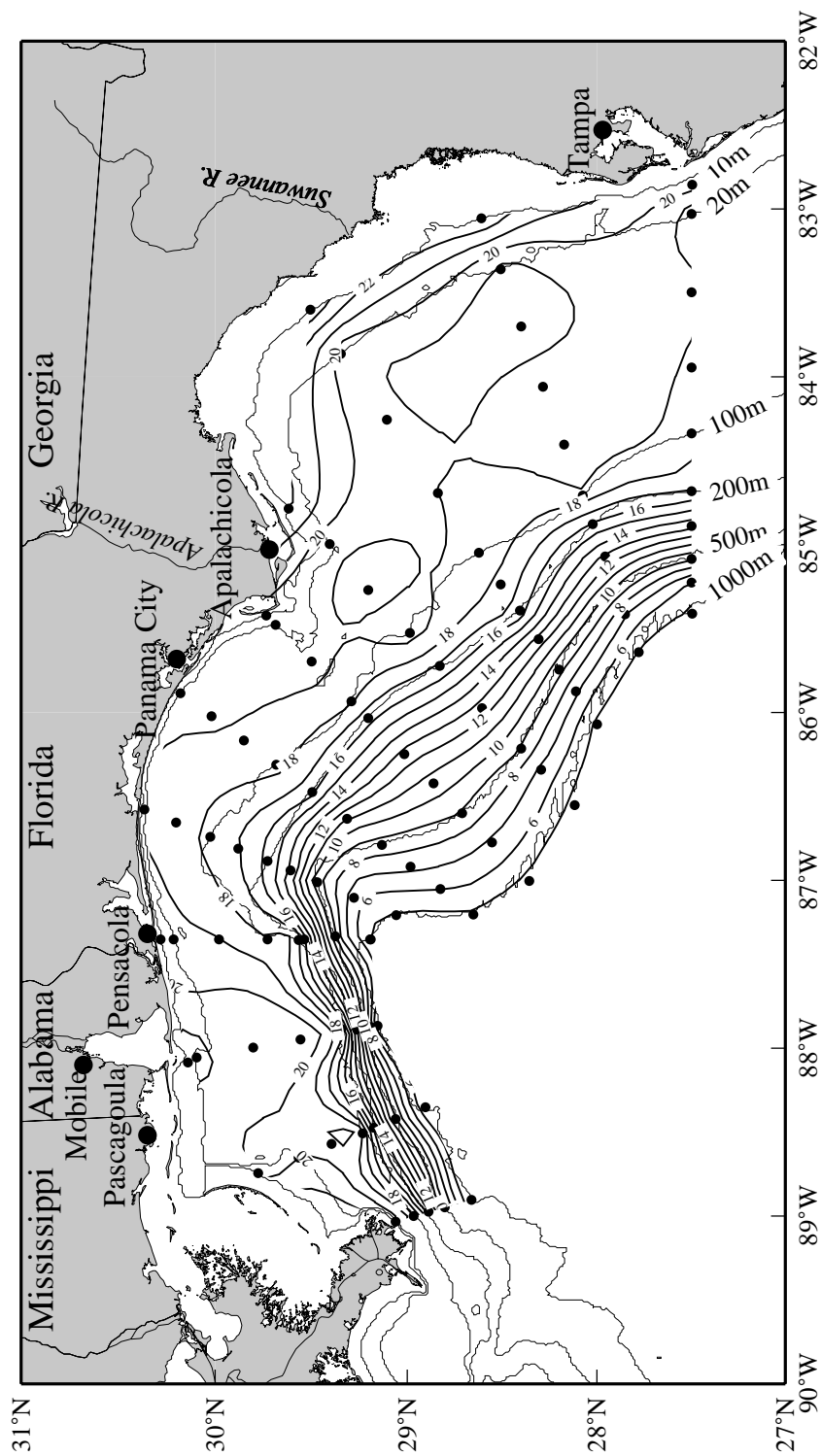


Figure 7. Potential temperature ($^{\circ}\text{C}$) near bottom on NEGOM Cruise N2, 5-16 May 1998.

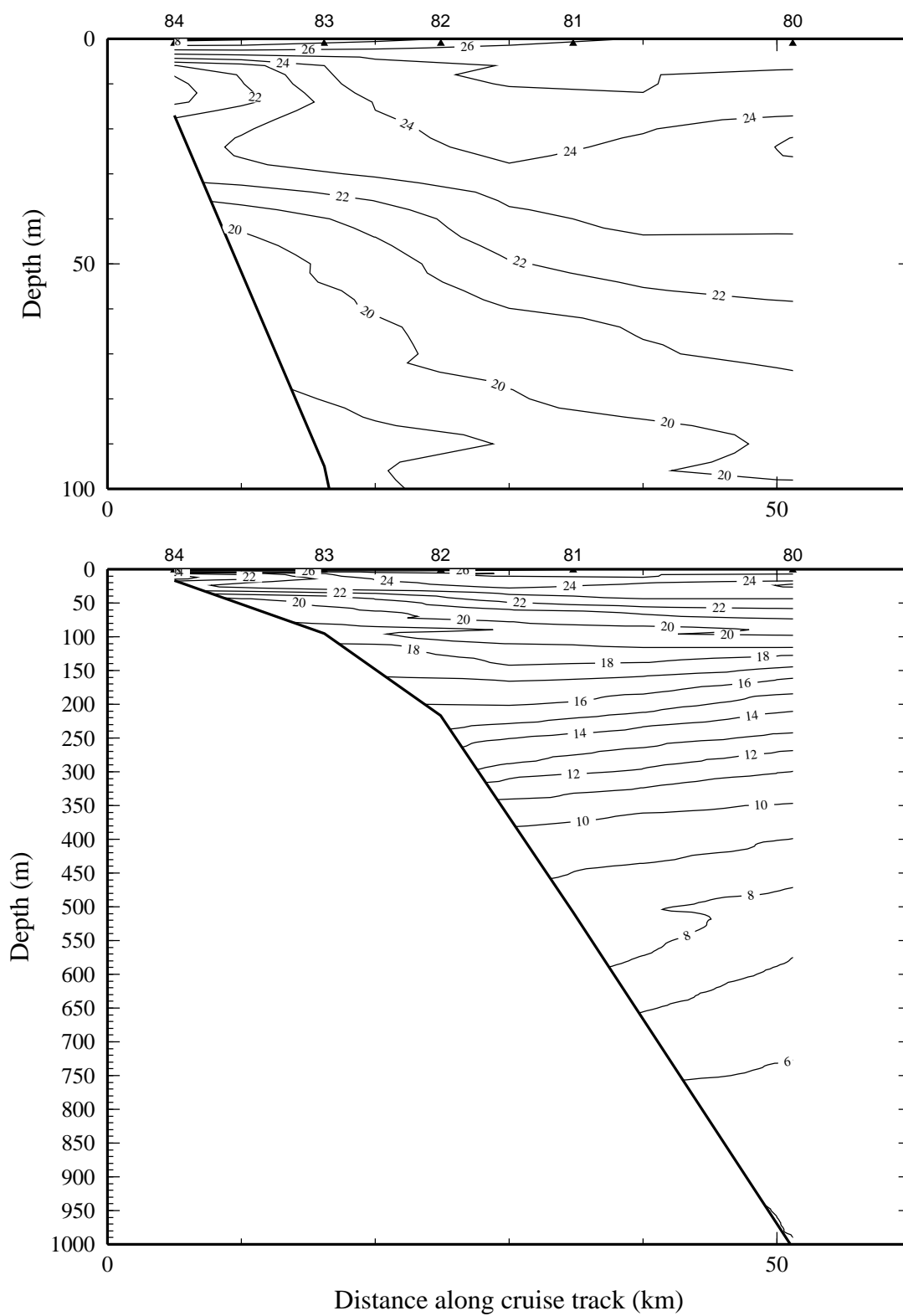


Figure 8a. Potential temperature ($^{\circ}\text{C}$) on line 1 of NEGOM cruise N2, 5-16 May 1998.

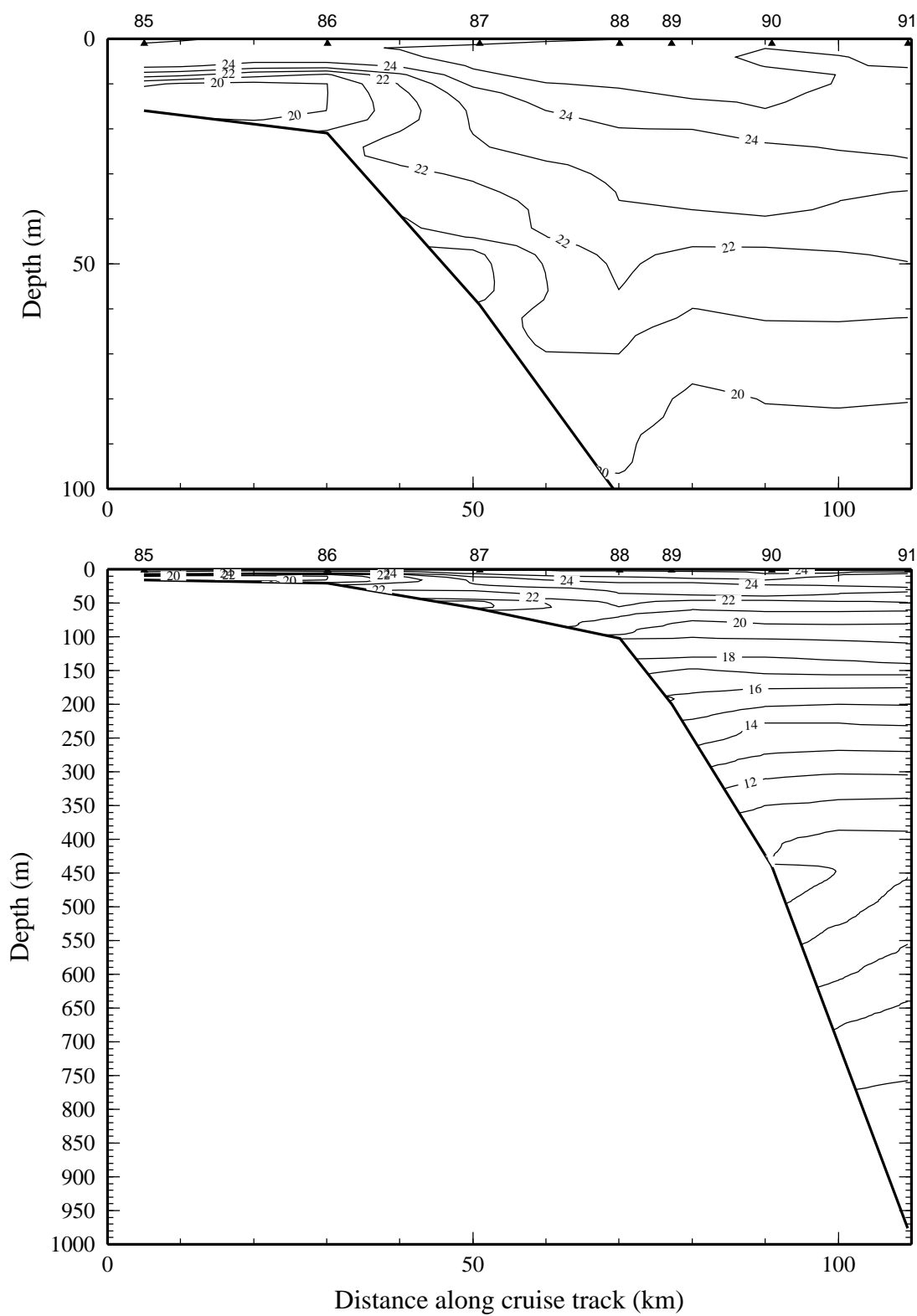


Figure 8b. Potential temperature ($^{\circ}\text{C}$) on line 2 of NEGOM cruise N2, 5-16 May 1998.

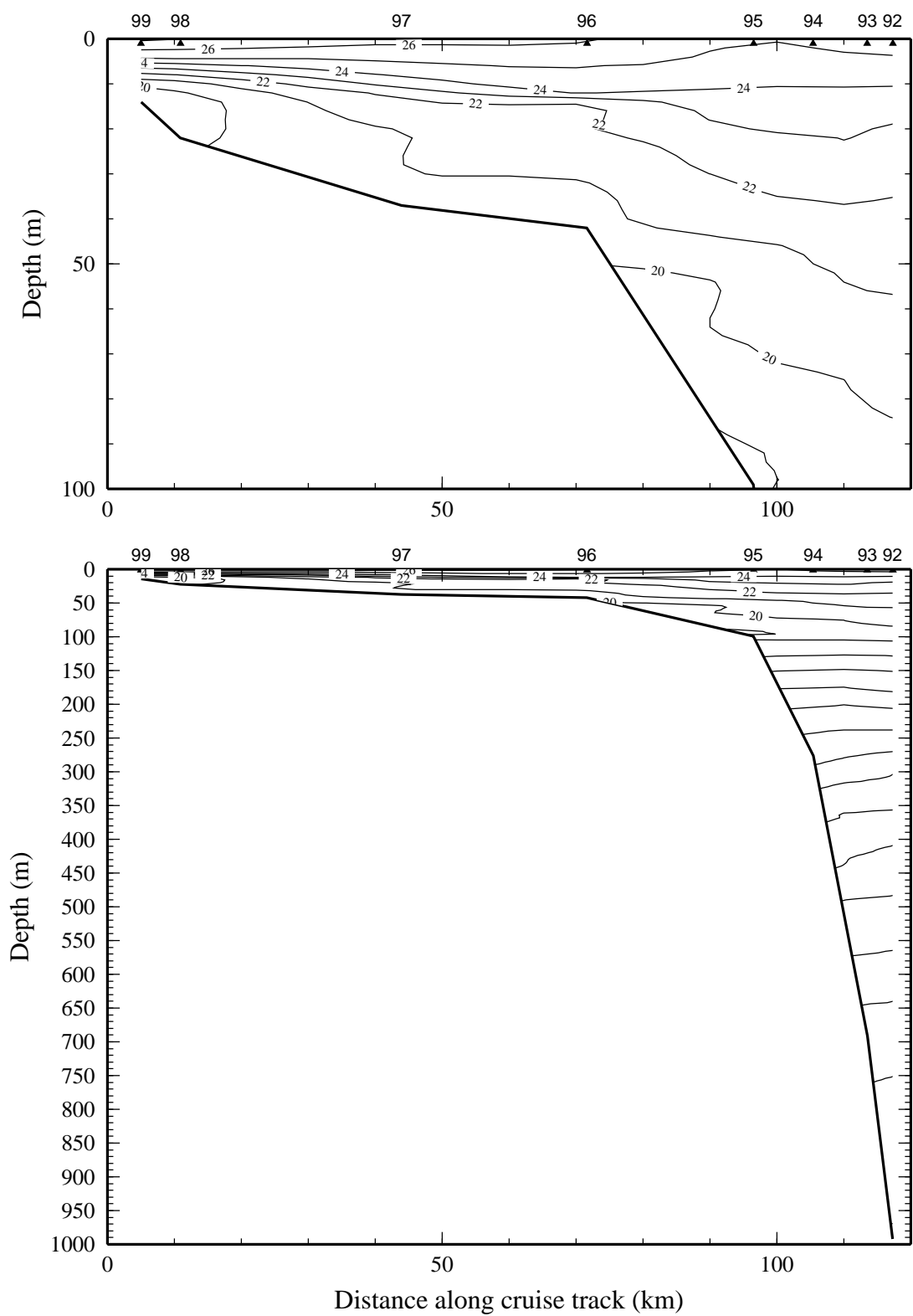


Figure 8c. Potential temperature ($^{\circ}\text{C}$) on line 3 of NEGOM cruise N2, 5-16 May 1998.

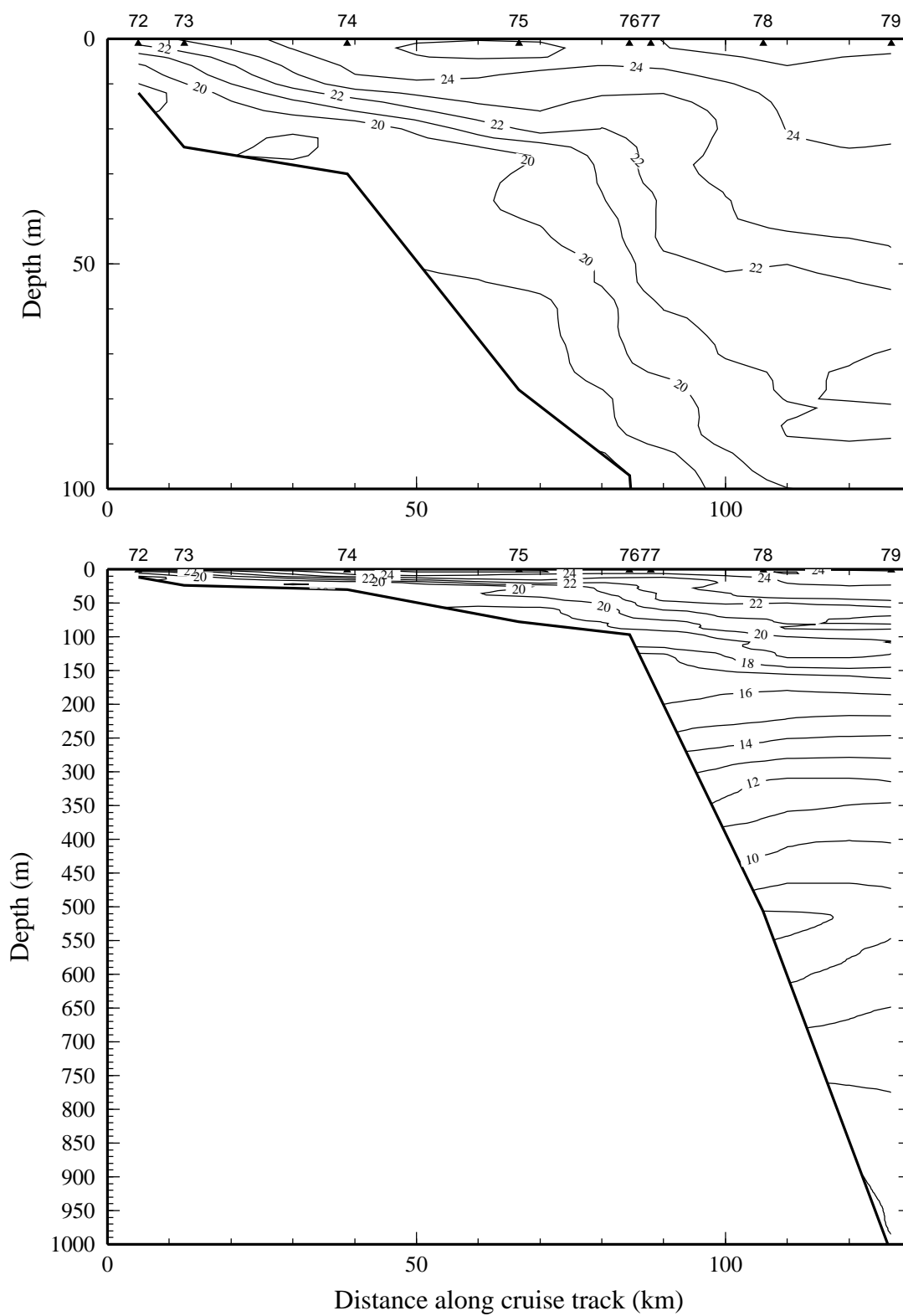


Figure 8d. Potential temperature (°C) on line 4 of NEGOM cruise N2, 5-16 May 1998.

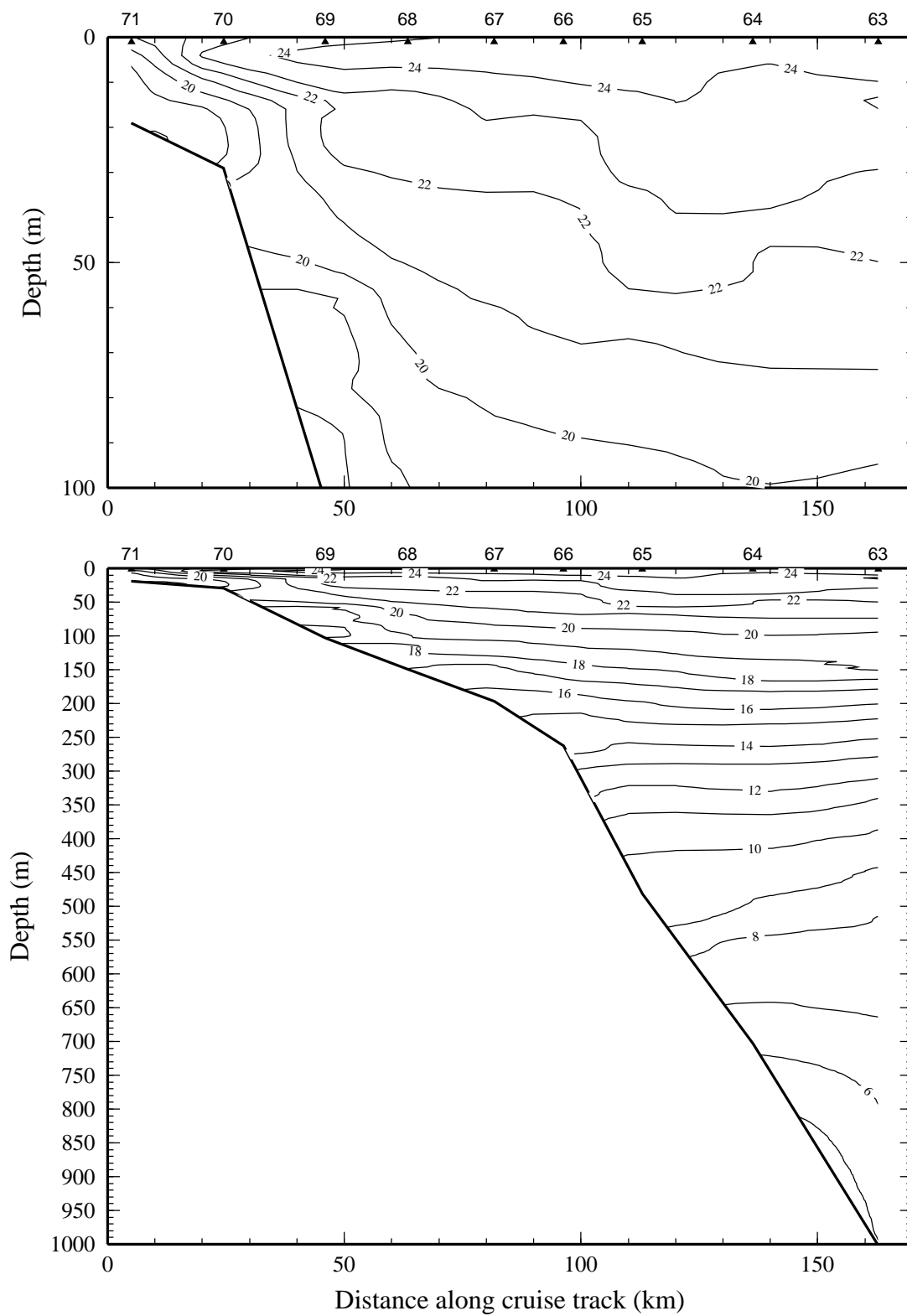


Figure 8e. Potential temperature (°C) on line 5 of NEGOM cruise N2, 5-16 May 1998.

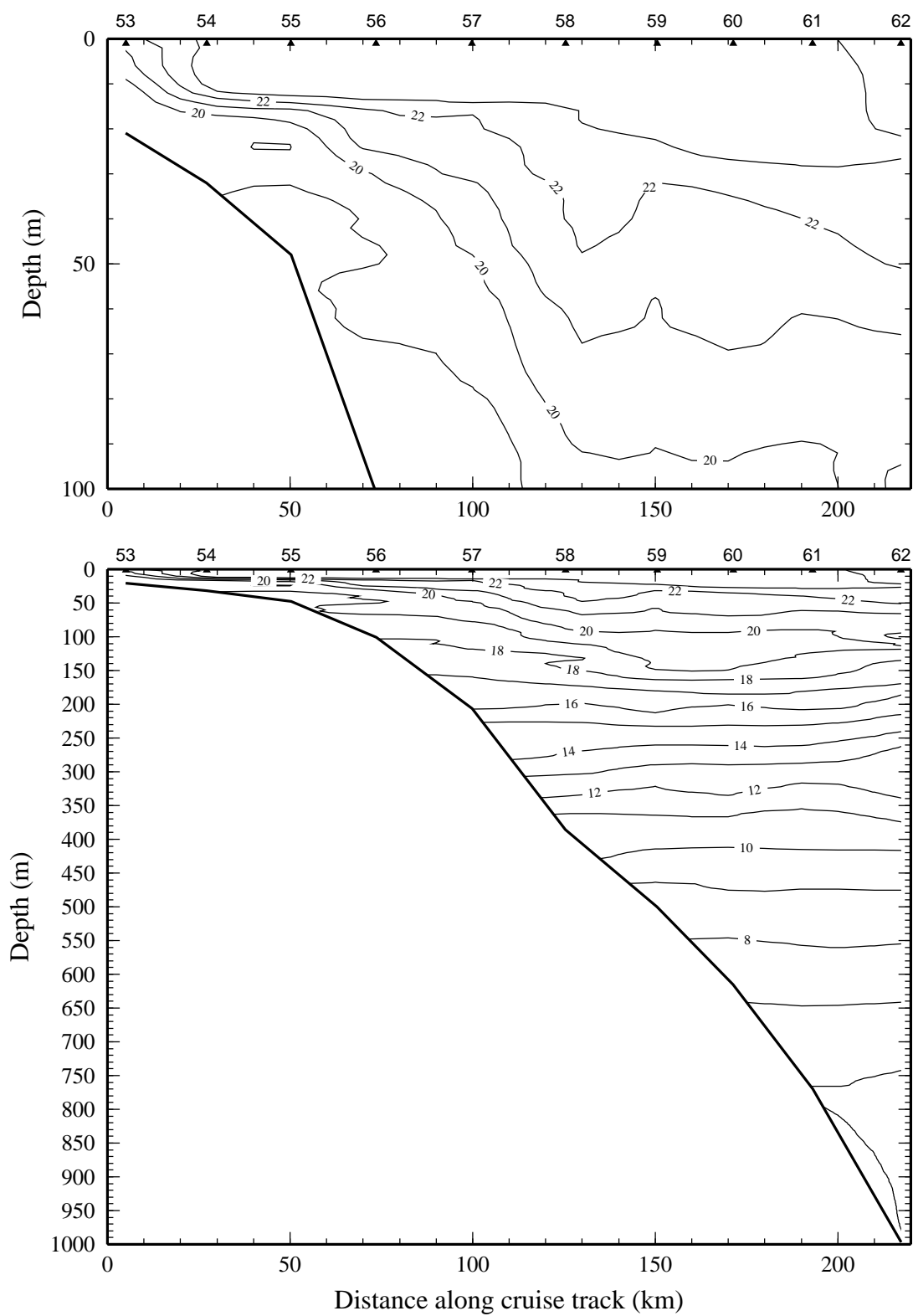


Figure 8f. Potential temperature (°C) on line 6 of NEGOM cruise N2, 5-16 May 1998.

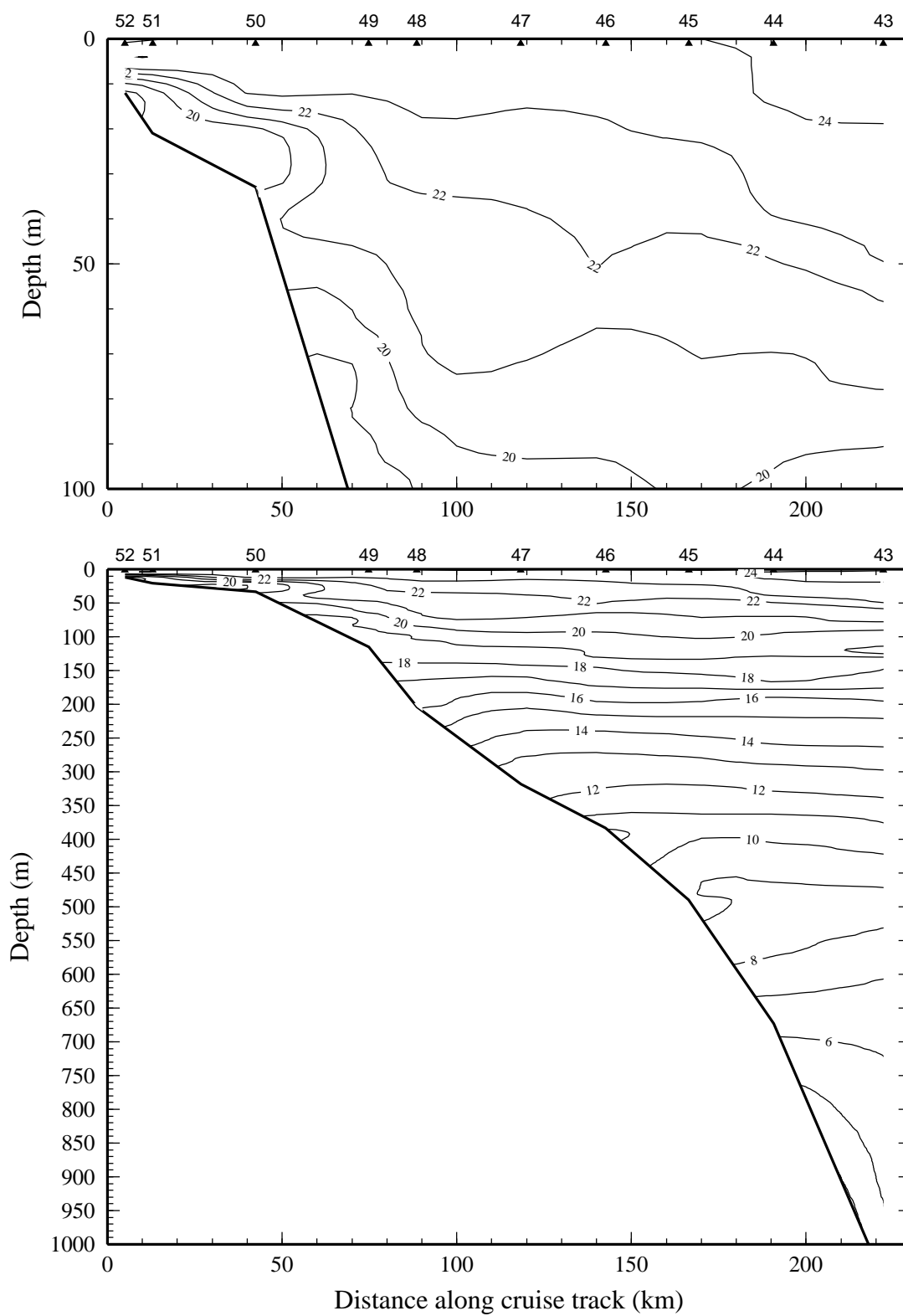


Figure 8g. Potential temperature (°C) on line 7 of NEGOM cruise N2, 5-16 May 1998.

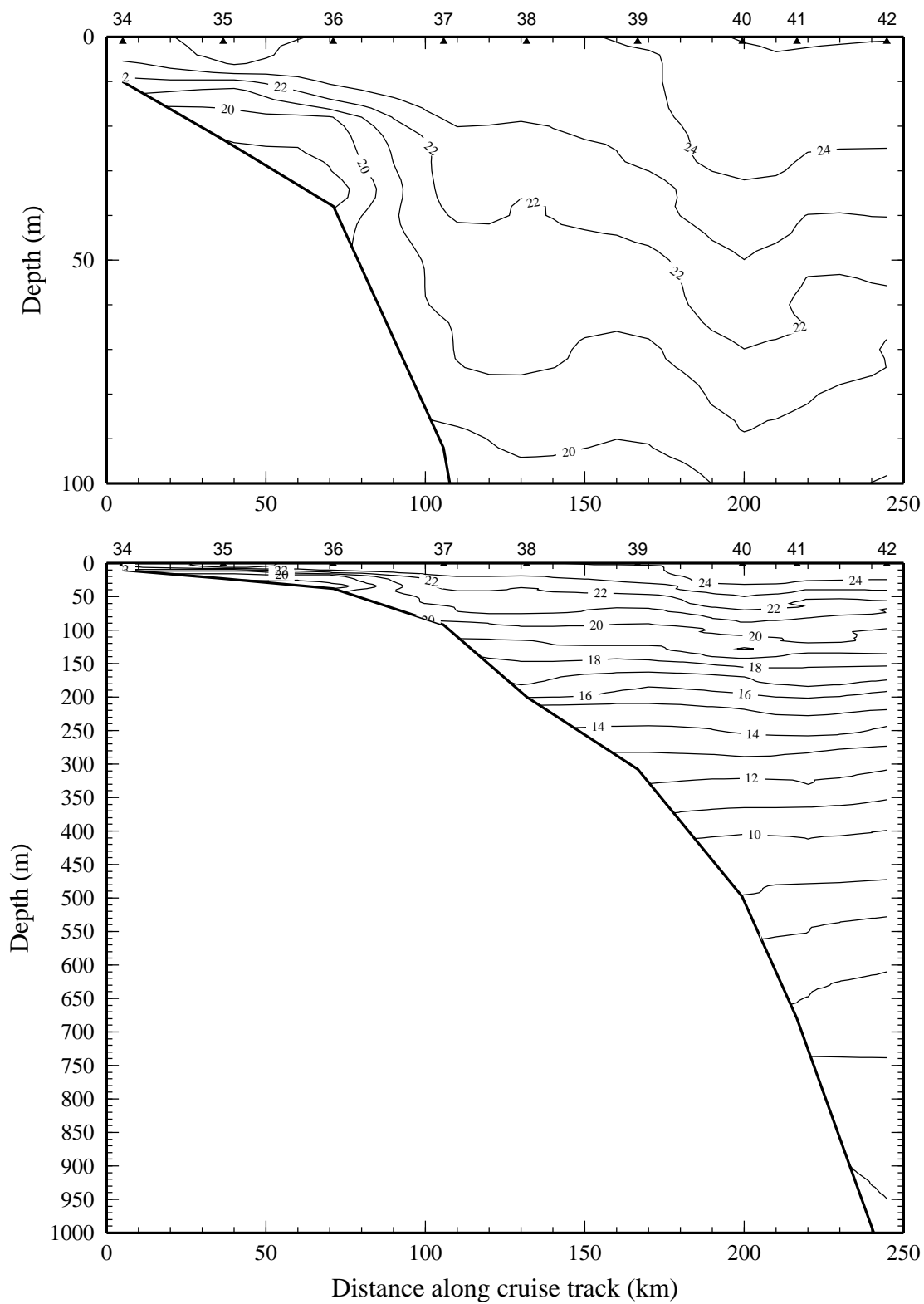


Figure 8h. Potential temperature (°C) on line 8 of NEGOM cruise N2, 5-16 May 1998.

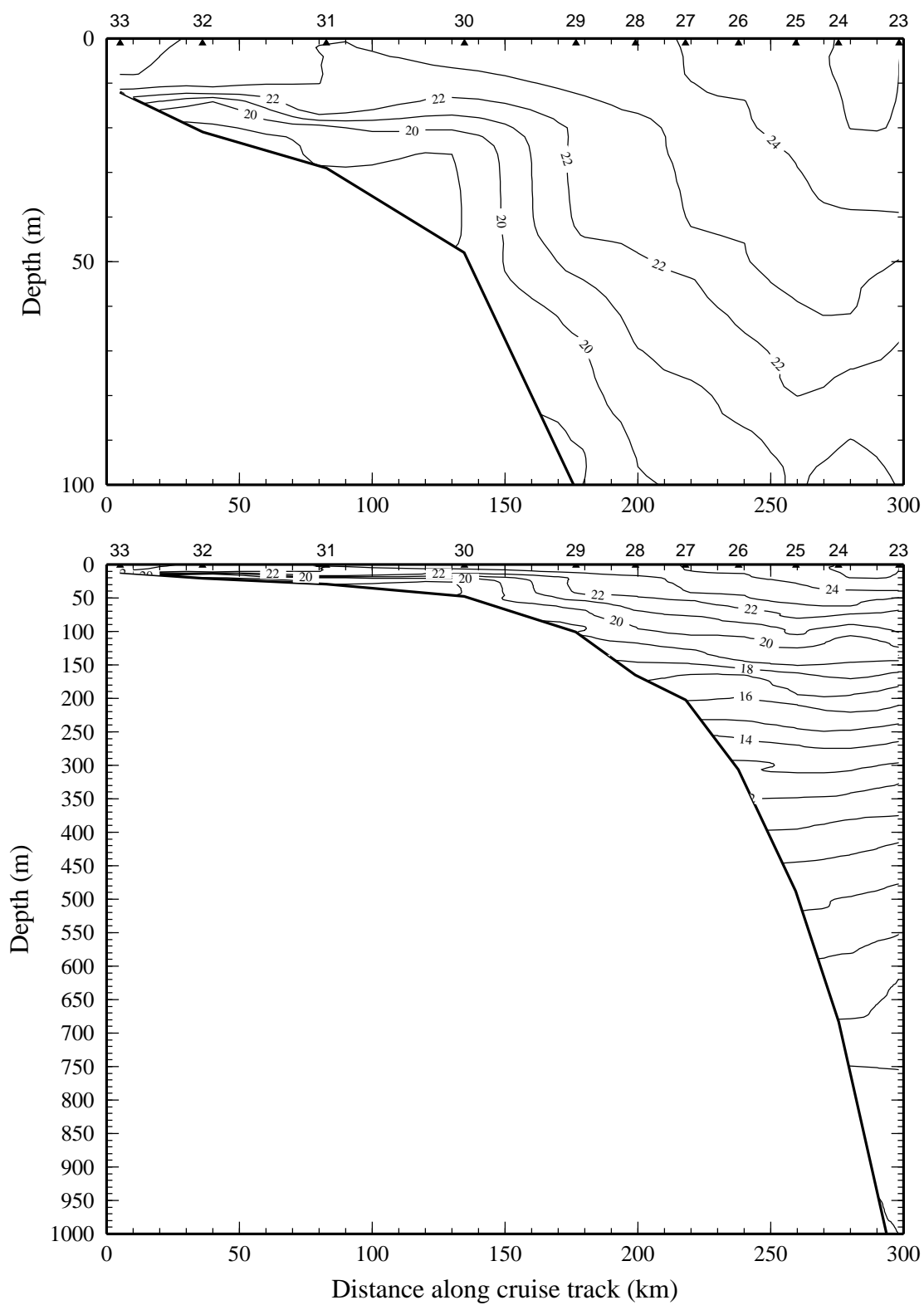


Figure 8i. Potential temperature ($^{\circ}\text{C}$) on line 9 of NEGOM cruise N2, 5-16 May 1998.

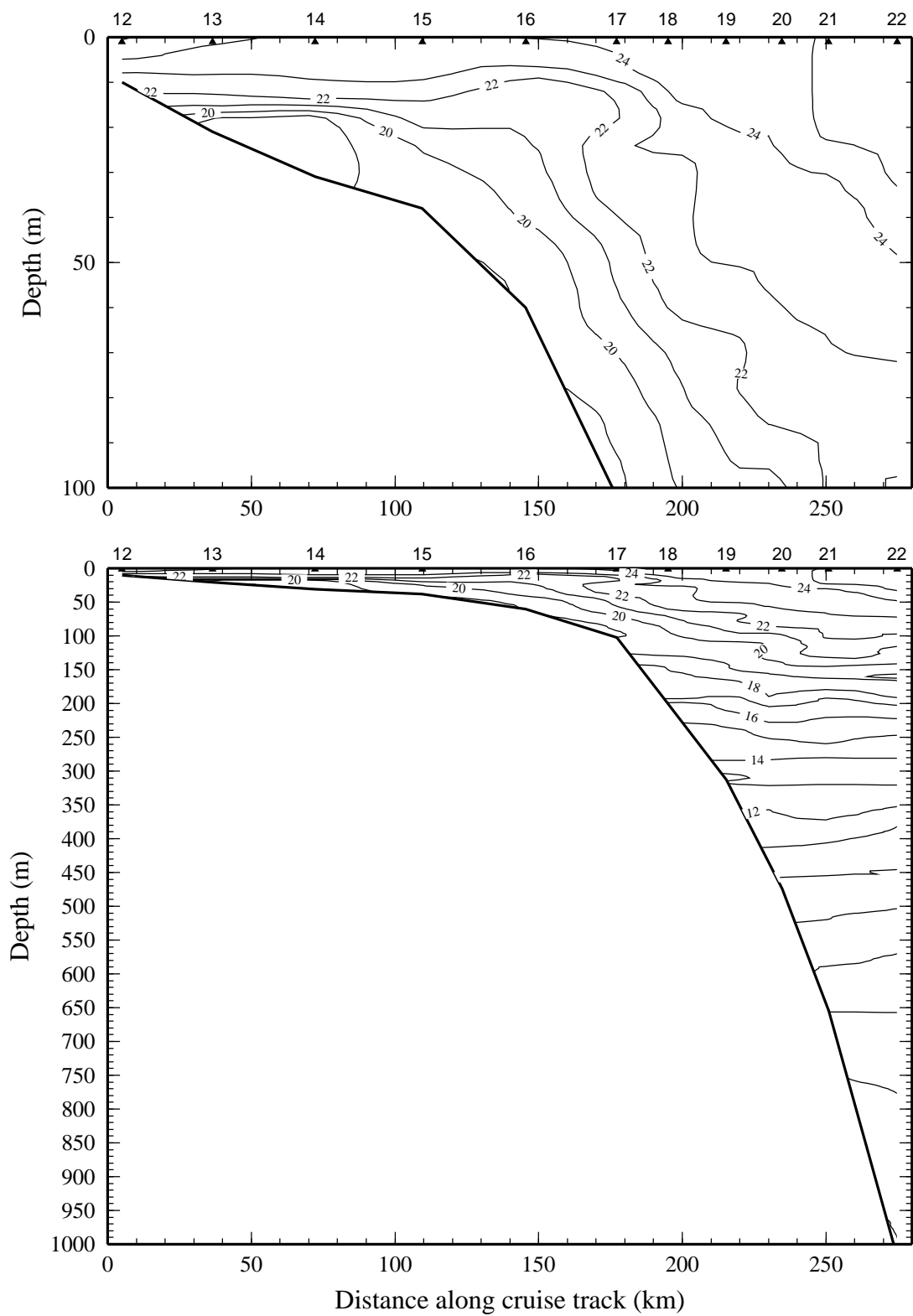


Figure 8j. Potential temperature ($^{\circ}\text{C}$) on line 10 of NEGOM cruise N2, 5-16 May 1998.

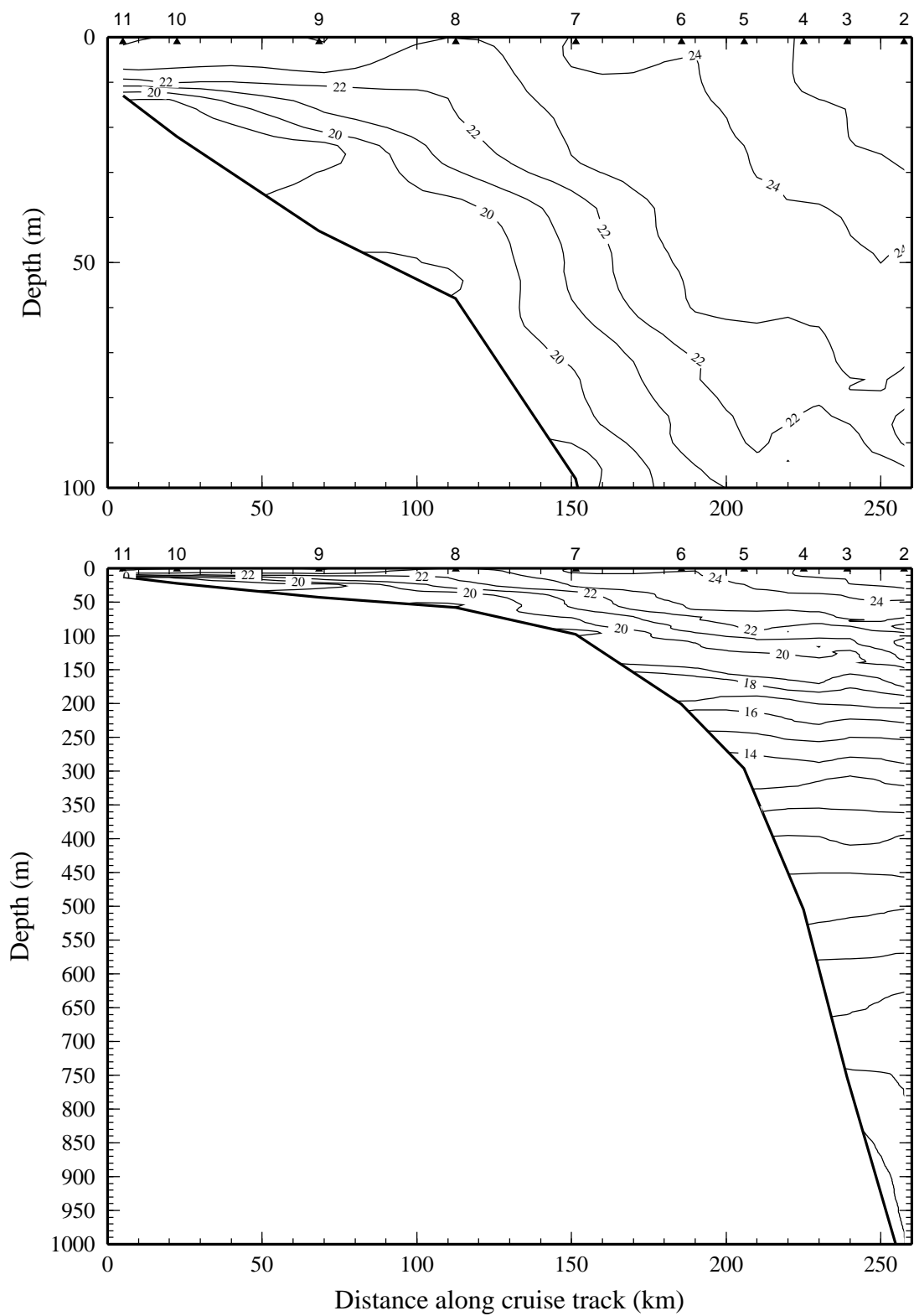


Figure 8k. Potential temperature (°C) on line 11 of NEGOM cruise N2, 5-16 May 1998.

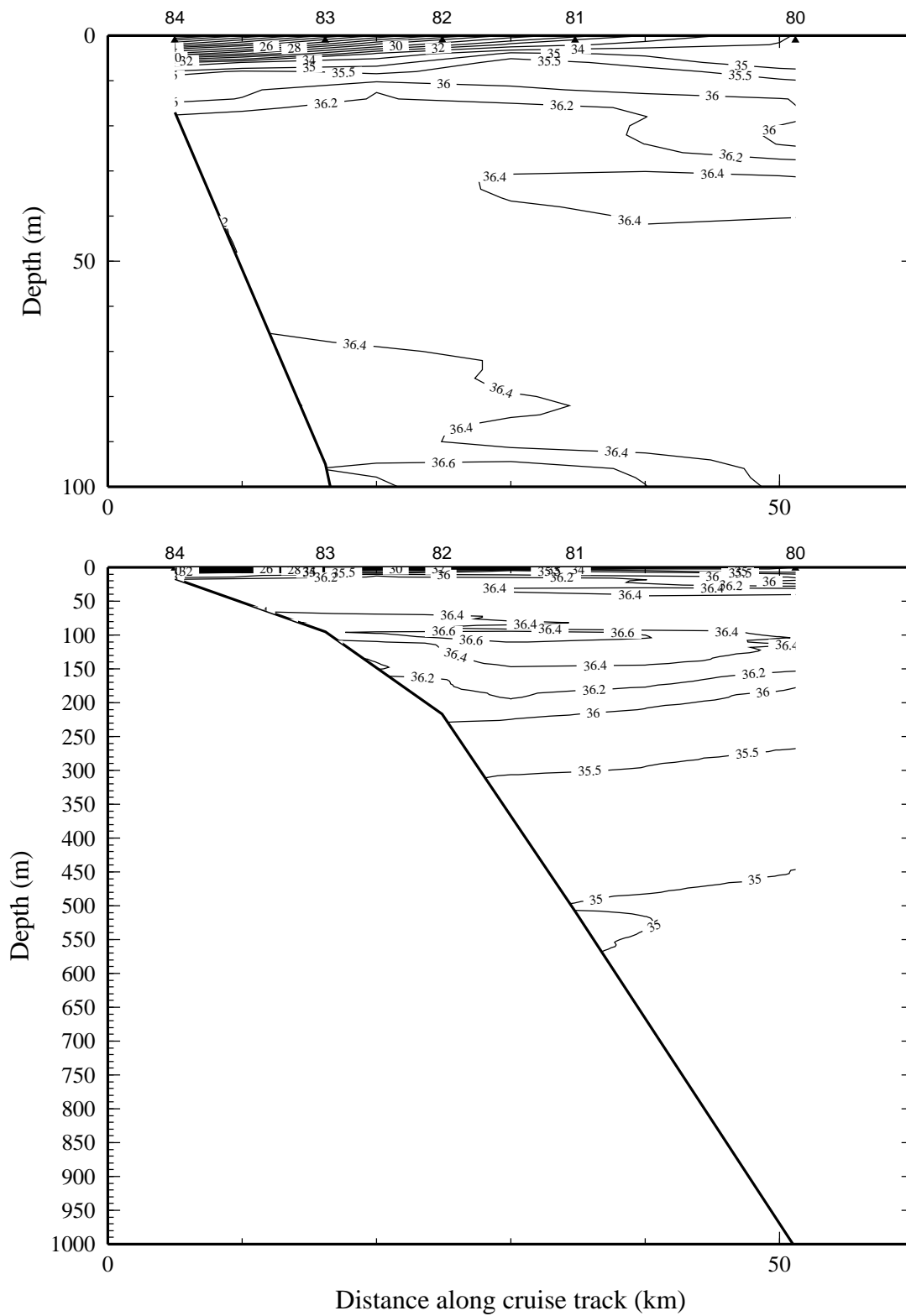


Figure 9a. Salinity, derived from CTD data, on line 1 of NEGOM cruise N2, 5-16 May 1998.

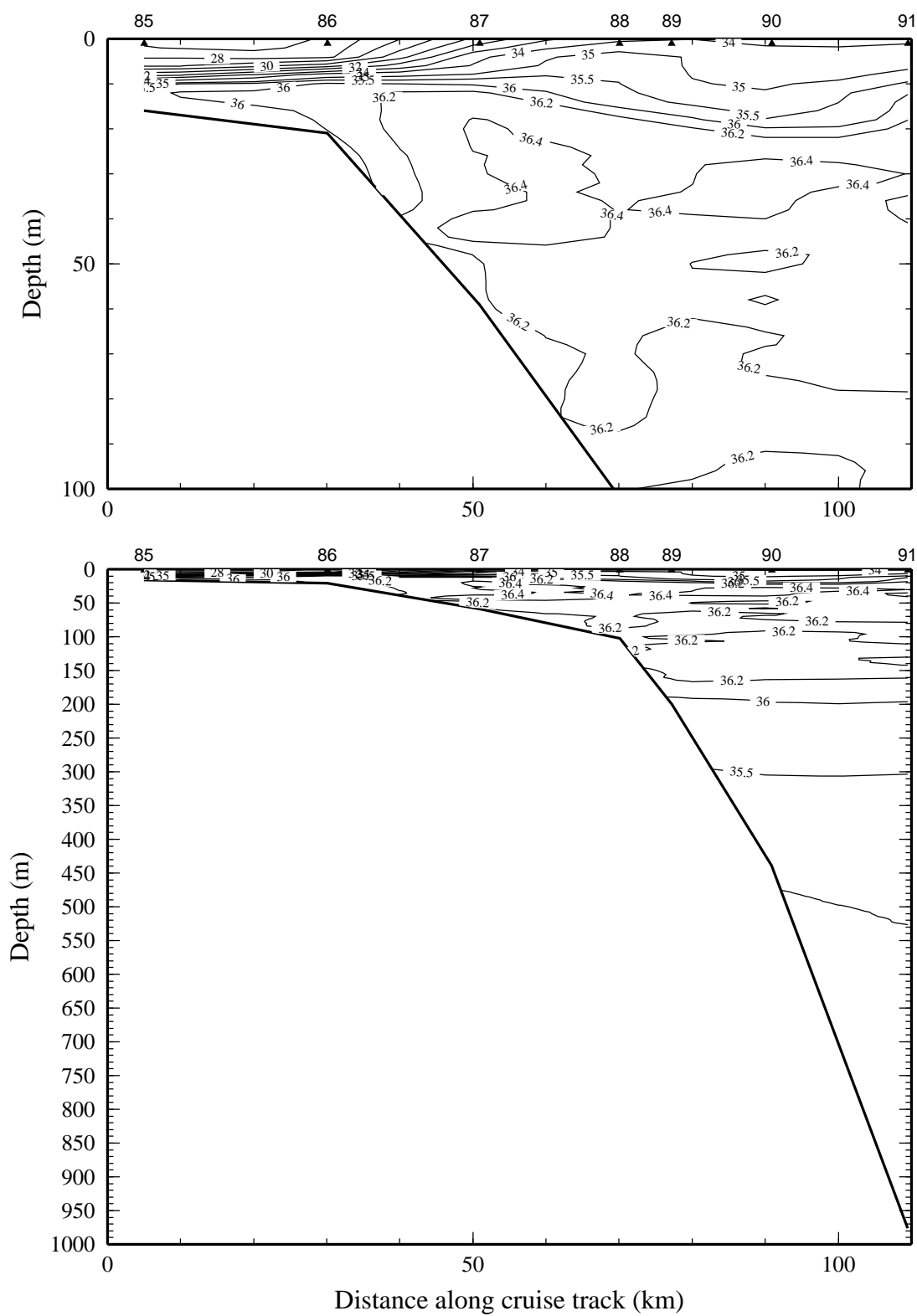


Figure 9b. Salinity, derived from CTD data, on line 2 of NEGOM cruise N2, 5-16 May 1998.

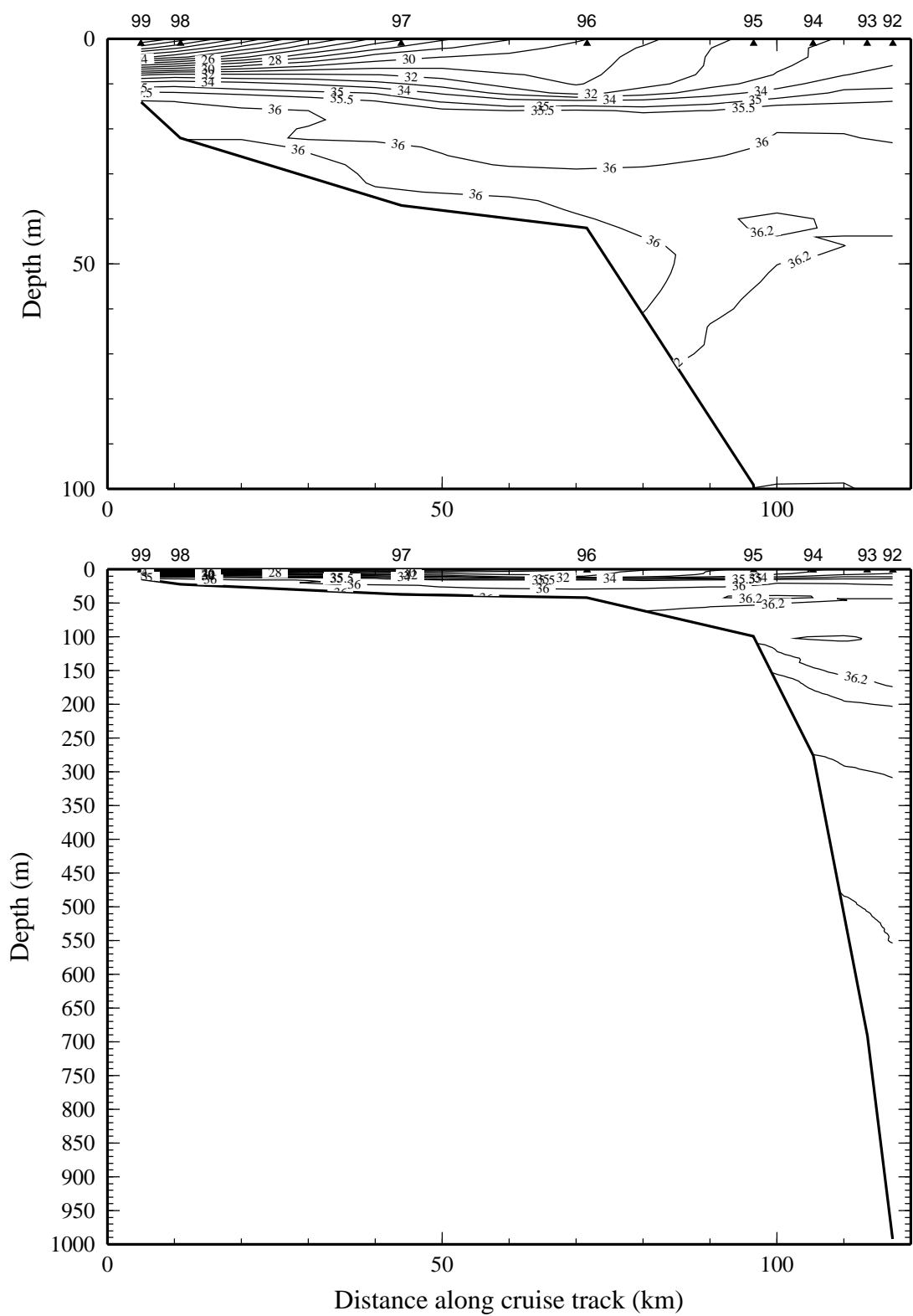


Figure 9c. Salinity, derived from CTD data, on line 3 of NEGOM cruise N2, 5-16 May 1998.

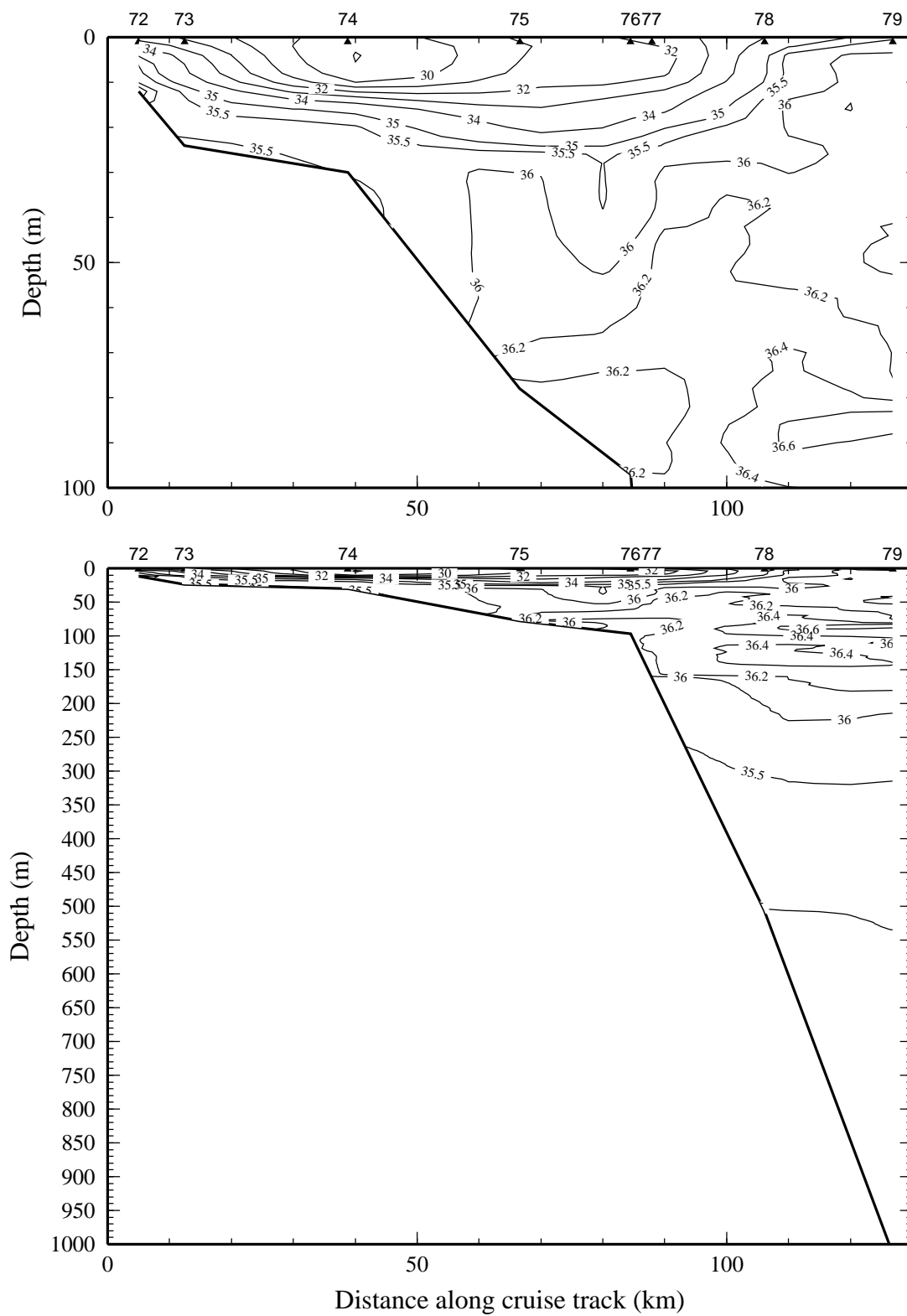


Figure 9d. Salinity, derived from CTD data, on line 4 of NEGOM cruise N2, 5-16 May 1998.

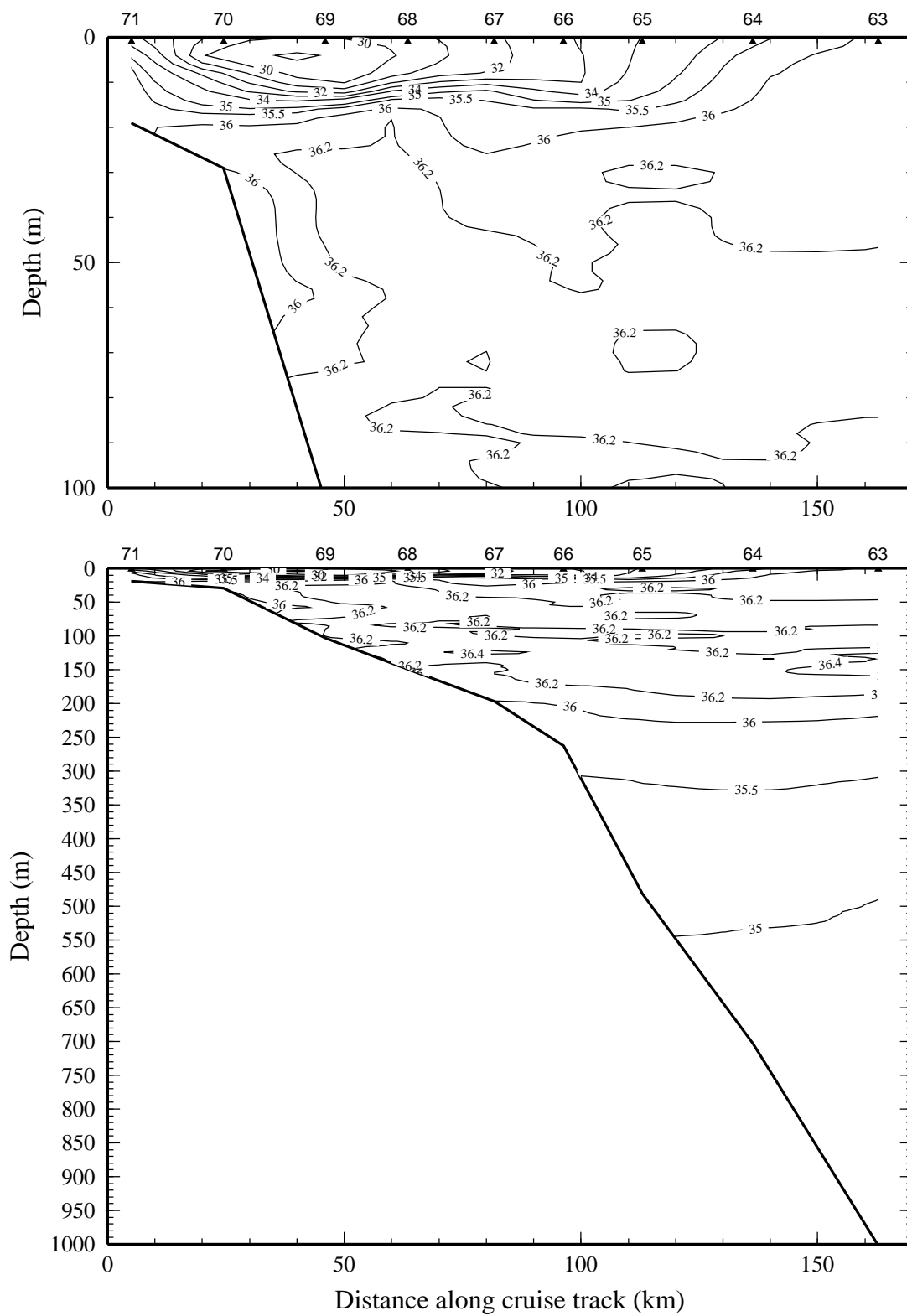


Figure 9e. Salinity, derived from CTD data, on line 5 of NEGOM cruise N2, 5-16 May 1998.

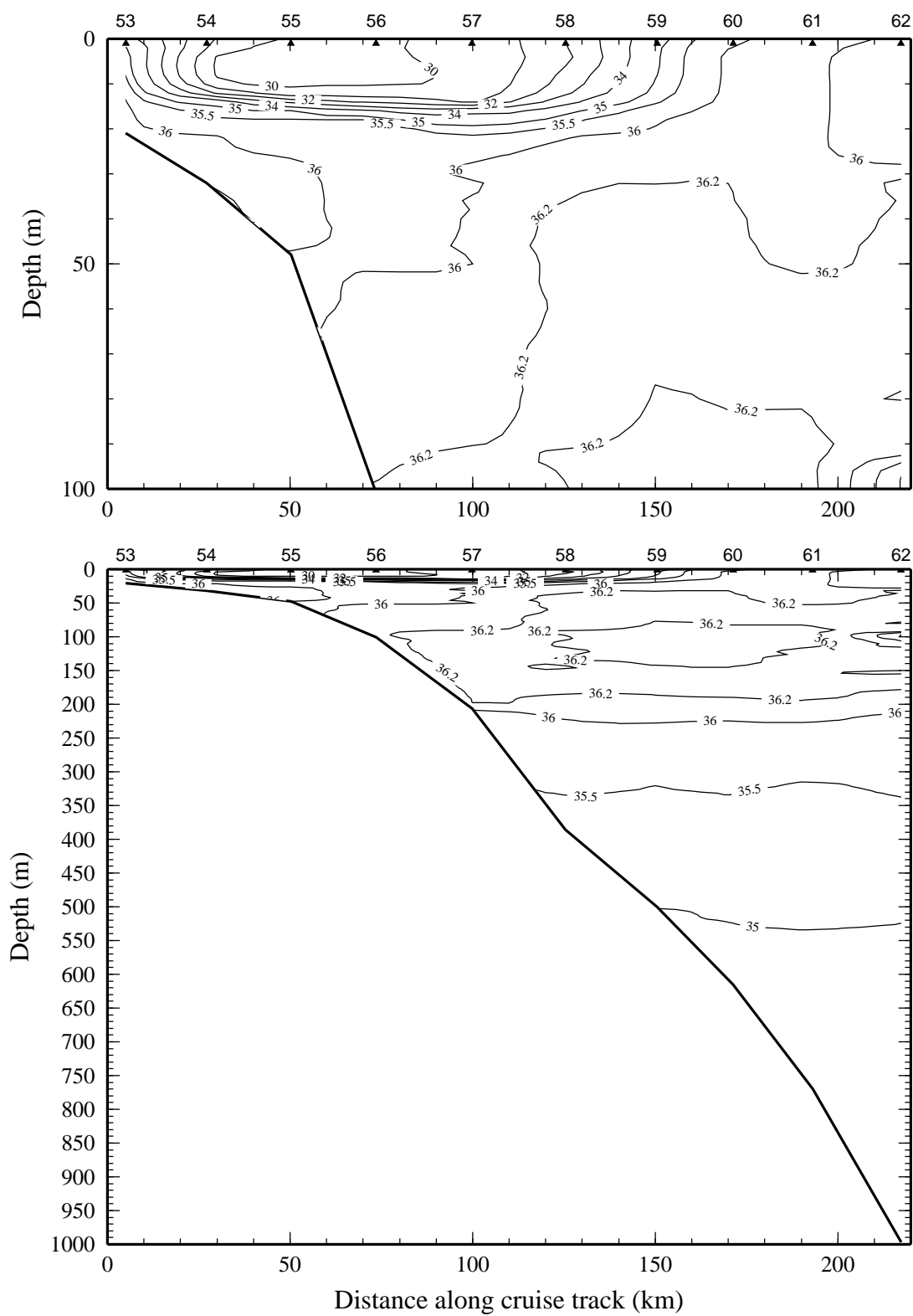


Figure 9f. Salinity, derived from CTD data, on line 6 of NEGOM cruise N2, 5-16 May 1998.

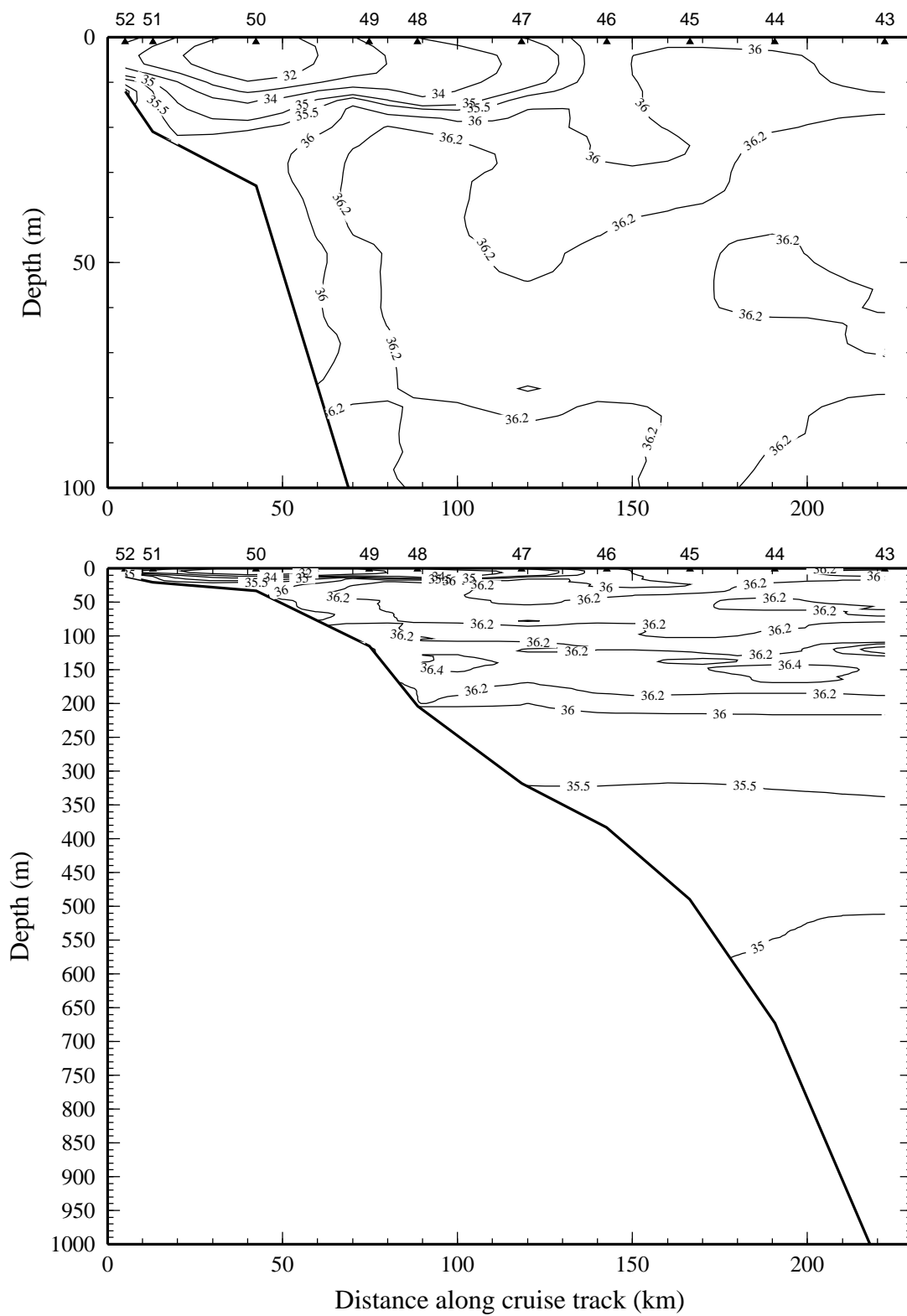


Figure 9g. Salinity, derived from CTD data, on line 7 of NEGOM cruise N2, 5-16 May 1998.

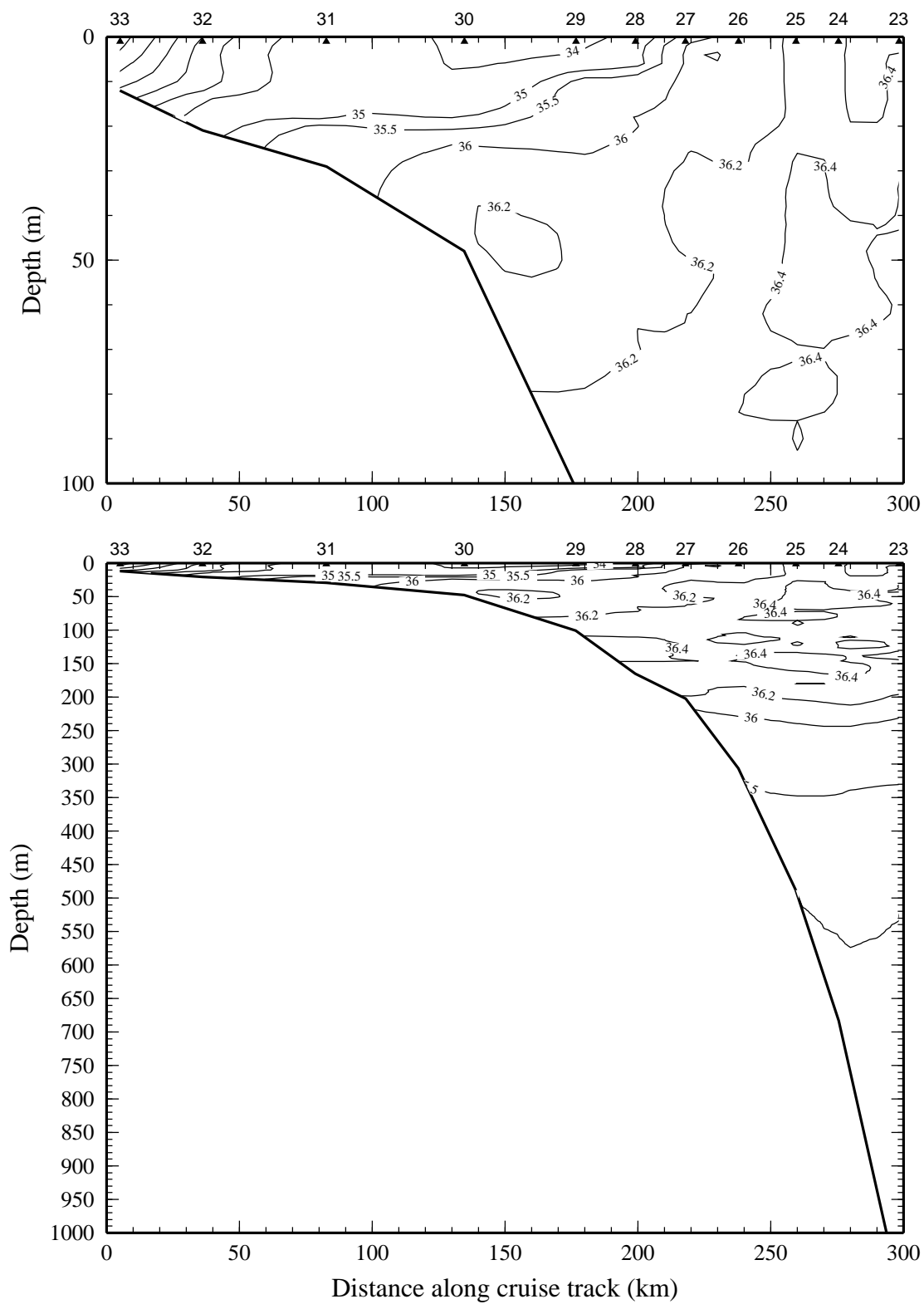


Figure 9h. Salinity, derived from CTD data, on line 9 of NEGOM cruise N2, 5-16 May 1998.

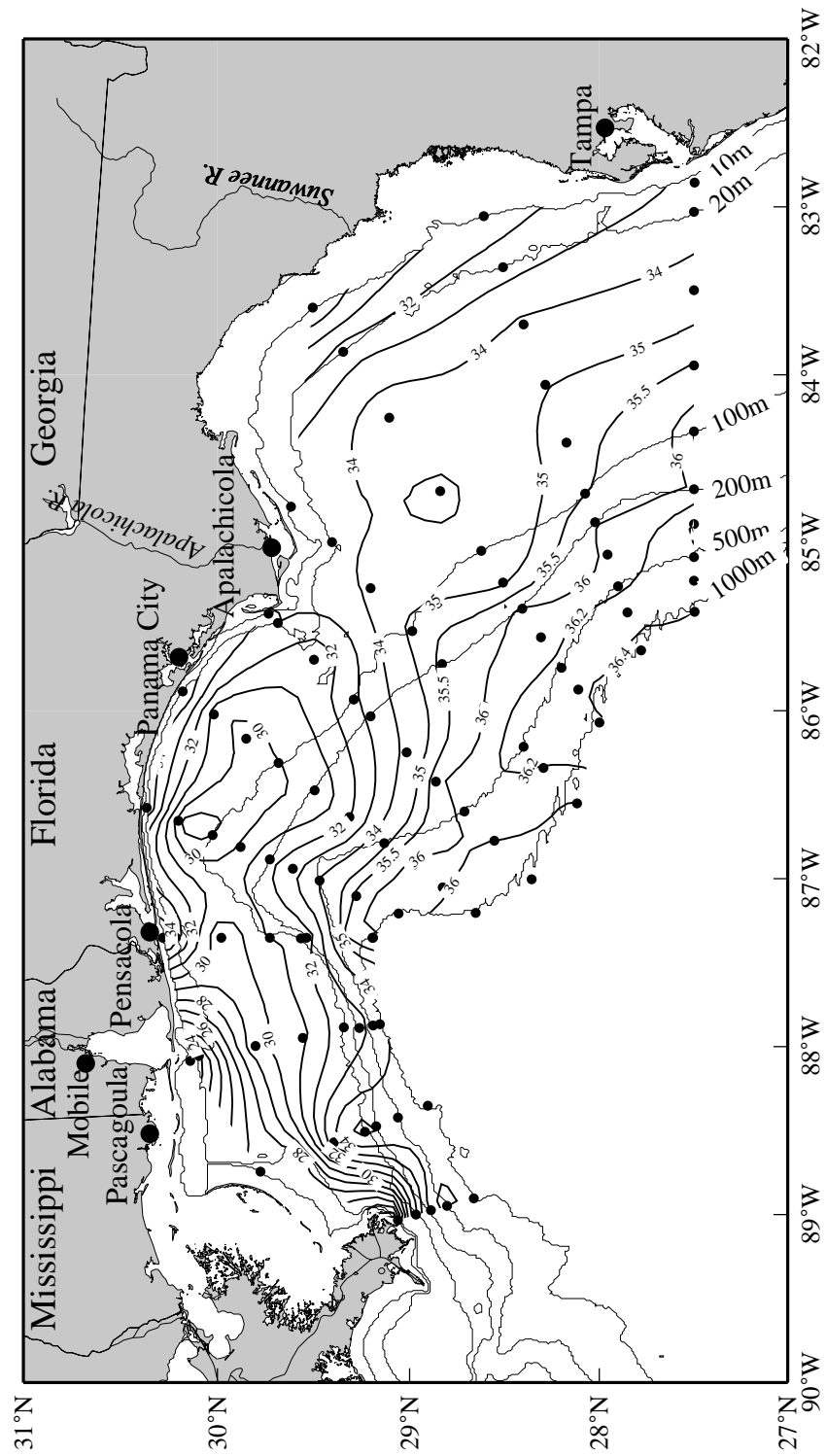


Figure 10. Salinity, derived from CTD data, at 3.5 m on NEGOM Cruise N2, 5-16 May 1998.

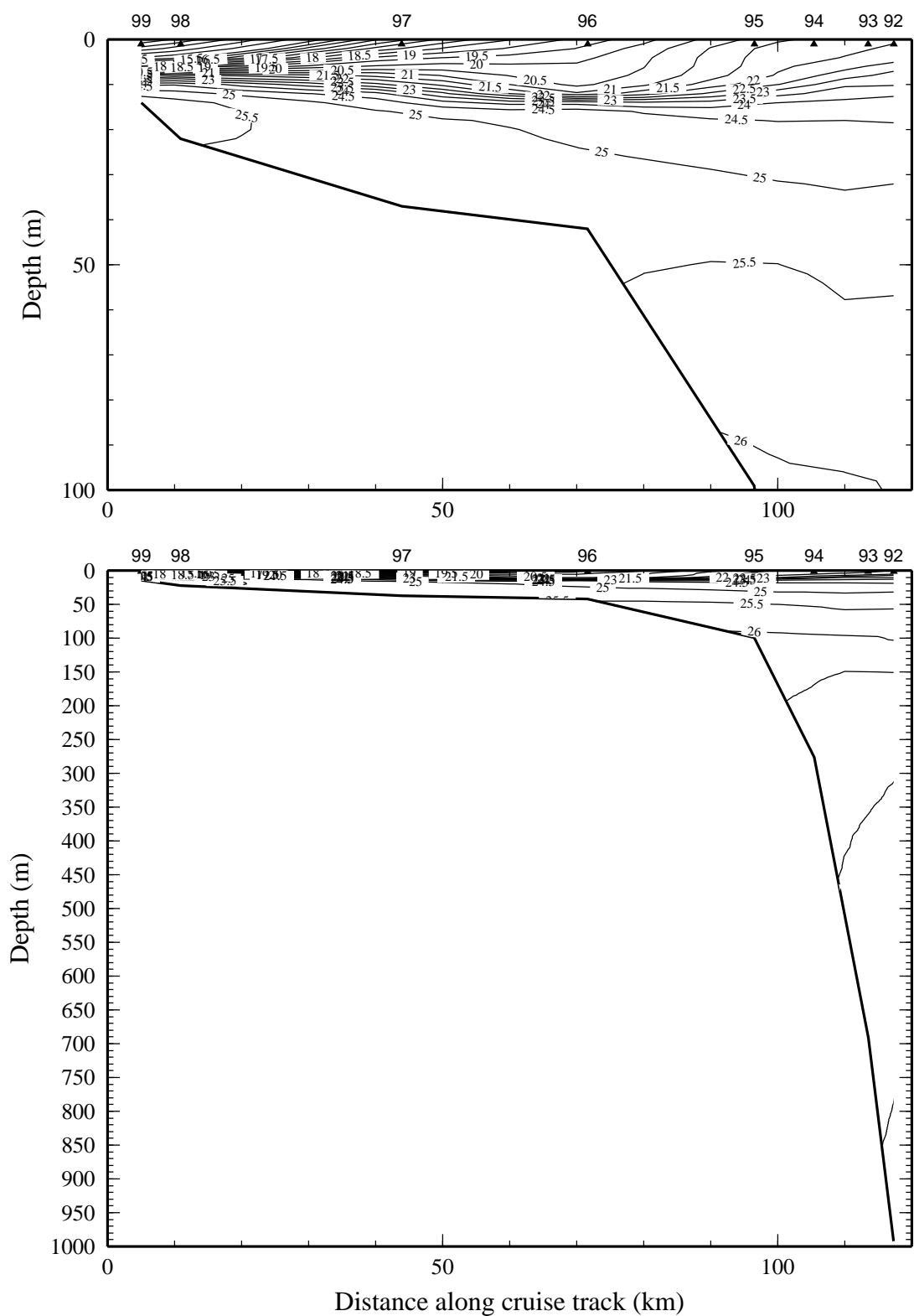


Figure 11a. Density anomaly (σ_t in $\text{kg}\cdot\text{m}^{-3}$) on line 3 of NEGOM cruise N2, 5-16 May 1998.

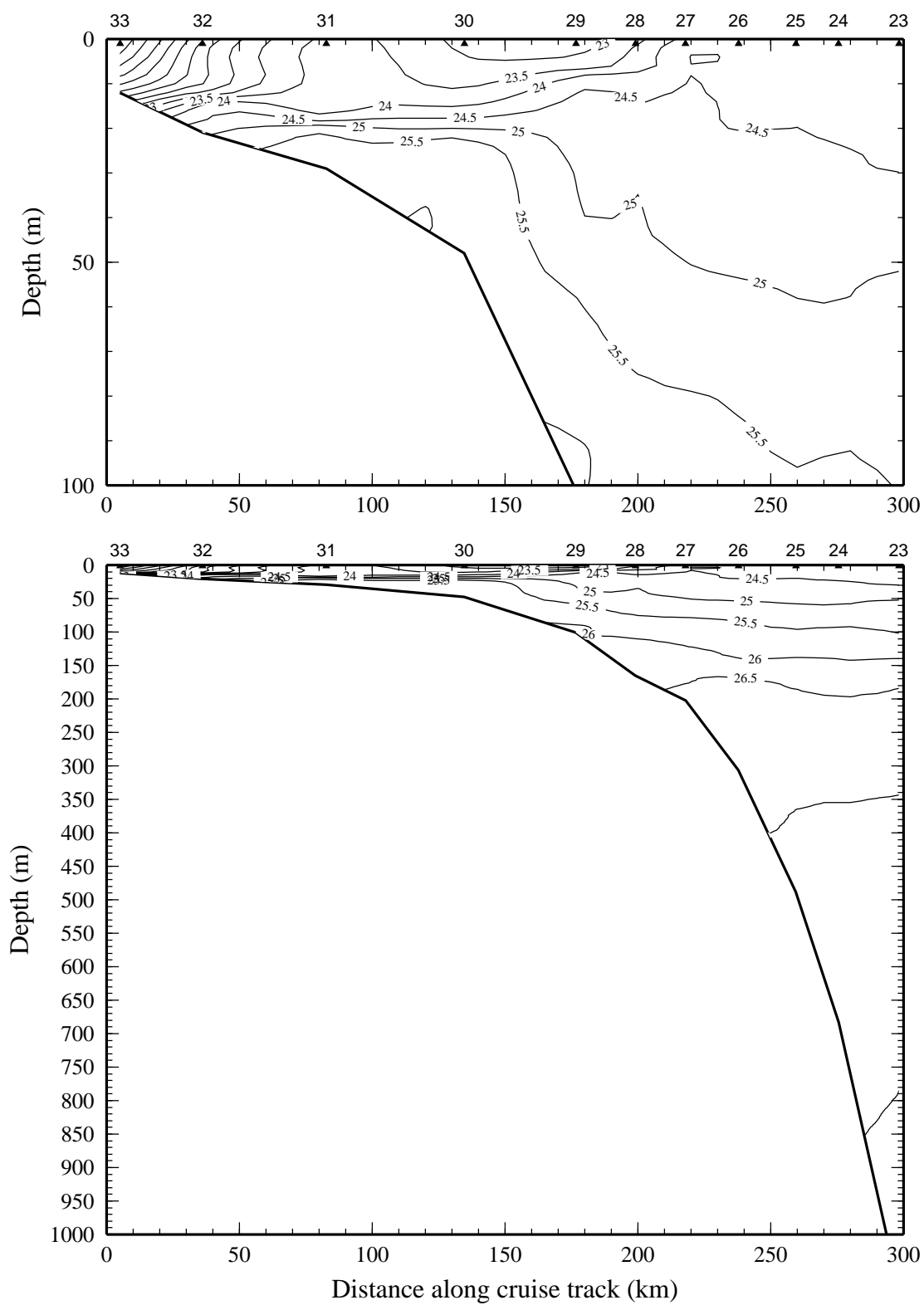


Figure 11b. Density anomaly (σ_t in $\text{kg}\cdot\text{m}^{-3}$) on line 9 of NEGOM cruise N2, 5-16 May 1998.

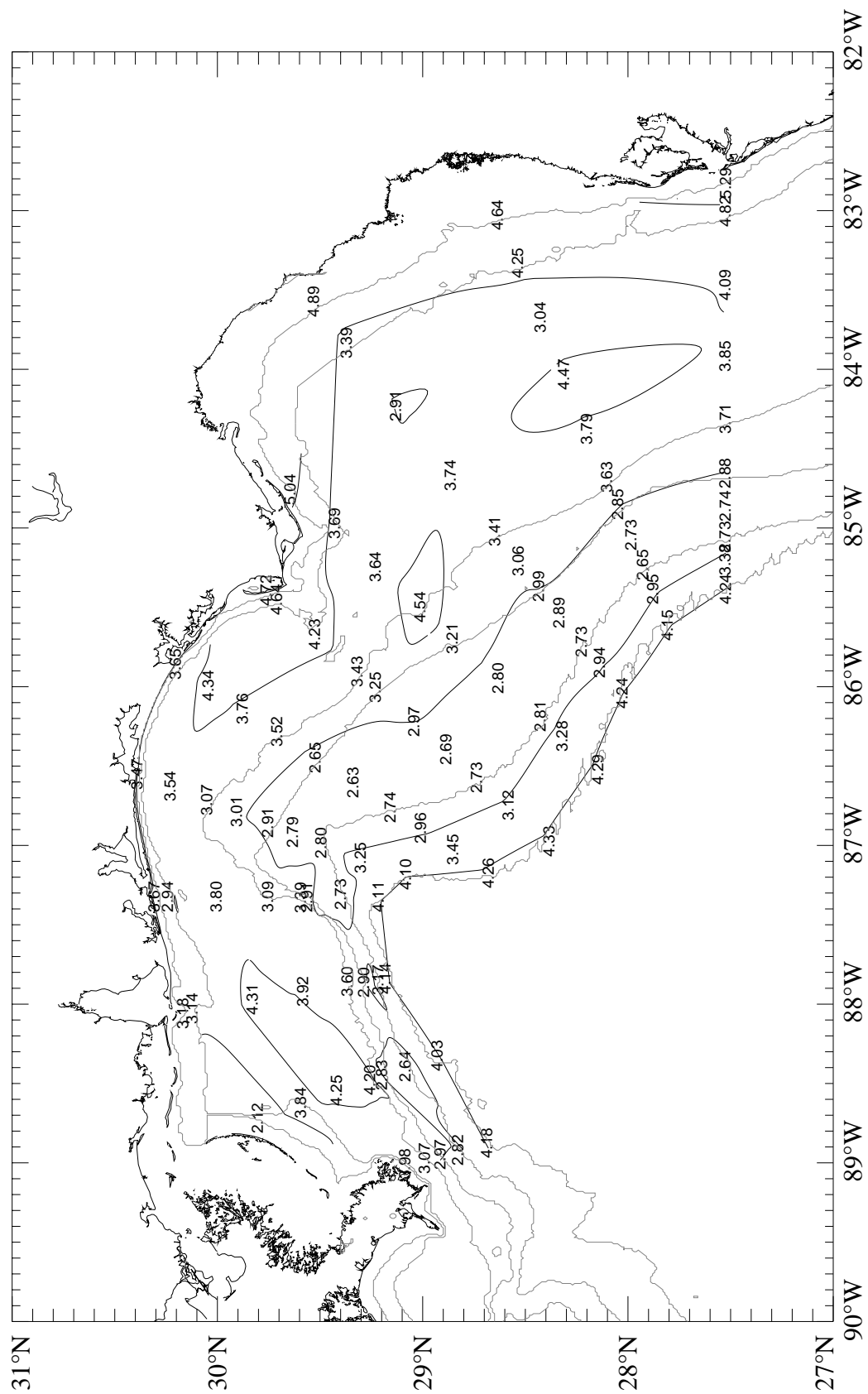


Figure 12. Dissolved oxygen (ml·l⁻¹) near bottom on NEGO Cruise N2, 5-16 May 1998.

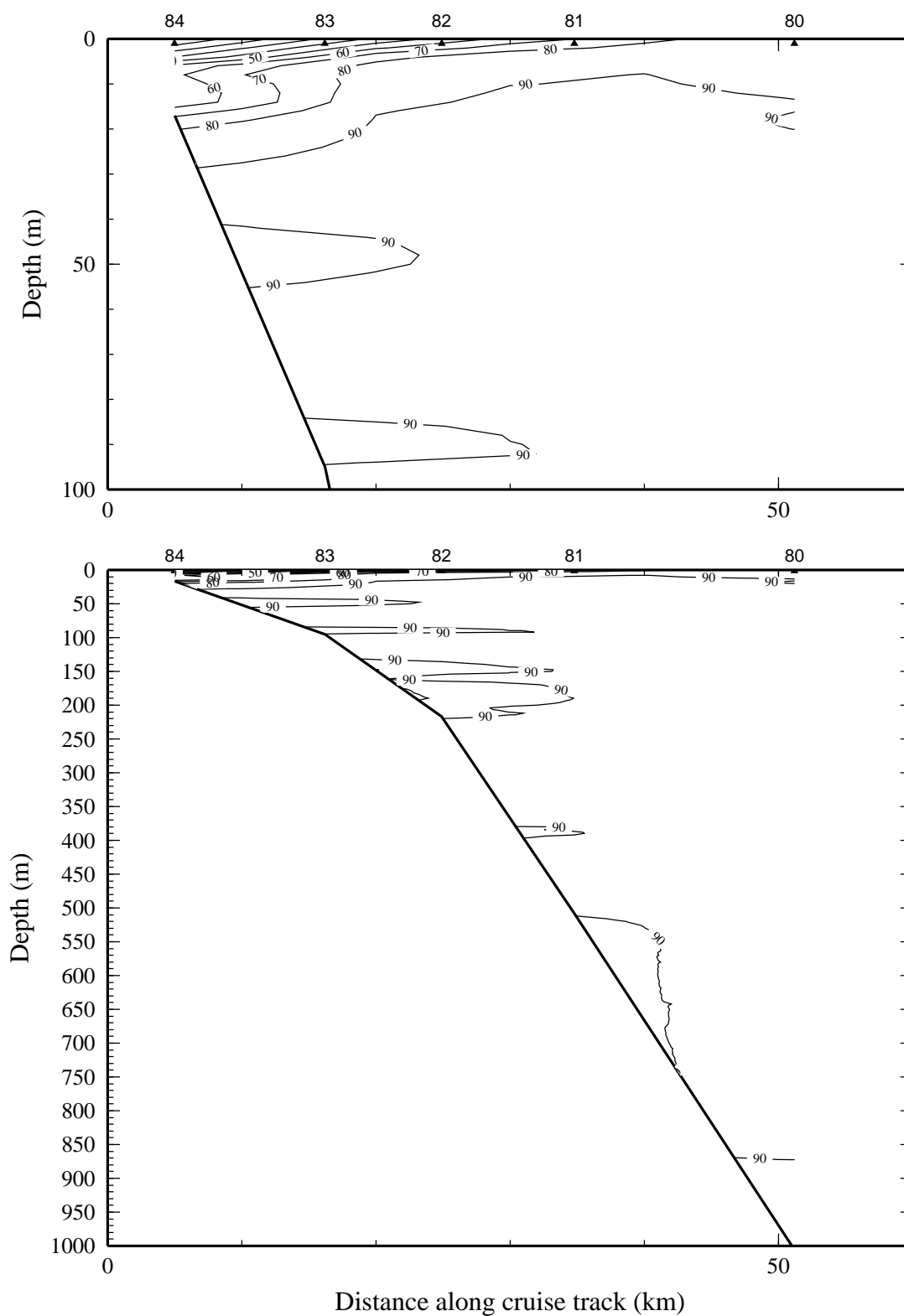


Figure 13a. Percent transmission (660 nm wave length; 25-cm path length) on line 1 of NEGOM cruise N2, 5-16 May 1998.

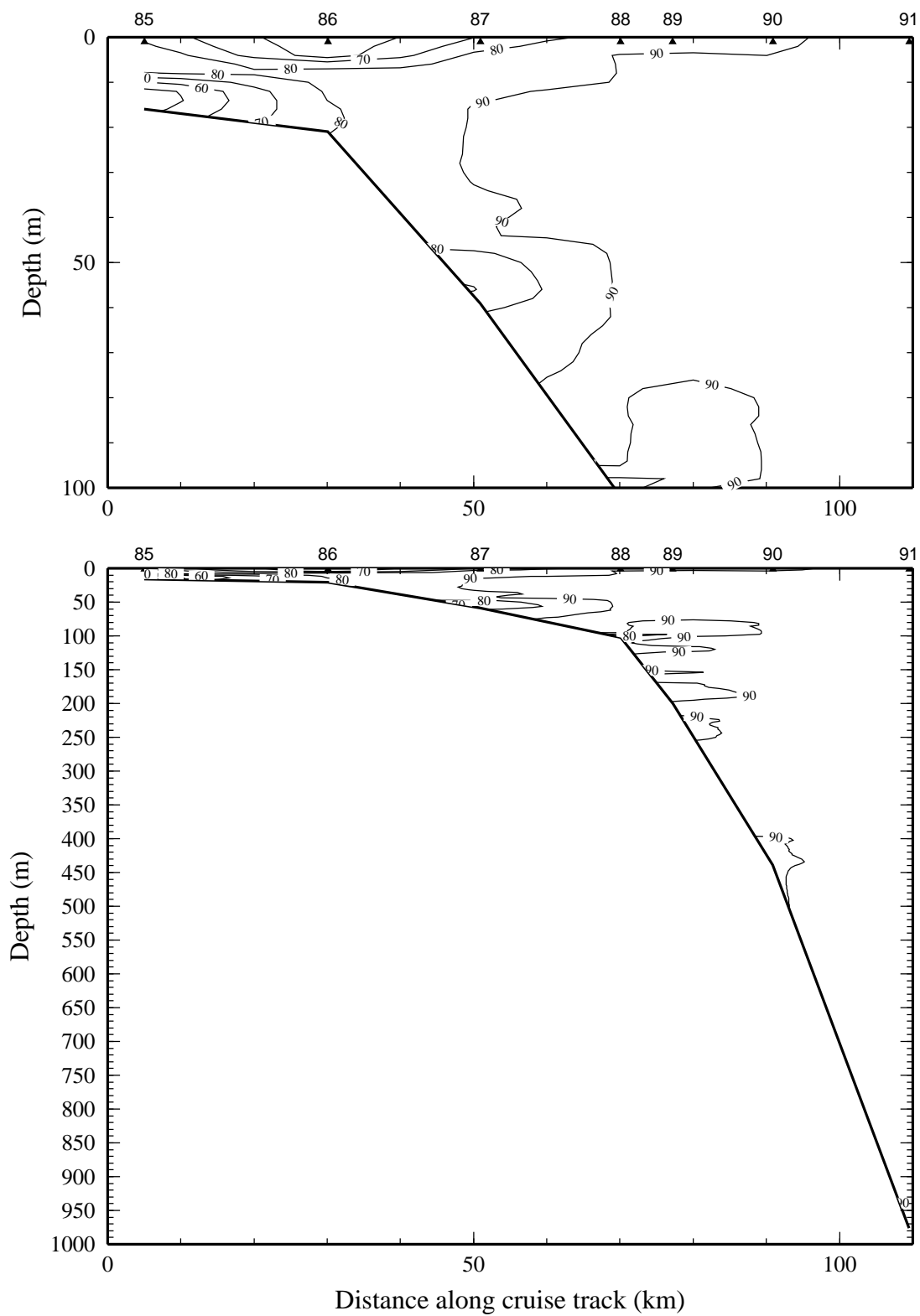


Figure 13b. Percent transmission (660 nm wave length; 25-cm path length) on line 2 of NEGOM cruise N2, 5-16 May 1998.

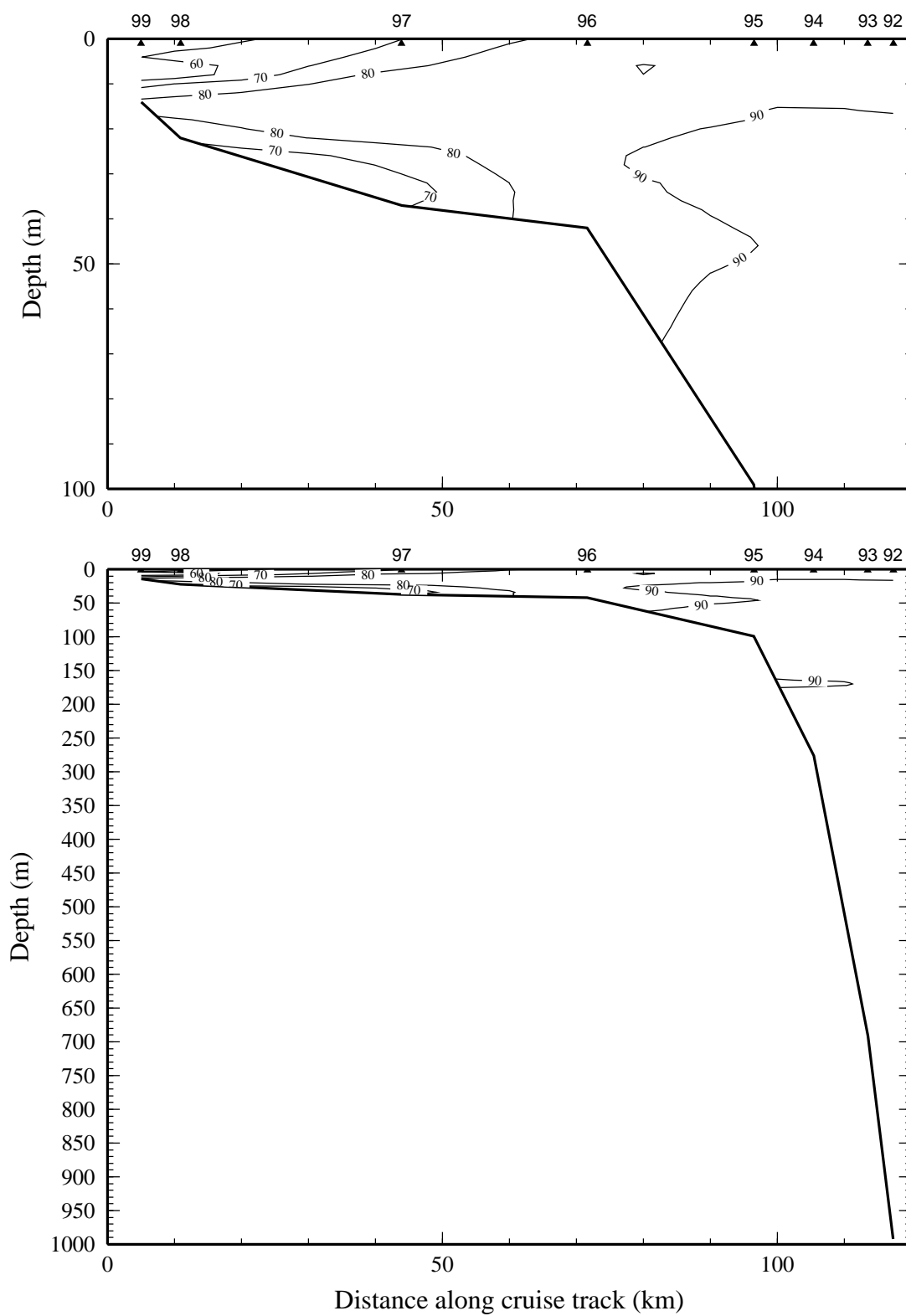


Figure 13c. Percent transmission (660 nm wave length; 25-cm path length) on line of NEGOM cruise N2, 5-16 May 1998.

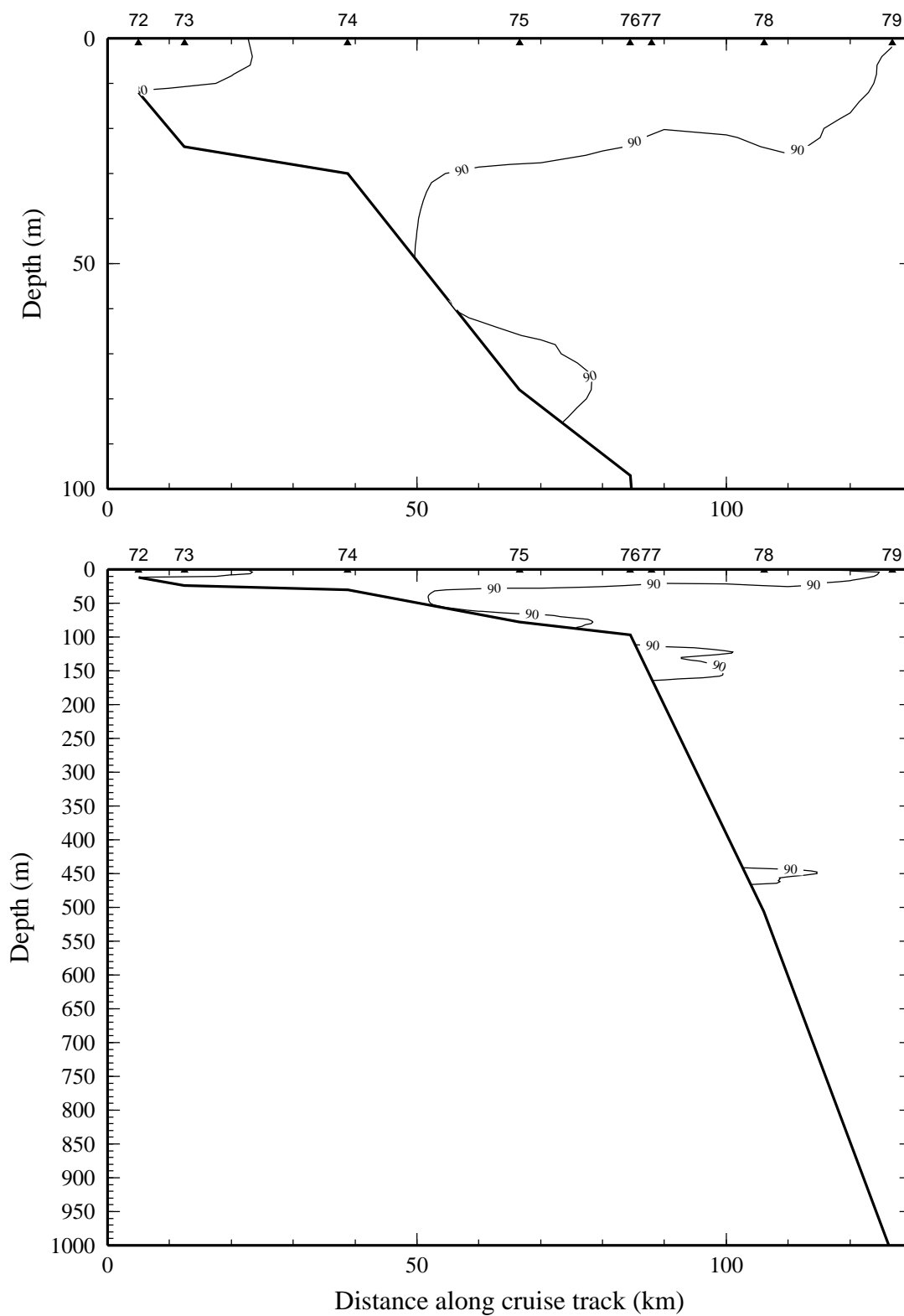


Figure 13d. Percent transmission (660 nm wave length; 25-cm path length) on line 4 of NEGOM cruise N2, 5-16 May 1998.

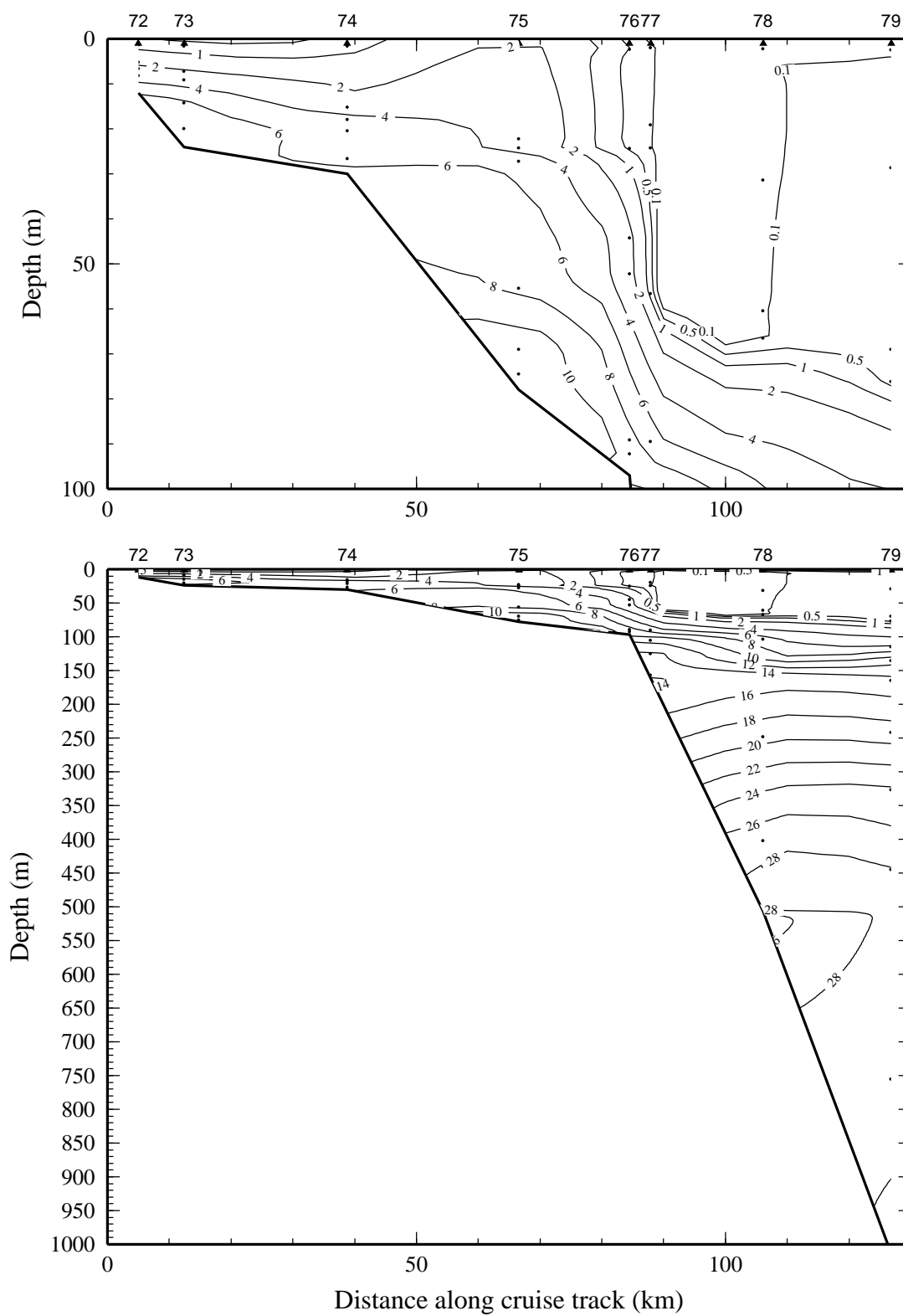


Figure 14. Nitrate ($\mu\text{mol}\cdot\text{l}^{-1}$) on line 4 of NEGOM cruise N2, 5-16 May 1998.

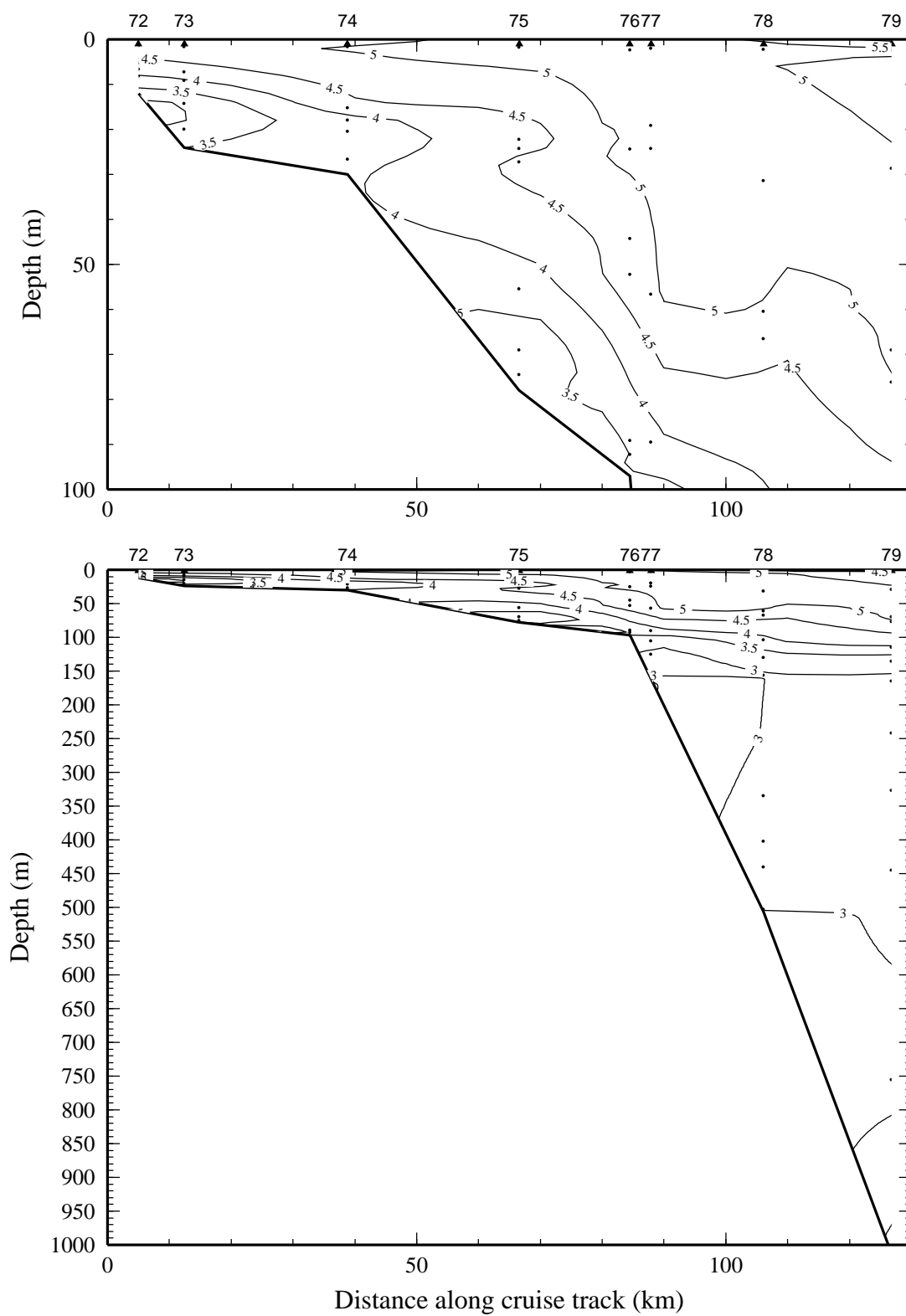


Figure 15. Dissolved oxygen (ml·l⁻¹) on line 4 of NEGOM cruise N2, 5-16 May 1998.

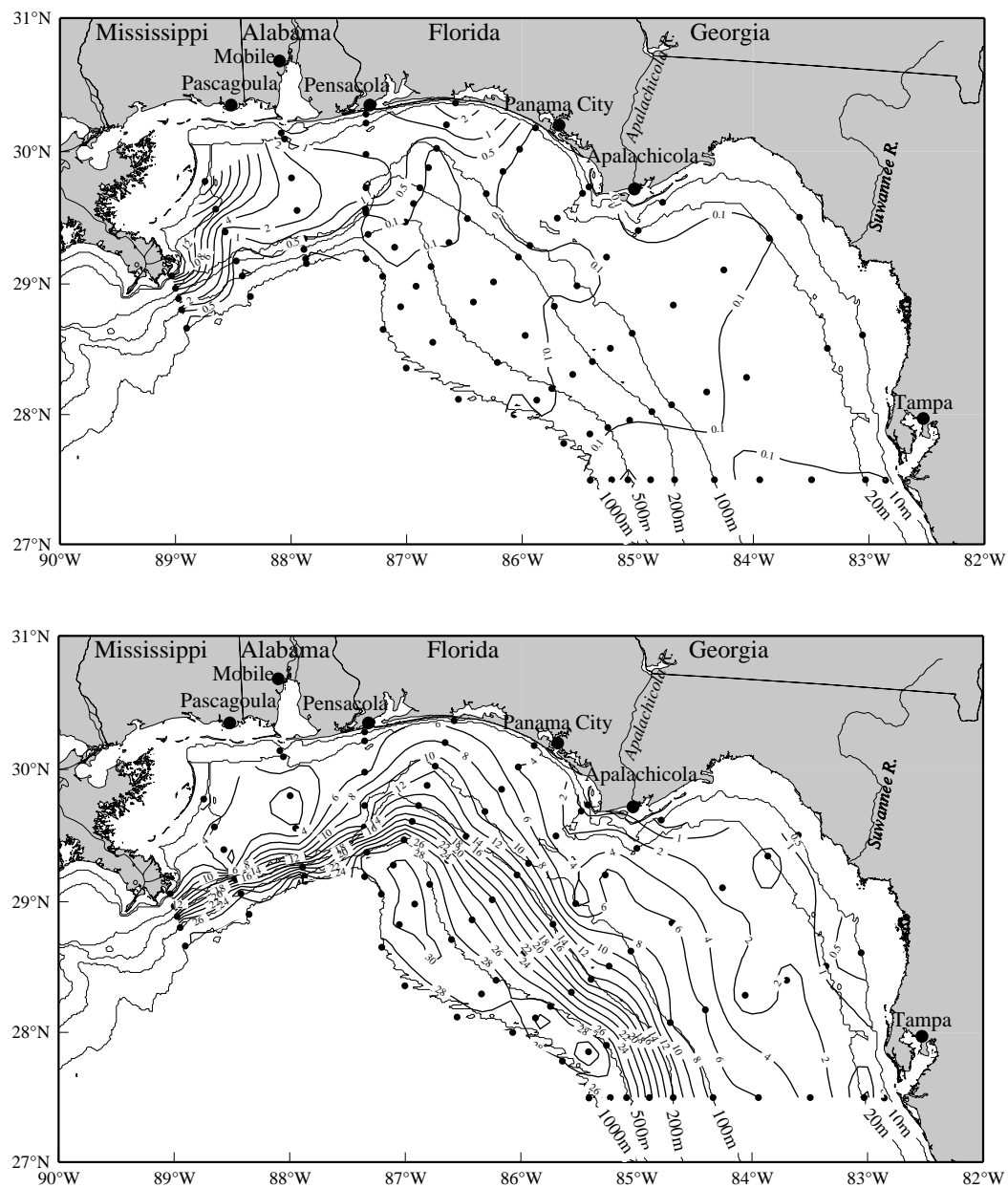


Figure 16. Nitrate ($\mu\text{mol}\cdot\text{l}^{-1}$) at 3.5 m (upper) and near bottom (lower) on NEGOM Cruise N2, 5-16 May 1998.

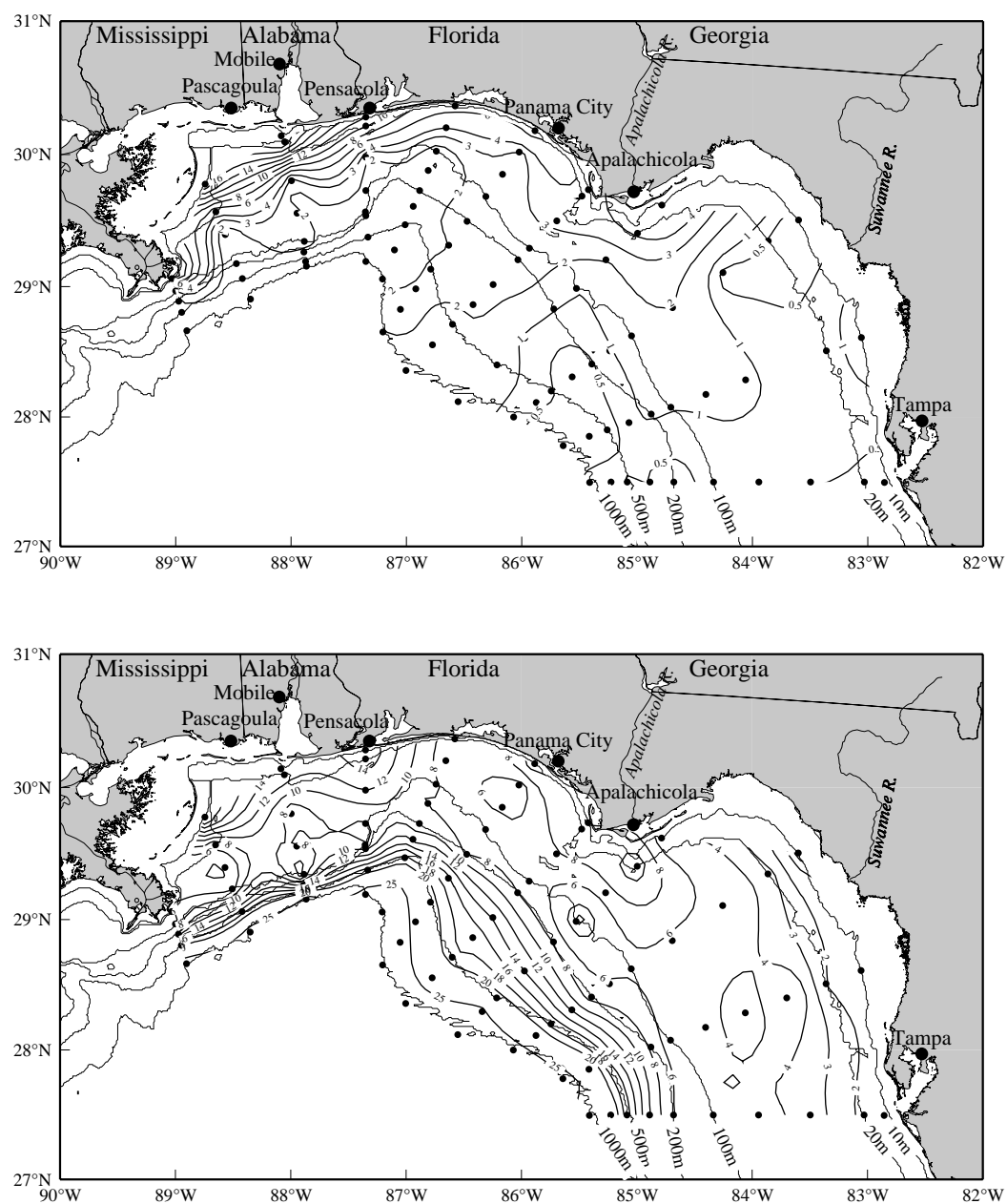


Figure 17. Silicate ($\mu\text{mol}\cdot\text{l}^{-1}$) at 3.5 m (upper) and near bottom (lower) on NEGOM Cruise N2, 5-16 May 1998.

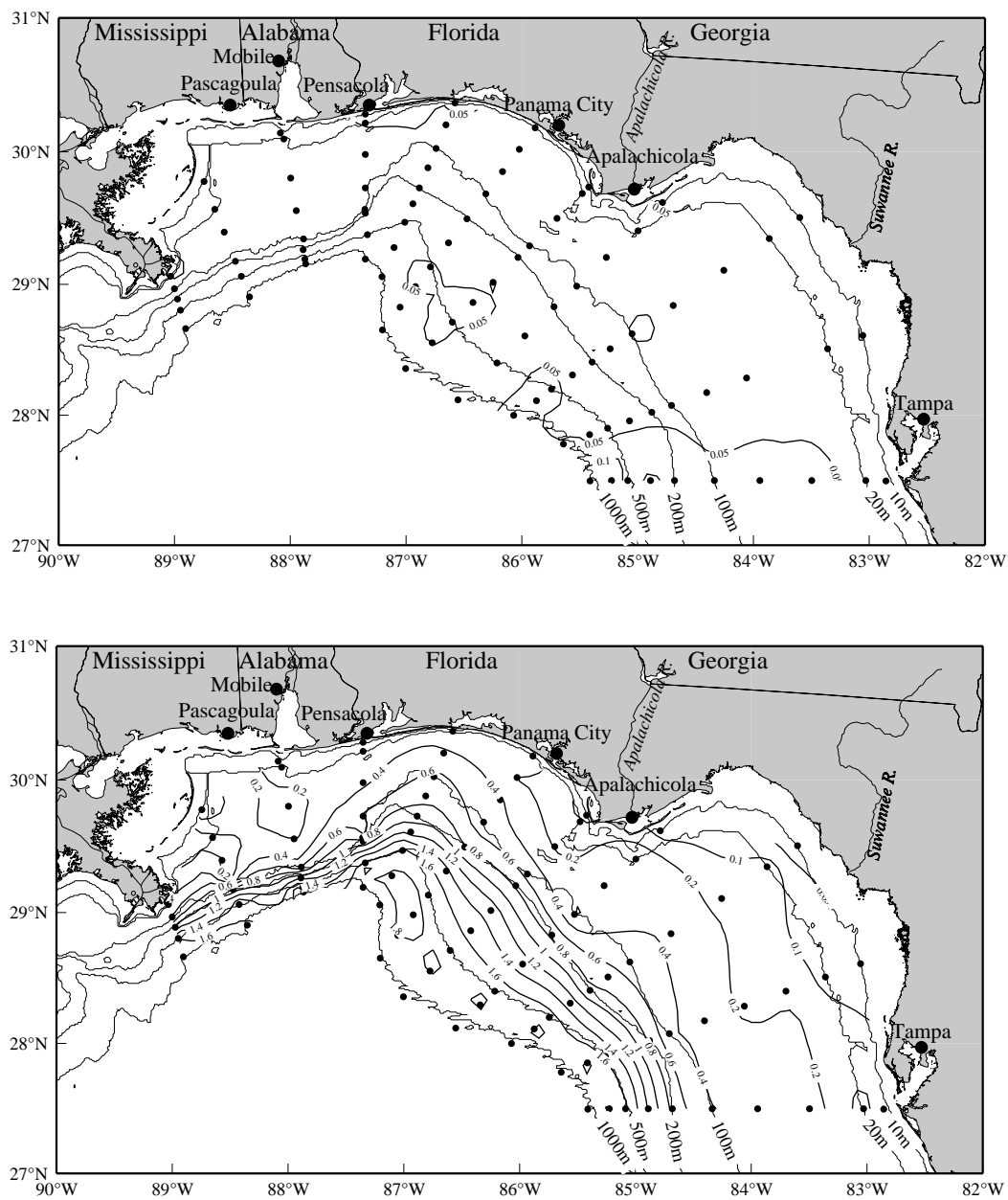


Figure 18. Phosphate ($\mu\text{mol}\cdot\text{l}^{-1}$) at 3.5 m (upper) and near bottom (lower) on NEGOM Cruise N2, 5-16 May 1998.

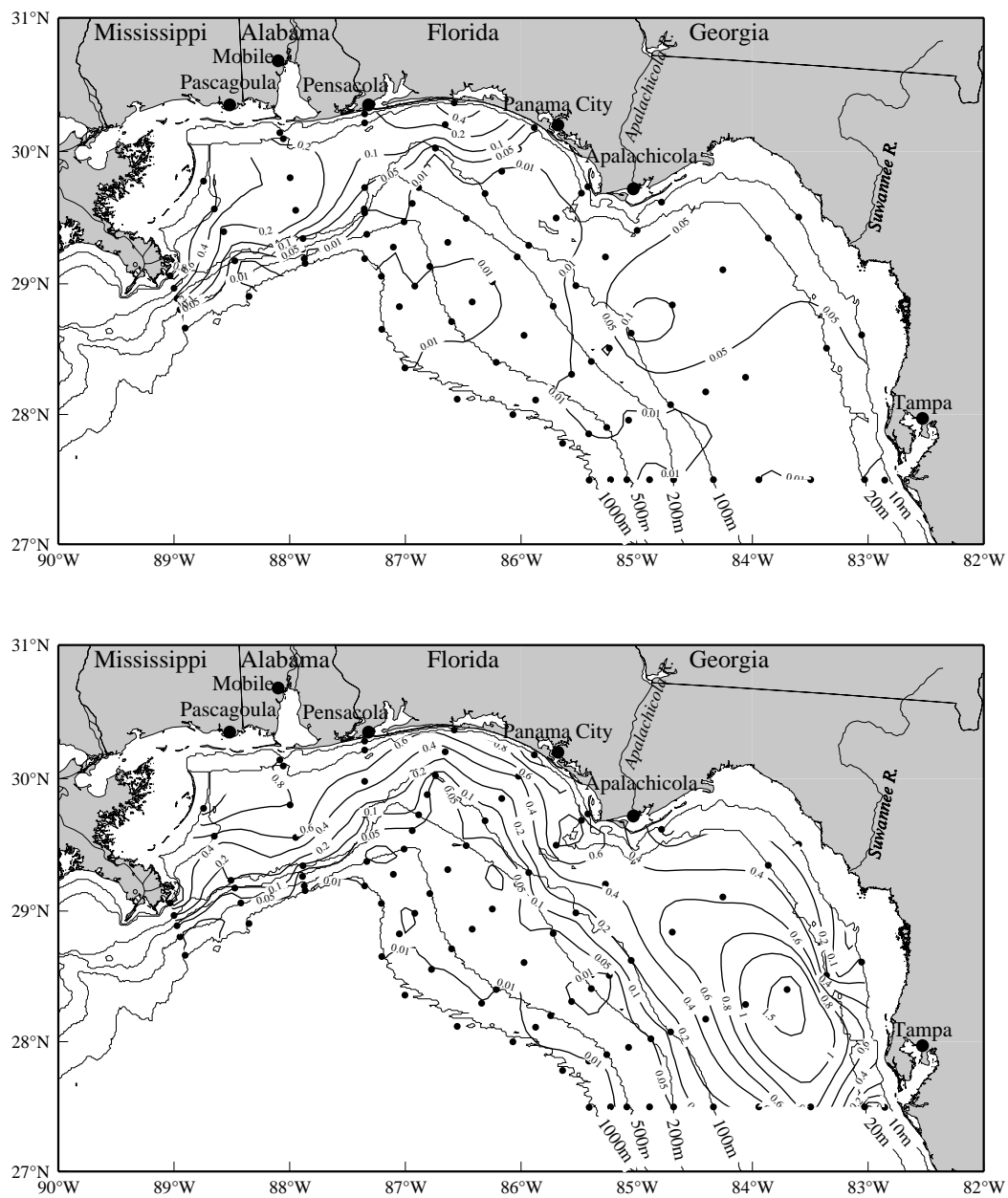


Figure 19. Nitrite ($\mu\text{mol}\cdot\text{l}^{-1}$) at 3.5 m (upper) and near bottom (lower) on NEGOM Cruise N2, 5-16 May 1998.

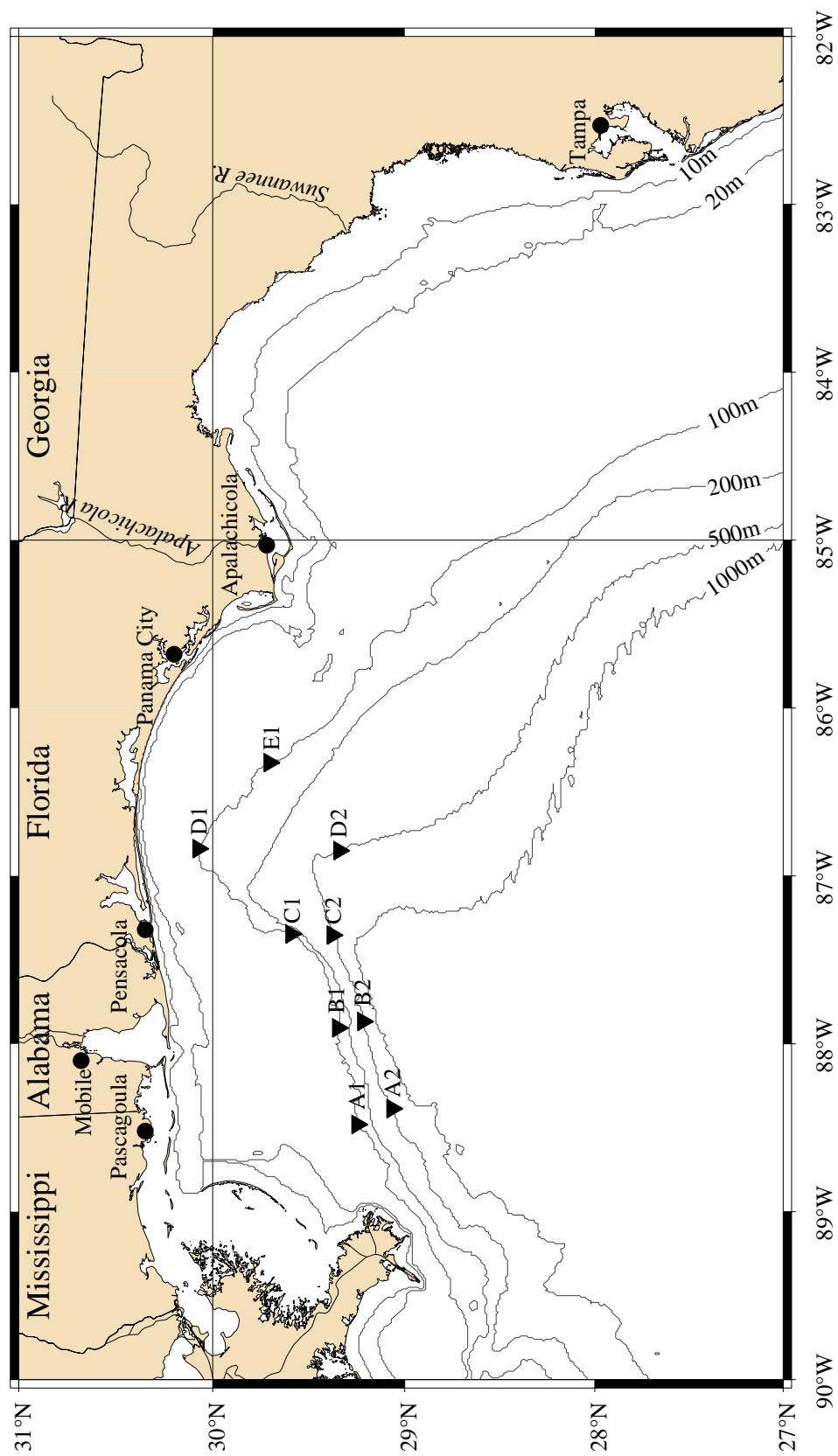


Figure 20. Positions (triangles) of SAIC moorings deployed as part of the DeSoto Canyon Eddy Intrusion Study during the period April-August 1998 (SAIC, 1998).

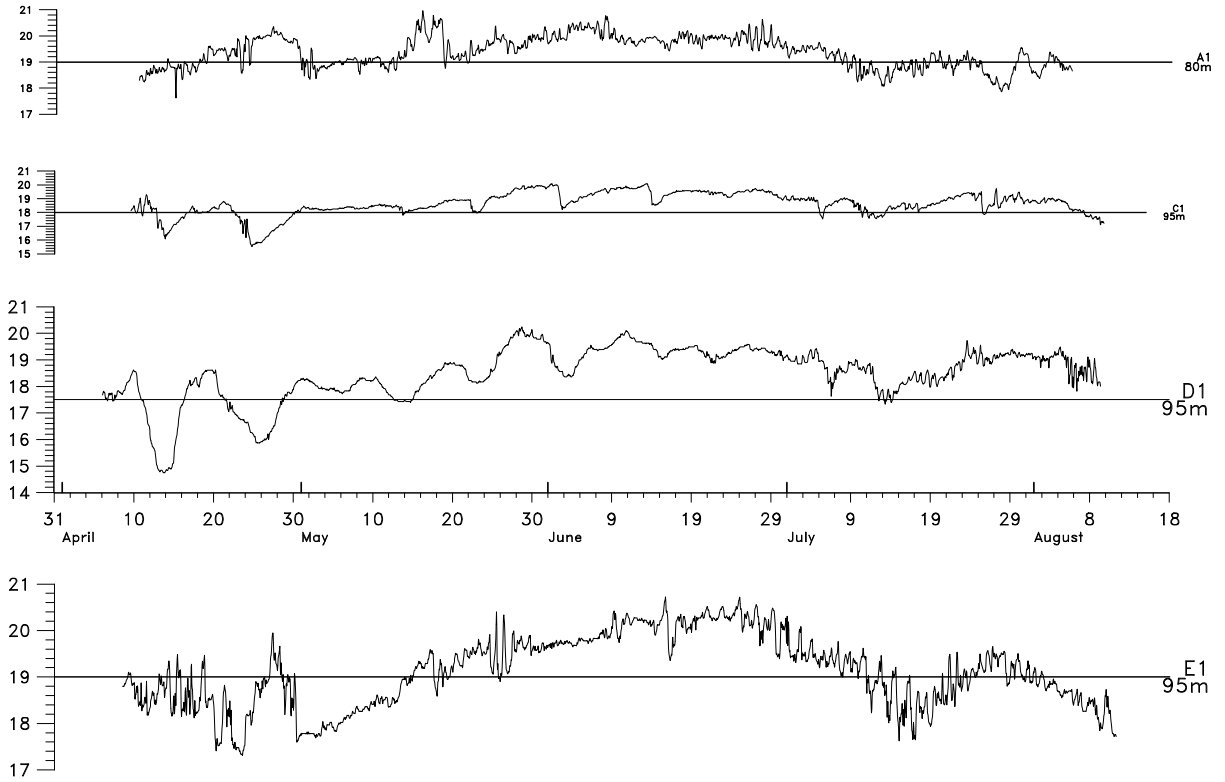


Figure 21. Temperature time series at near-bottom instrument positions on moorings A1, C1, D1, and E1 for April-August 1998. Locations are shown in Figure 20 (SAIC, 1998).

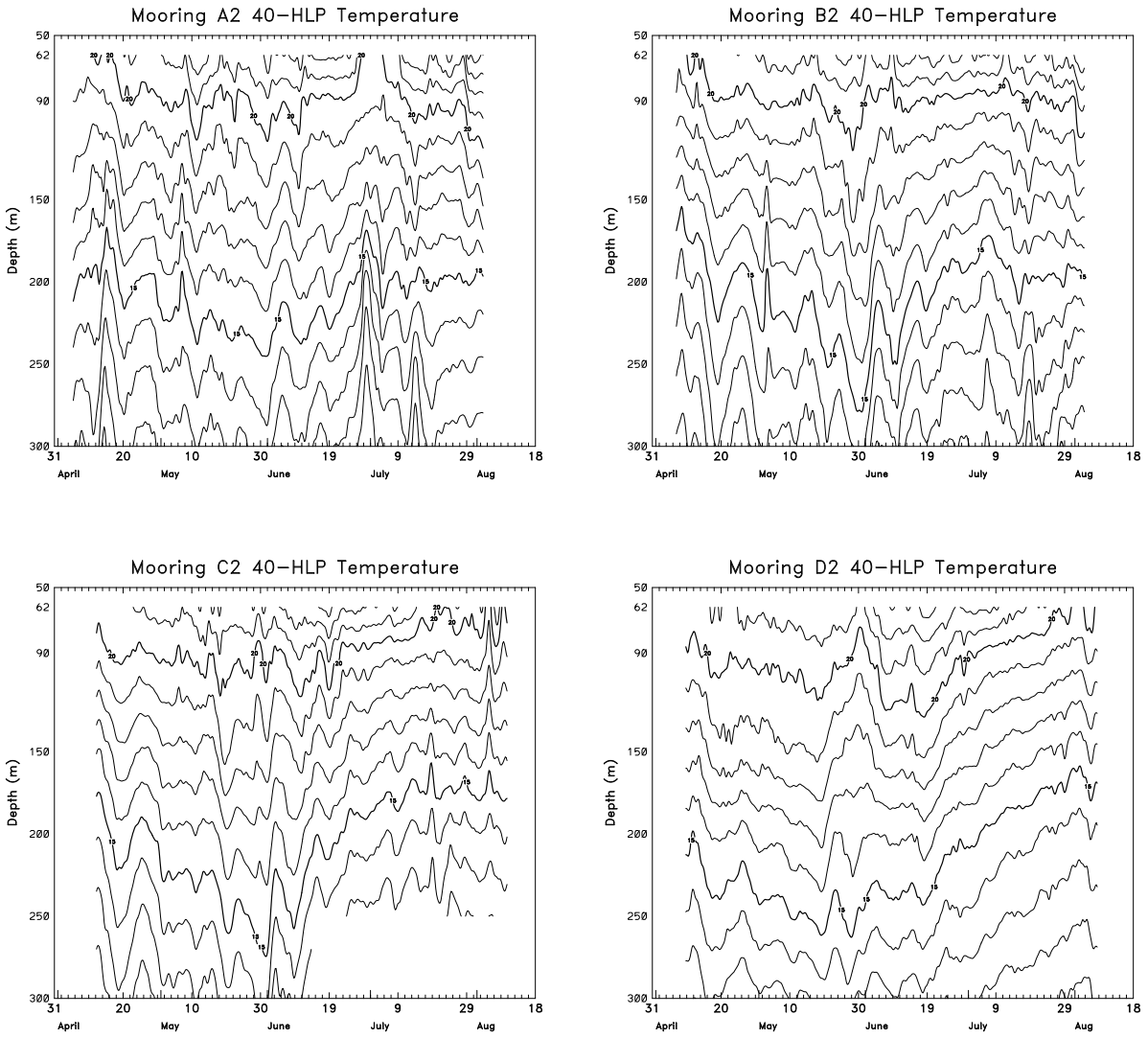


Figure 22. Time histories of isotherm depths between 50 and 300 m constructed by SAIC (1998) from data collected at moorings A2, B2, C2, and D2 (positions shown in Figure 20) for April-August 1998.

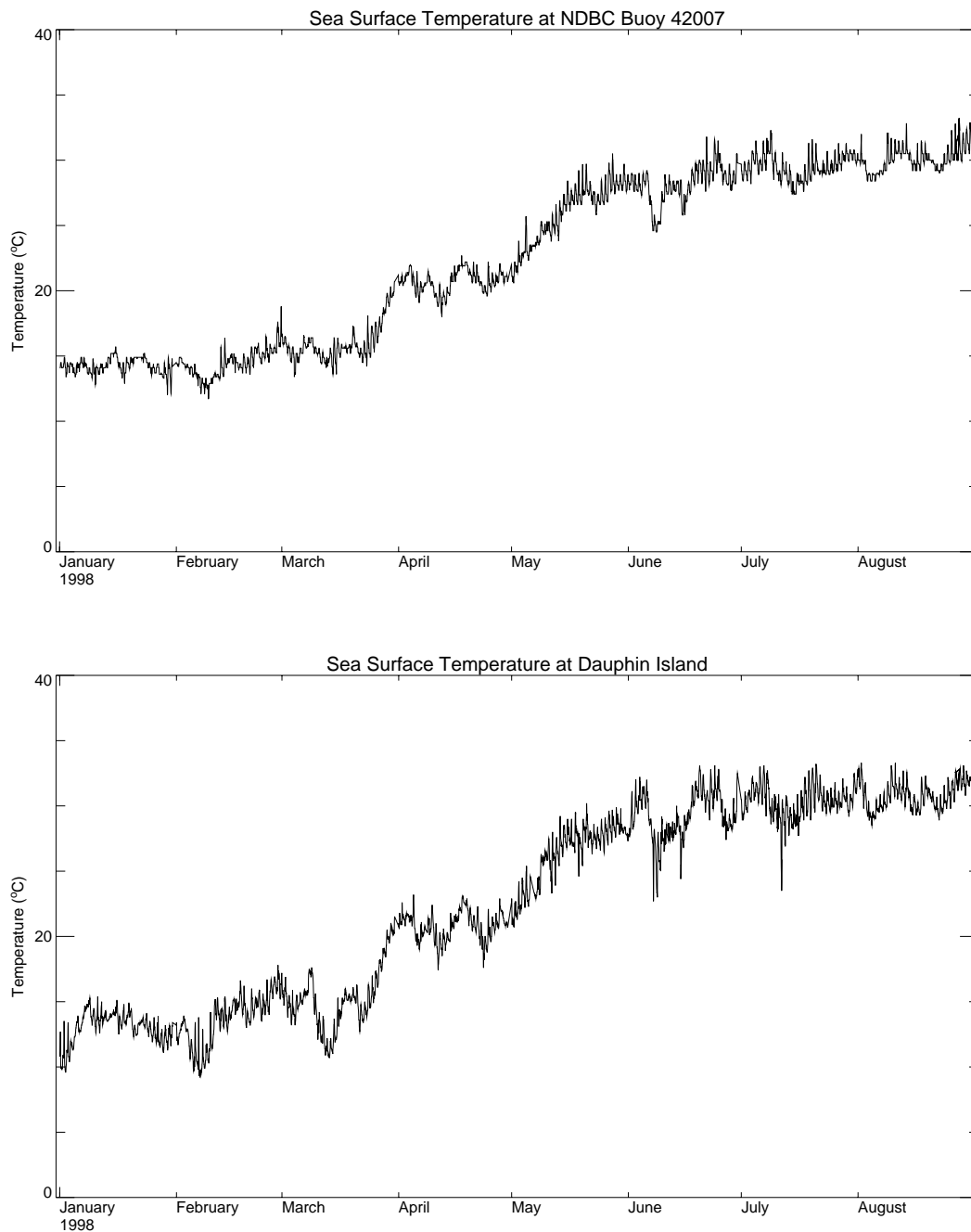


Figure 23. Time series of sea surface temperature (°C) from meteorological stations 42007 (upper) and off Dauphin Island (lower).

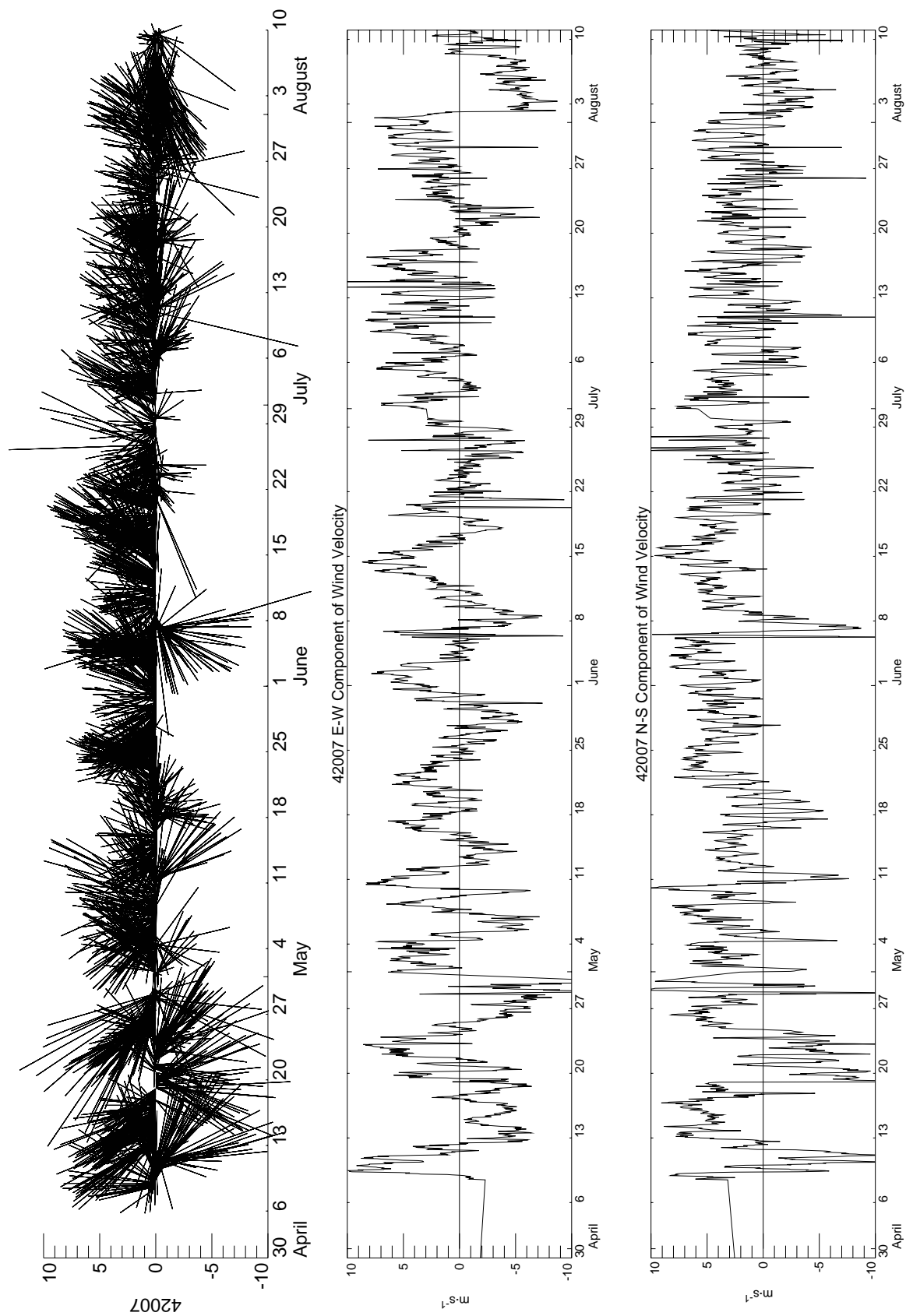


Figure 24a. Surface winds from April through August 1998 for buoy 42007. See Figure 2 for location.

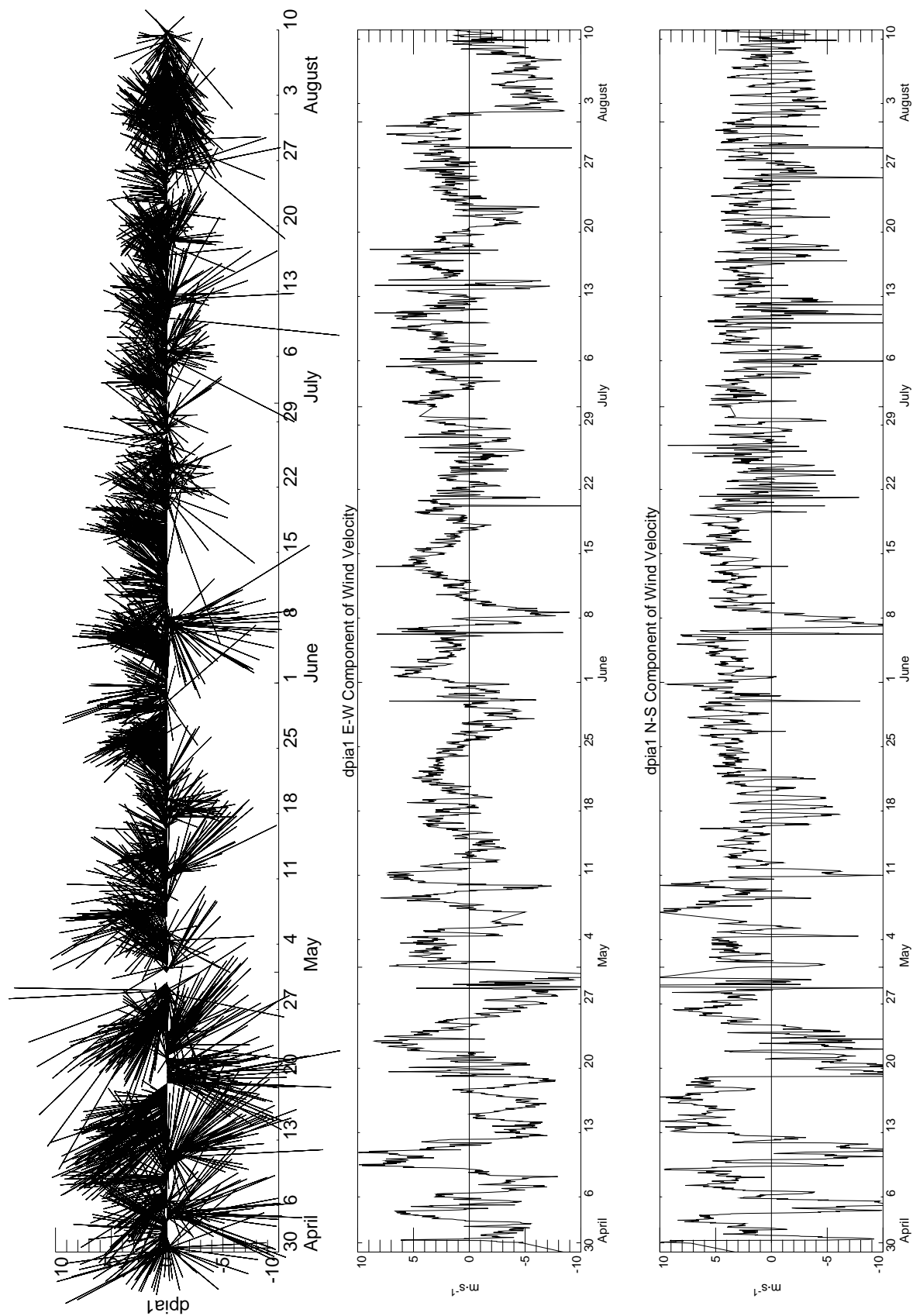


Figure 24b. Surface winds from April through August 1998 for Dauphin Island. See Figure 2 for location.

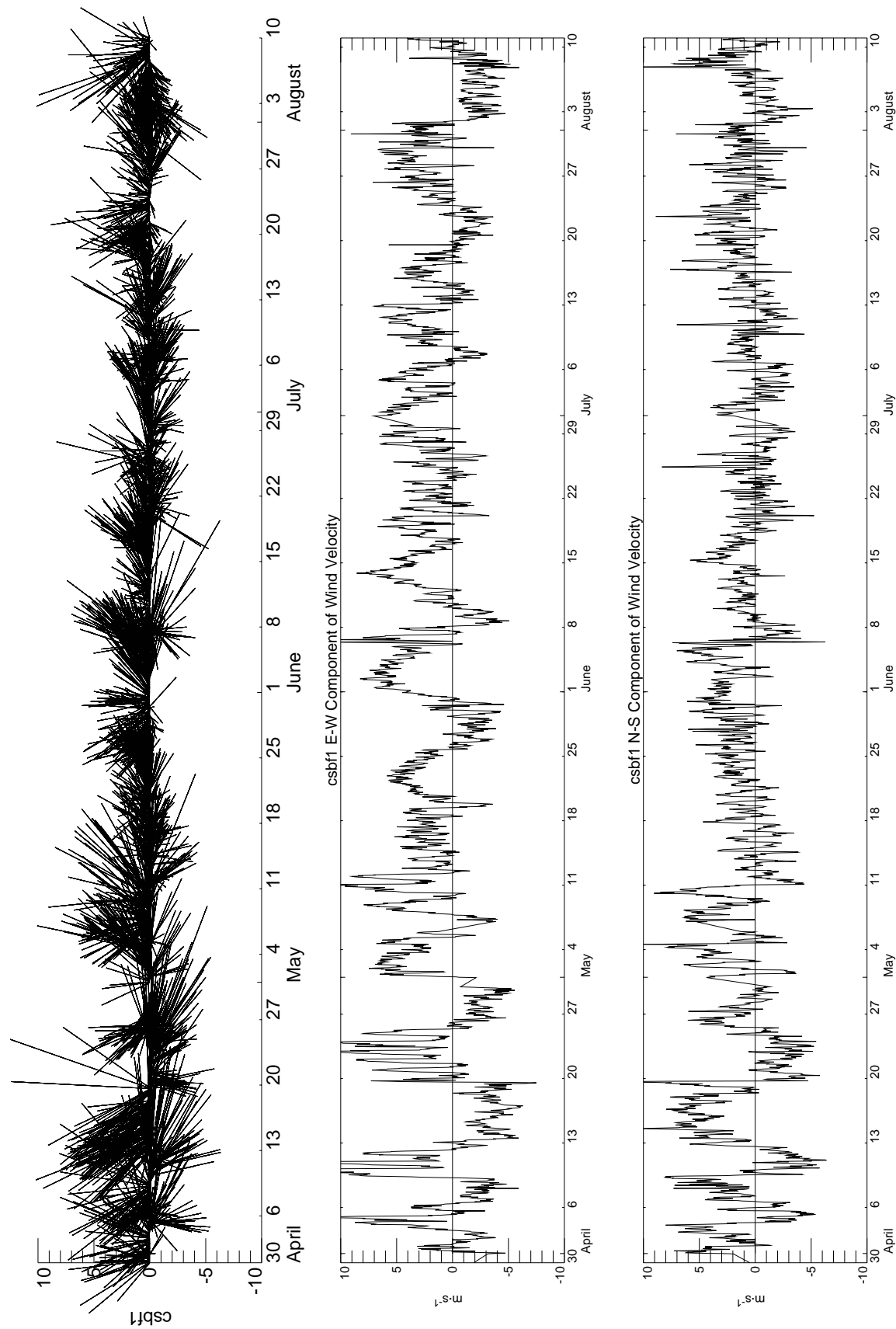


Figure 24c. Surface winds from April through August 1998 for Cape San Blas. See Figure 2 for location.

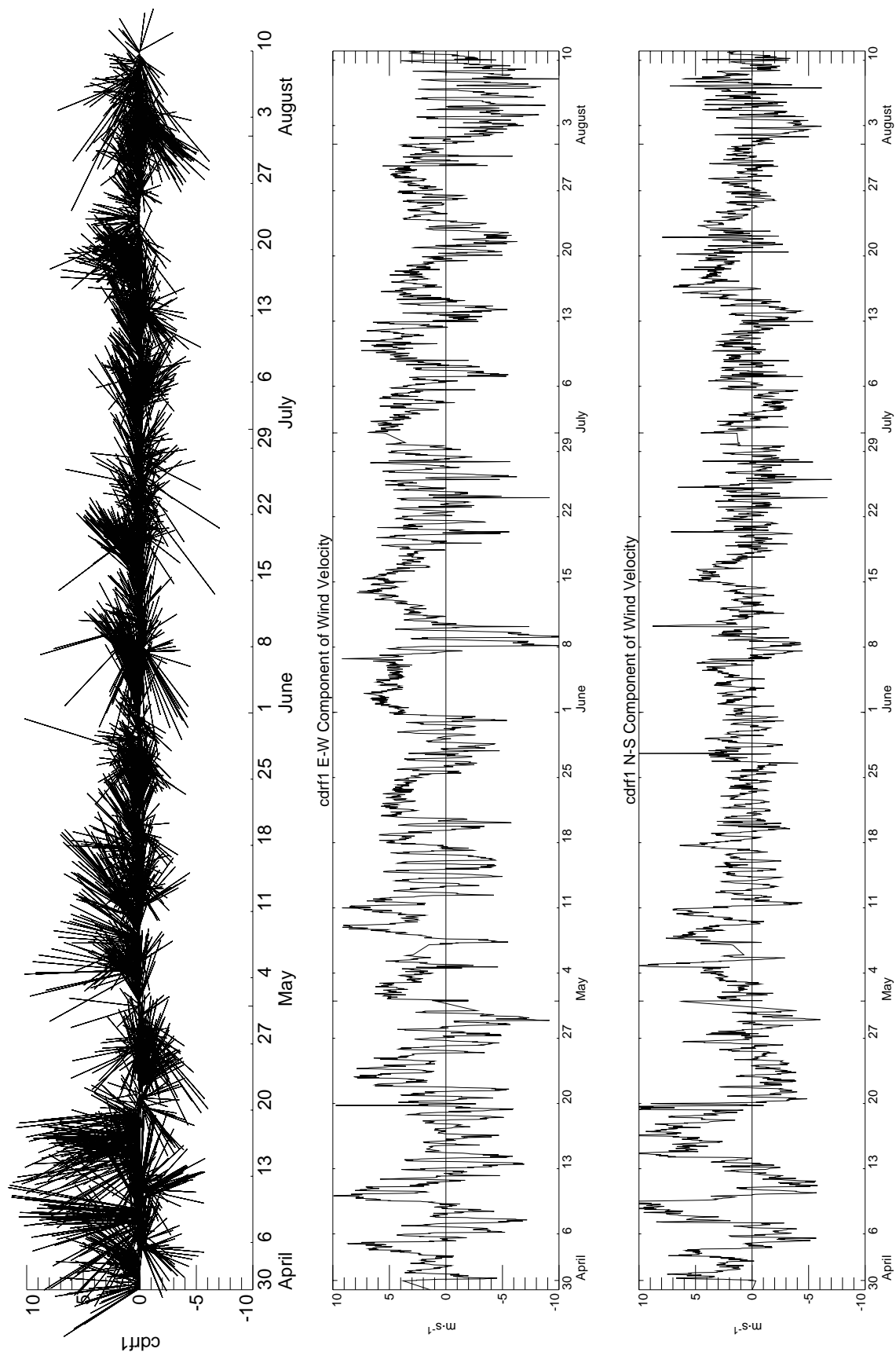


Figure 24d. Surface winds from April through August 1998 for Cedar Key. See Figure 2 for location.

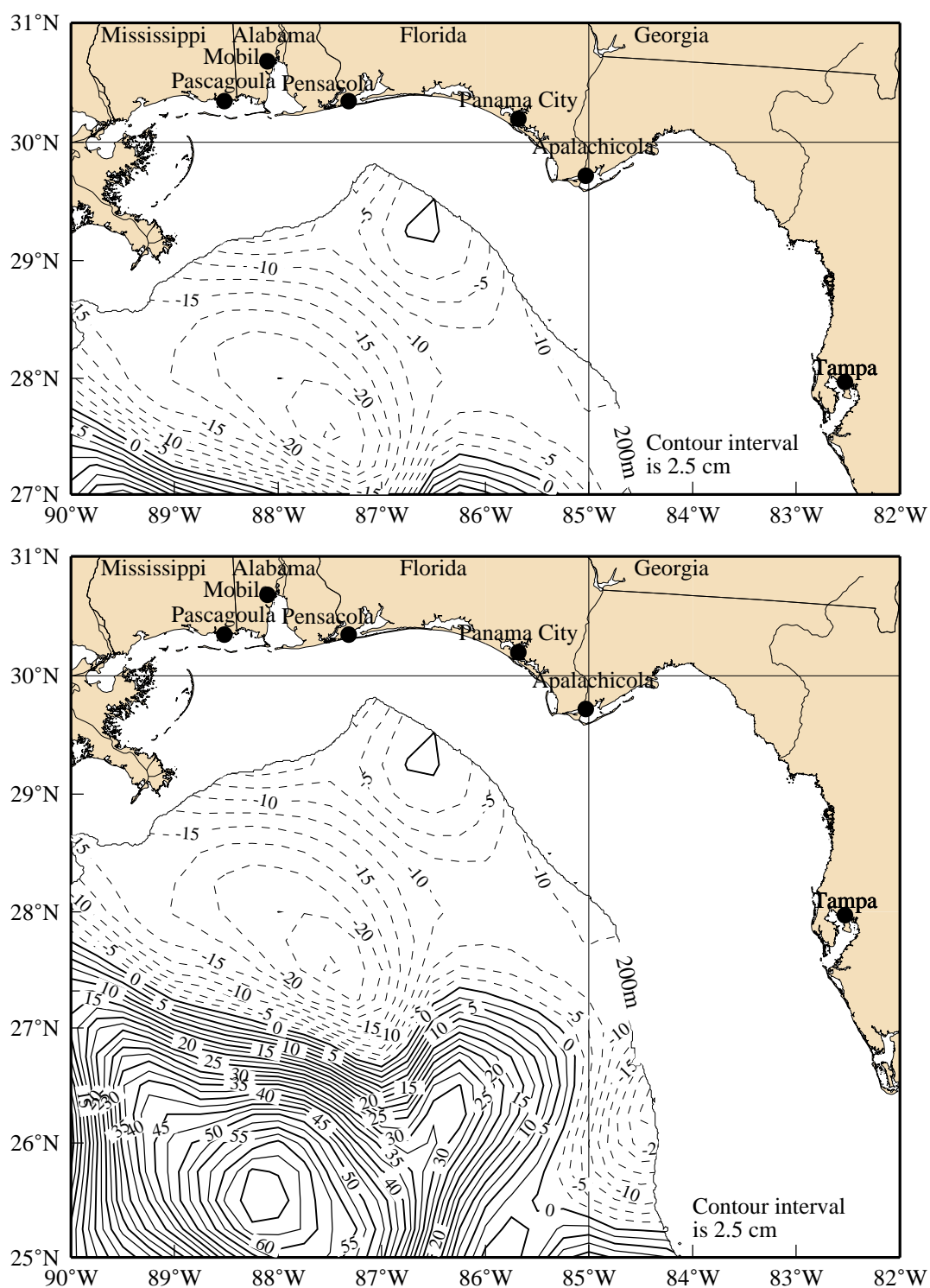


Figure 25. Sea surface height anomaly from satellite altimeter data showing NEGOM study area (upper) and extended region (lower) for 1 April 1998.

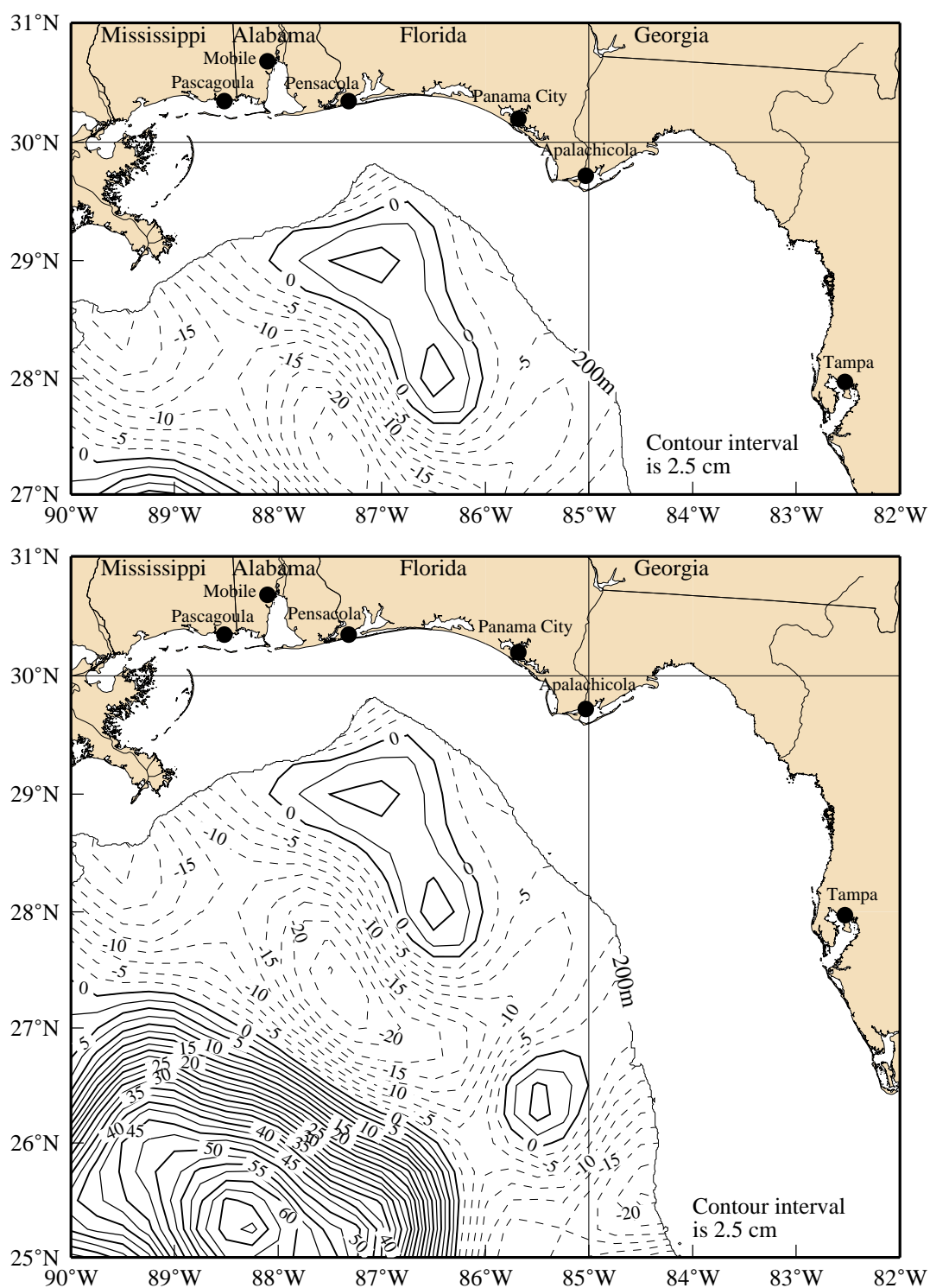


Figure 26. Sea surface height anomaly from satellite altimeter data showing NEGOM study area (upper) and extended region (lower) for 29 April 1998.

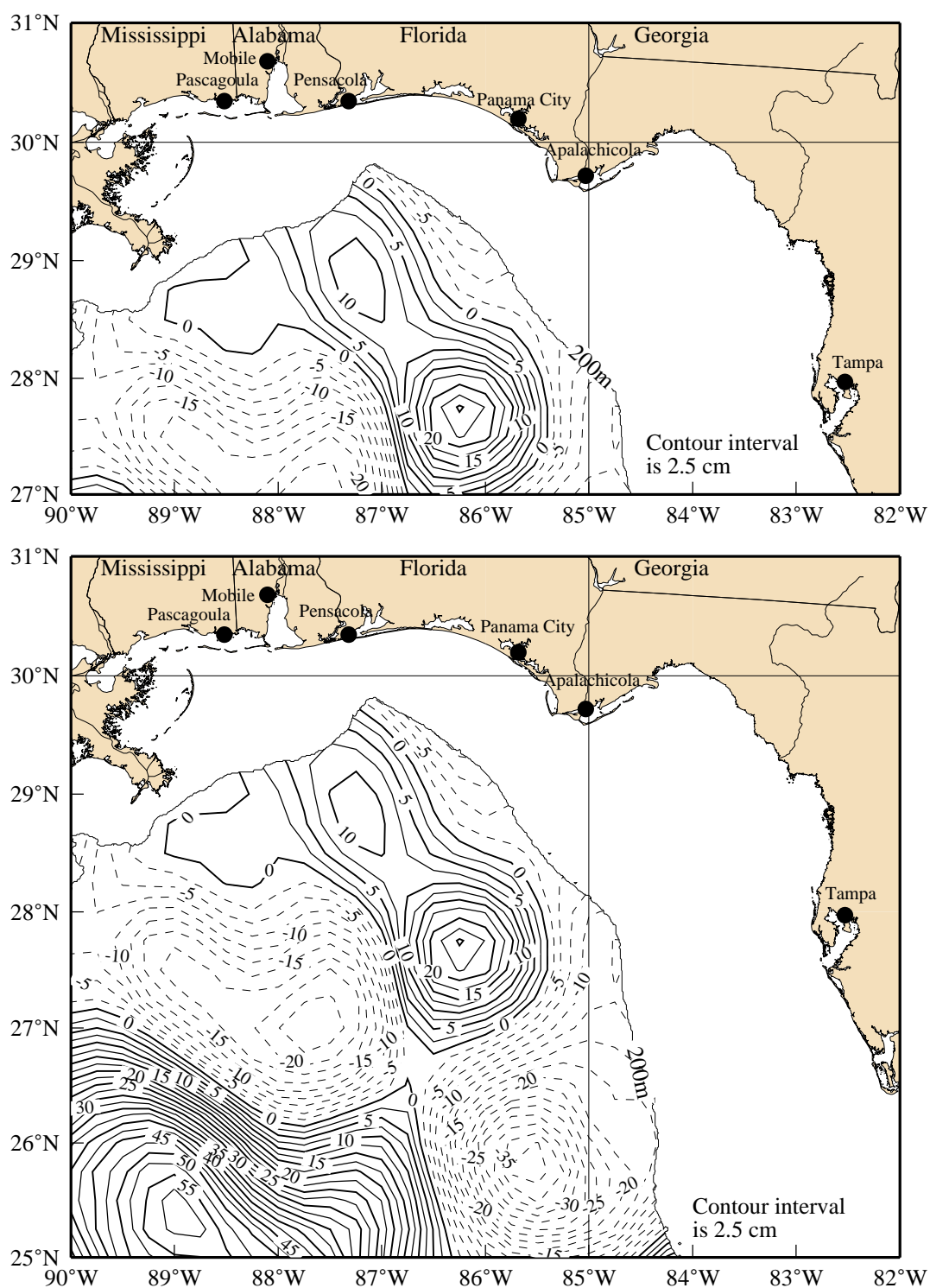


Figure 27. Sea surface height anomaly from satellite altimetry data showing NEGOM study area (upper) and extended region (lower) for 20 May 1998.

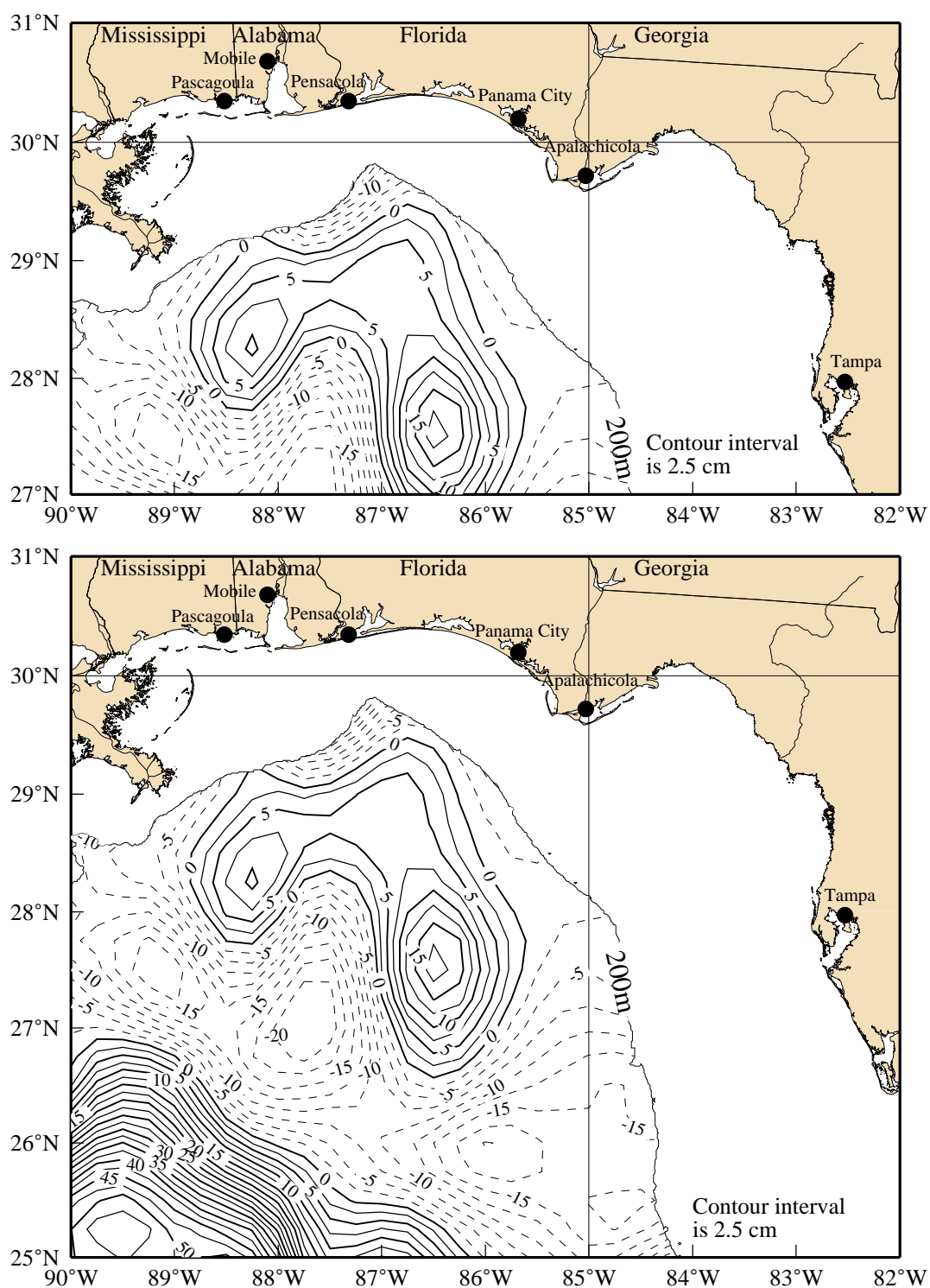


Figure 28. Sea surface height anomaly from satellite altimeter data showing NEGOM study area (upper) and extended region (lower) for 3 June 1998.

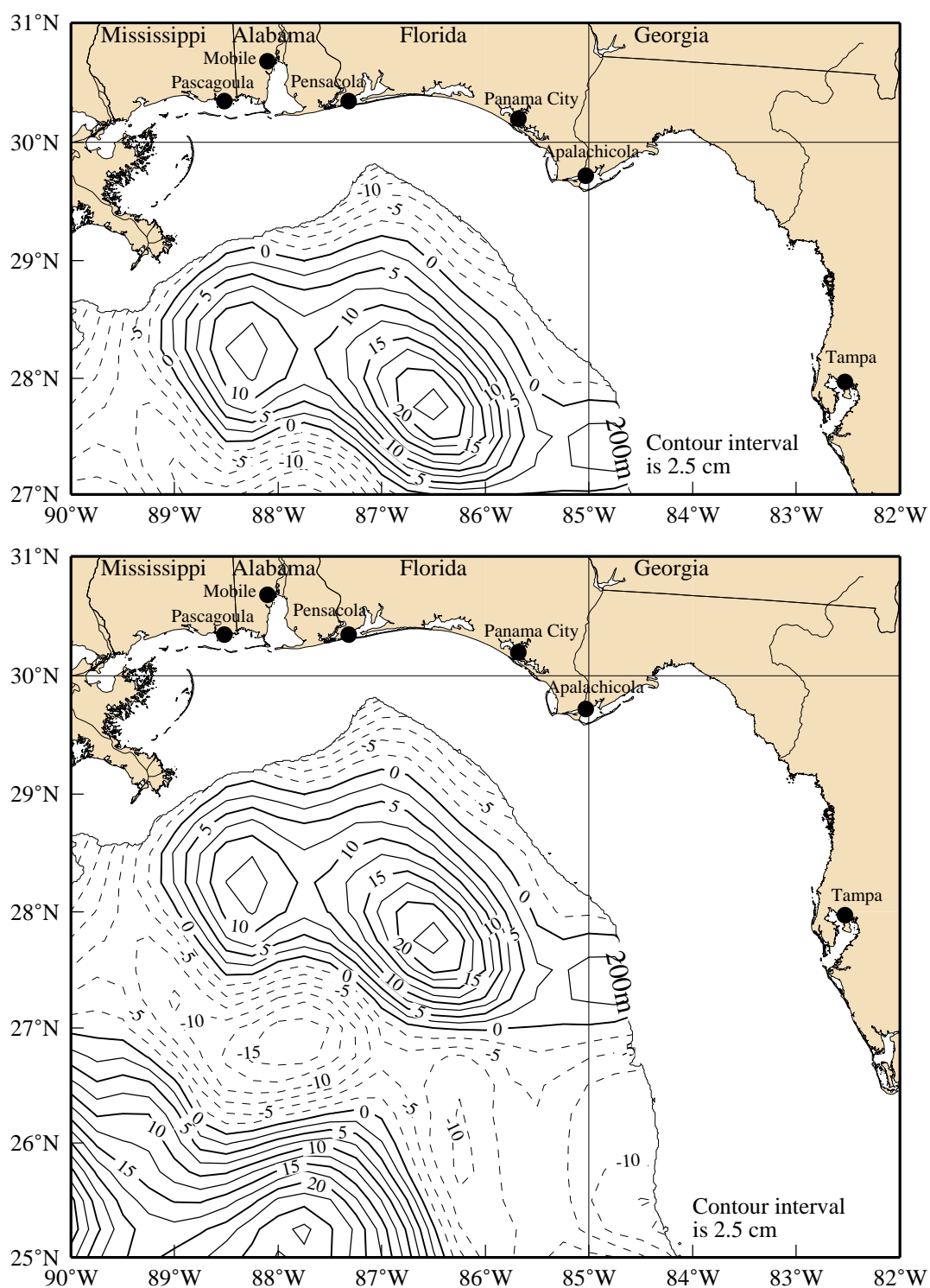


Figure 29. Sea surface height anomaly from satellite altimeter data showing NEGOM study area (upper) and extended region (lower) for 1 July 1998.

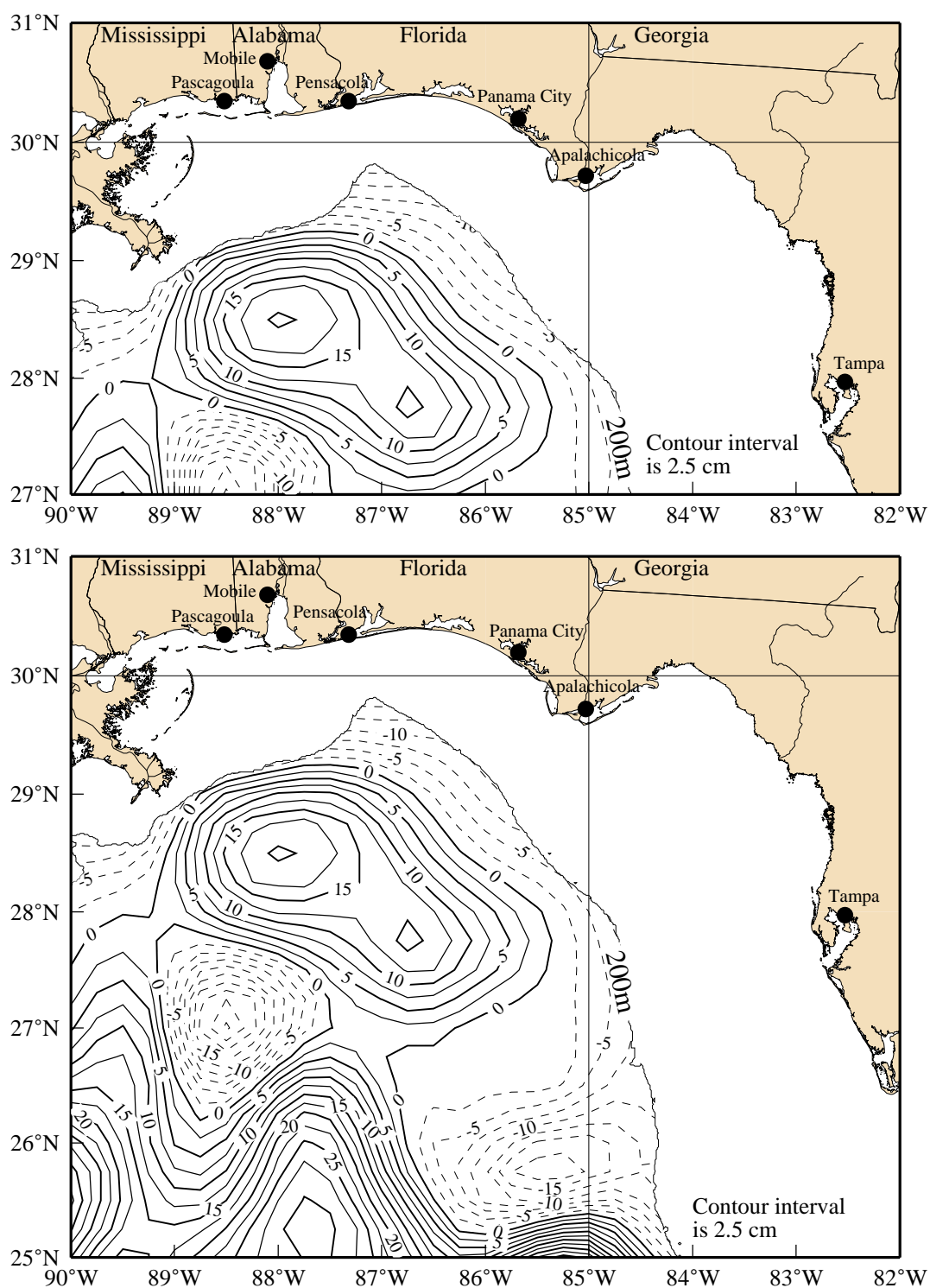


Figure 30. Sea surface height anomaly from satellite altimeter data showing NEGOM study area (upper) and extended region (lower) for 22 July 1998.

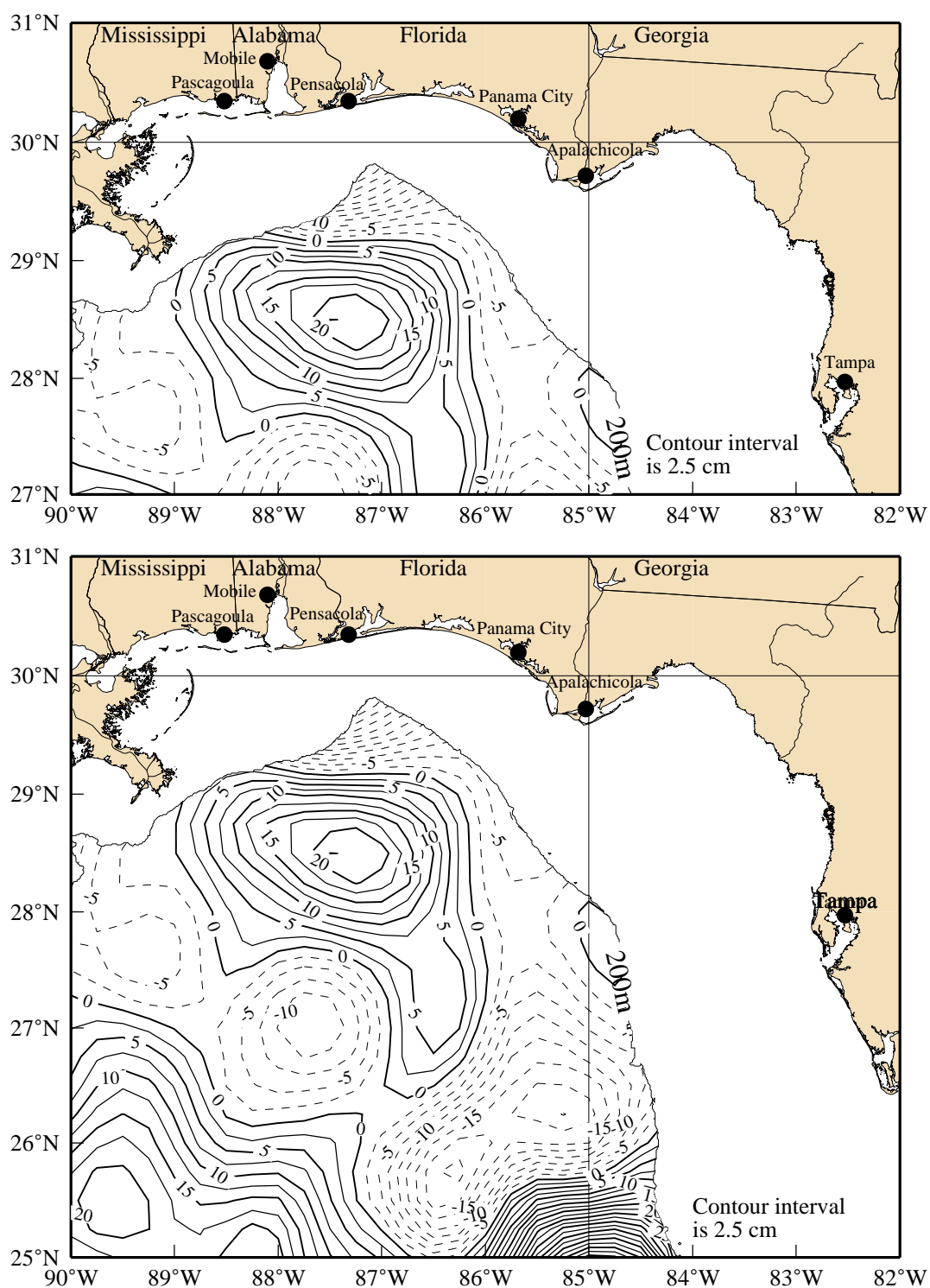


Figure 31. Sea surface height anomaly from satellite altimeter data showing NEGOM study area (upper) and extended region (lower) for 12 August 1998.

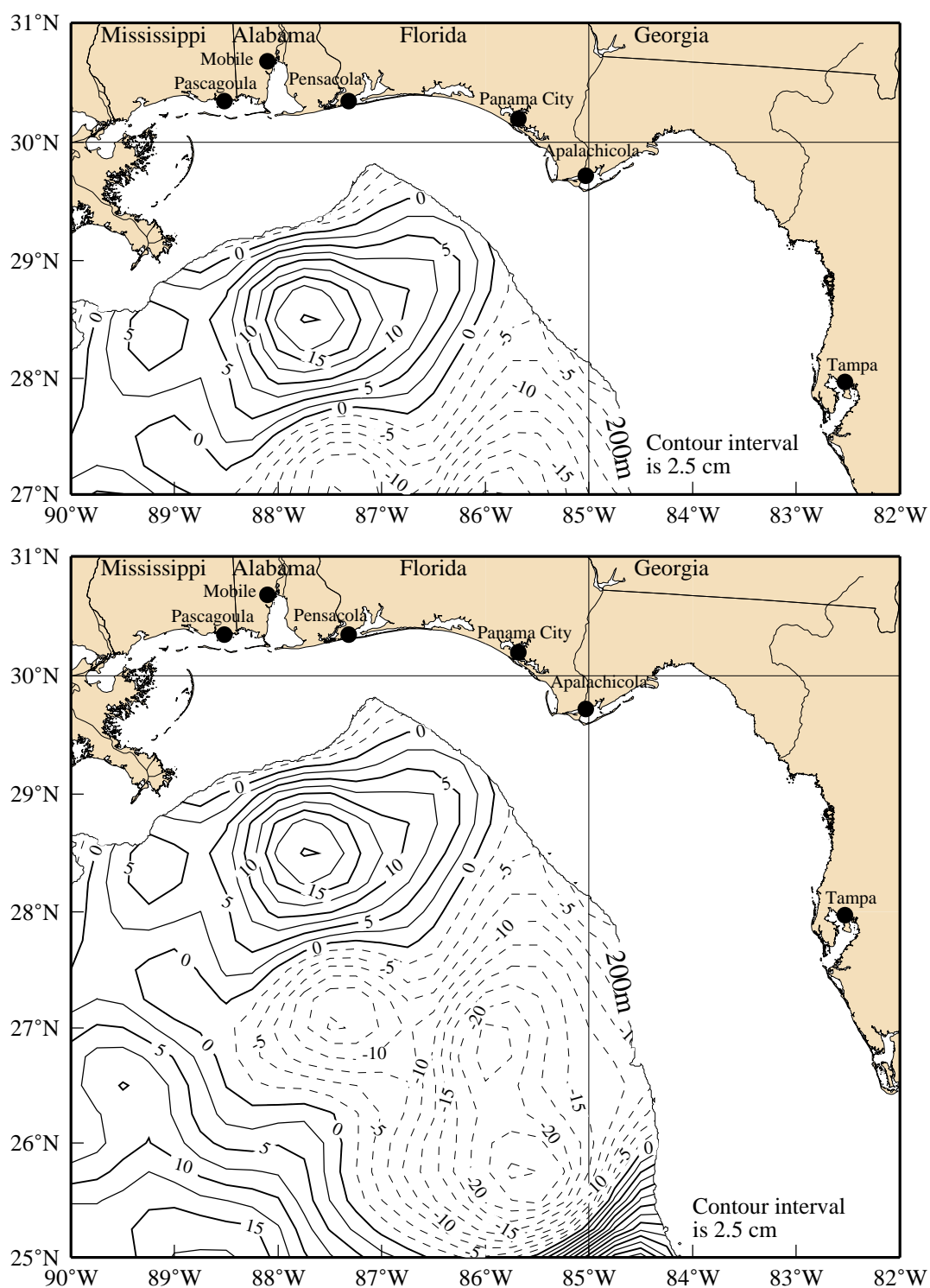


Figure 32. Sea surface height anomaly from satellite altimetry data showing NEGOM study area (upper) and extended region (lower) for 26 August 1998.